รายงานวิจัยฉบับสมบูรณ์

โครงการ

ระบาดวิทยาและการจำแนกสายพันธุ์ระดับโมเลกุลของเชื้อไวรัสอุบัติใหม่ในประเทศไทยตั้งแต่ปี 2012-2013

Prevalence and molecular characterization of emerging respiratory viruses in Thailand during 2012-2013

โดย

รองศาสตราจารย์ ดร.สัญชัย พยุงภร

ภาควิชาชีวเคมี คณะแพทยศาสตร์

จุฬาลงกรณ์มหาวิทยาลัย

ตุลาคม 2559

สัญญาเลขที่ RSA5680031

รายงานวิจัยฉบับสมบูรณ์

โครงการ

ระบาดวิทยาและการจำแนกสายพันธุ์ระดับโมเลกุลของเชื้อไวรัสอุบัติใหม่ในประเทศไทยตั้งแต่ปี 2012-2013

Prevalence and molecular characterization of emerging respiratory viruses in Thailand during 2012-2013

ผู้วิจัย

รองศาสตราจารย์ ดร.สัญชัย พยุงภร
ภาควิชาชีวเคมี คณะแพทยศาสตร์
จุฬาลงกรณ์มหาวิทยาลัย

สนับสนุนโดยสำนักงานกองทุนสนับสนุนการวิจัย
และจุฬาลงกรณ์มหาวิทยาลัย

กิตติกรรมประกาศ

โครงงานวิจัยเรื่อง ระบาดวิทยาและการจำแนกสายพันธุ์ระดับโมเลกุลของเชื้อไวรัสอุบัติใหม่ในประเทศไทยตั้งแต่ปี 2012-2013 (Prevalence and molecular characterization of emerging respiratory viruses in Thailand during 2012-2013) ได้รับทุนอุดหนุนการวิจัยจากสำนักงานกองทุนสนับสนุนการวิจัย (สกว.) และจุฬาลงกรณ์มหาวิทยาลัย โดยมีระยะเวลาในการทำวิจัย 3 ปี (พ.ศ. 2556-2559) คณะผู้วิจัยขอขอบคุณสำนักงานกองทุนสนับสนุนการวิจัย (สกว.) ที่เป็นผู้สนับสนุนหลักในการทำวิจัยโครงการนี้ นอกจากนี้ได้รับการสนับสนุนเพิ่มเติมในด้านเงินทุน สถานที่และอุปกรณ์การวิจัยจากจุฬาลงกรณ์มหาวิทยาลัย

คณะผู้วิจัยขอขอบคุณ ศาสตราจารย์ นายแพทย์ยง ภู่วรวรรณ ซึ่งเป็นที่ปรึกษาอาวุโสในการให้คำแนะนำและแก้ไขปัญหาโดยรวมของโครงการ นอกจากนี้ขอขอบคุณนักวิทยาศาสตร์ นักวิจัย เจ้าหน้าที่ และนิสิตจากหน่วยงานต่างๆ โดยเฉพาะอย่างยิ่งศูนย์เชี่ยวชาญเฉพาะทางไวรัสวิทยาคลินิก คณะแพทยศาสตร์ จุฬาลงกรณ์มหาวิทยาลัย ที่ได้ให้ความร่วมมือเป็นอย่างดีในการดำเนินงานวิจัยให้สำเร็จลุล่วงตามเป้าหมาย

รองศาสตราจารย์ ดร.สัญชัย พยุงภร
และคณะผู้วิจัย

บทคัดย่อ

สัญญาเลขที่ RSA5680031

โครงการวิจัย ระบาดวิทยาและการจำแนกสายพันธุ์ระดับโมเลกุลของเชื้อไวรัสอุบัติใหม่ในประเทศไทยตั้งแต่ปี 2012-2013

ผู้วิจัยหลัก รองศาสตราจารย์ ดร.สัญชัย พยุงภร

อีเมลล์ sp.medbiochemcu@gmail.com

ระยะเวลา 3 ปี (พ.ศ. 2556-2559)

โรคติดเชื้อในระบบทางเดินหายใจ เป็นสาเหตุหลักที่ทำให้เกิดอาการเจ็บป่วย และเสียชีวิต โดยมีสาเหตุหลักมาจากการติดเชื้อไวรัส ซึ่งไวรัสที่ก่อโรคติดเชื้อในระบบทางเดินหายใจในมนุษย์ มีหลายชนิด ได้แก่ influenza viruses, parainfluenza viruses, respiratory syncytial viruses, rhinoviruses, adenoviruses, coronaviruses และ metapneumoviruses เป็นต้น ในงานวิจัยนี้มุ่งเน้นในการศึกษาระบาดวิทยาและการจำแนกสายพันธุ์ระดับโมเลกุลของเชื้อไวรัส human polyomavirus (HPyV) และ human coronavirus (HCoV) จากผู้ป่วยติดเชื้อระบบทางเดินหายใจ ในประเทศไทย ตั้งแต่ปี ค.ศ. 2012-2013 โดยใช้เทคนิค semi-nested PCR และหาลำดับพันธุกรรม เพื่อใช้ในการจำแนกลักษณะทางพันธุกรรม จากผลการทดลองพบการติดเชื้อ WU polyomavirus (WUPyV) ประมาณ 0.16% ในขณะที่ไม่พบการติดเชื้อ human polyomavirus สายพันธุ์อื่นๆ เช่น KIPyV, HPyV9 และ MCPyV สำหรับการติดเชื้อ human coronavirus (HCoV) พบประมาณ 0.79% ซึ่งจำแนกได้เป็นสายพันธุ์ HCoV-HKU1 จำนวน 19 ตัวอย่าง (0.32%), HCoV-NL63 จำนวน 19 ตัวอย่าง (0.32%), HCoV-229E จำนวน 5 ตัวอย่าง (0.09%) และ HCoV-OC43 จำนวน 3 ตัวอย่าง (0.05%) ทั้งนี้ไม่พบการติดเชื้อ MERS-CoV โดยสรุปข้อมูลที่ได้จากการศึกษาทำให้ได้องค์ความรู้ในแง่ระบาดวิทยาและการจำแนกสายพันธุ์ของเชื้อไวรัส HPyV และ HCoV ในประเทศไทย ตั้งแต่ปี ค.ศ. 2012-2013 ซึ่งมีประโยชน์อย่างยิ่งในด้านระบาดวิทยาและการจำแนกสายพันธุ์ของเชื้อไวรัส รวมทั้งสามารถประยุกต์ใช้ในการควบคุมการระบาดและการพัฒนาวัคซีนในอนาคต

คำหลัก: Human coronavirus; human polyomavirus; ระบาดวิทยา; โรคติดเชื้อระบบทางเดินหายใจ

Abstract

Project Code: RSA5680031

Project Title: Prevalence and molecular characterization of emerging respiratory viruses in Thailand during 2012-2013

Investigator: Associate Professor Sunchai Payungporn, Ph.D.

E-mail Address: sp.medbiochemcu@gmail.com

Project Period: 3 years (2013-2016)

Acute respiratory diseases are a major cause of morbidity and mortality in humans and most acute respiratory infections are caused by viruses. The viruses associated with respiratory disease that are well documented in human populations include influenza viruses, parainfluenza viruses, respiratory syncytial viruses, rhinoviruses, adenoviruses, coronaviruses, and metapneumoviruses. This study focuses on the prevalence and genetic characterization of human polyomavirus (HPyV) and human coronavirus (HCoV) obtained from patients with respiratory diseases in Thailand during 2012-2013. HPyV and HCoV were detected by using semi-nested PCR and then characterized by multiple sequences alignment and phylogenetic tree. The result revealed that 0.16% was positive for WU polyomavirus (WUPyV) whereas KIPyV, HPyV9 and MCPyV were not detected in this study. HCoV infection was found in 46 (0.79%) of the total samples: 19 (0.32%) for HCoV-HKU1, 19 (0.32%) for HCoV-NL63, 5 (0.09%) for HCoV-229E, and 3 (0.05%) for HCoV-OC43. None of the sample tested positive for MERS-CoV. In conclusion, data obtained from this study provides the HPyV and HCoV infection rate in a Thai cohort during 2012-2013 which might be useful in terms of epidemiology and genetic characterization of HPyV and HCoV for disease prevention and vaccine development in the future.

Keywords: Human coronavirus; human polyomavirus; epidemiology; respiratory tract infection (RTI)

บทนำ (Introduction)

Acute respiratory diseases are a major cause of morbidity and mortality in humans and most acute respiratory infections are caused by viruses. The viruses associated with respiratory disease that are well documented in human populations include influenza viruses, parainfluenza viruses, respiratory syncytial viruses, rhinoviruses, adenoviruses, coronaviruses, and metapneumoviruses. Many of these viruses cause the highest problem of disease in particular risk groups such as little infants, elderly and immune-compromised personnel. Although most important respiratory viruses in humans have been recognized in the last century, new emerging viruses that may cause a symptom of acute respiratory disease in humans have been recently discovered. In this study, we focus on the prevalence and characterization of novel strains of human coronavirus and human polyomavirus that may involve with emerging respiratory diseases in human.

Coronaviruses (CoVs)

Coronaviruses (CoVs) belong to *Coronaviridae* family, are a group of enveloped viruses with a linear, non-segmented, positive-sense, single-stranded RNA genome, having a characteristic crown morphology [Fauquet *et al*., 2005]. According to the International Committee for Taxonomy of Viruses (ICTV), the *Coronaviridae* family was classified into two subfamilies: *Coronavirinae* and *Torovirinae*. At present, the *Coronavirinae* subfamily can be classified into three groups: group I (Alphacoronavirus) includes both human (HCoV-229E and HCoV-NL63) and animal pathogens; group II (Betacoronavirus) includes both human (HCoV-OC43, HCoV-HKU1 & SARS-CoV) and animal pathogens; and group III (Gammacoronavirus) includes only avian CoVs. The coronaviral genome is non-segmented viral RNA genome (approximately 30 kbp) and is subdivided into a variable number of 6 to 9 open reading frames (ORFs) which encode non-structural proteins with RNA-polymerase function (Pol-1a,b) and four structural proteins: Spike (S), Membrane (M), Envelope (E) and Nucleocapsid (N) proteins (Figure 1) [Fauquet *et al*., 2005].

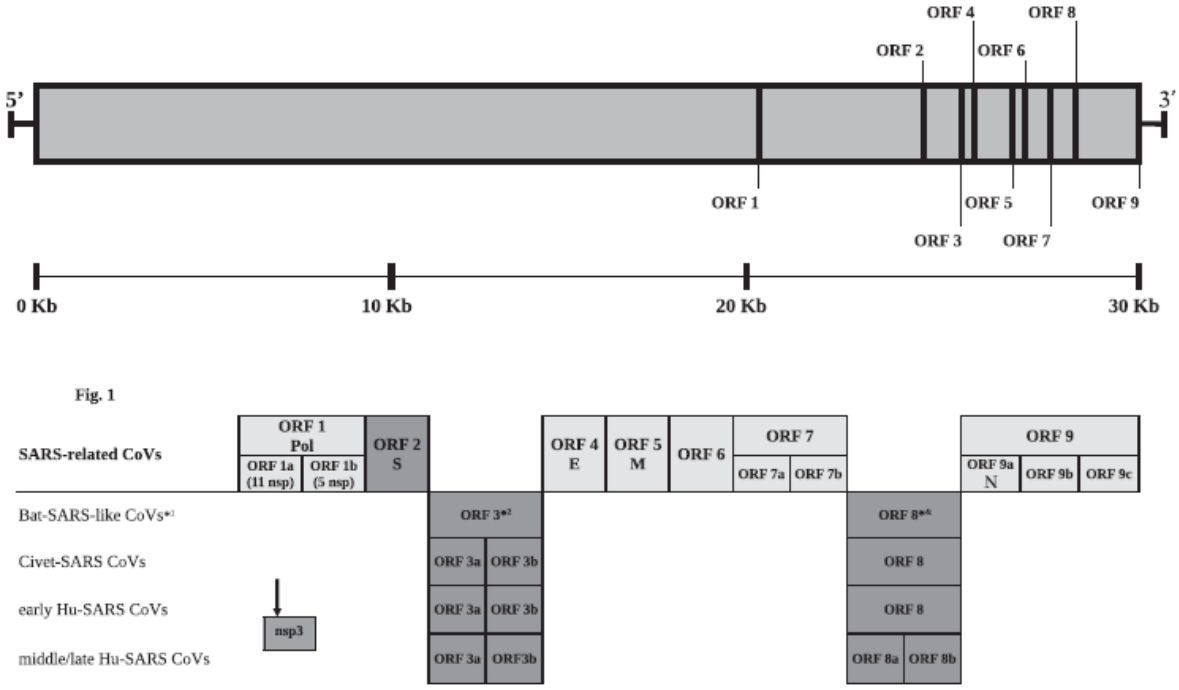

Figure 1: Genome organization of human CoVs and other related-CoVs. [Balboni *et al*, 2012]

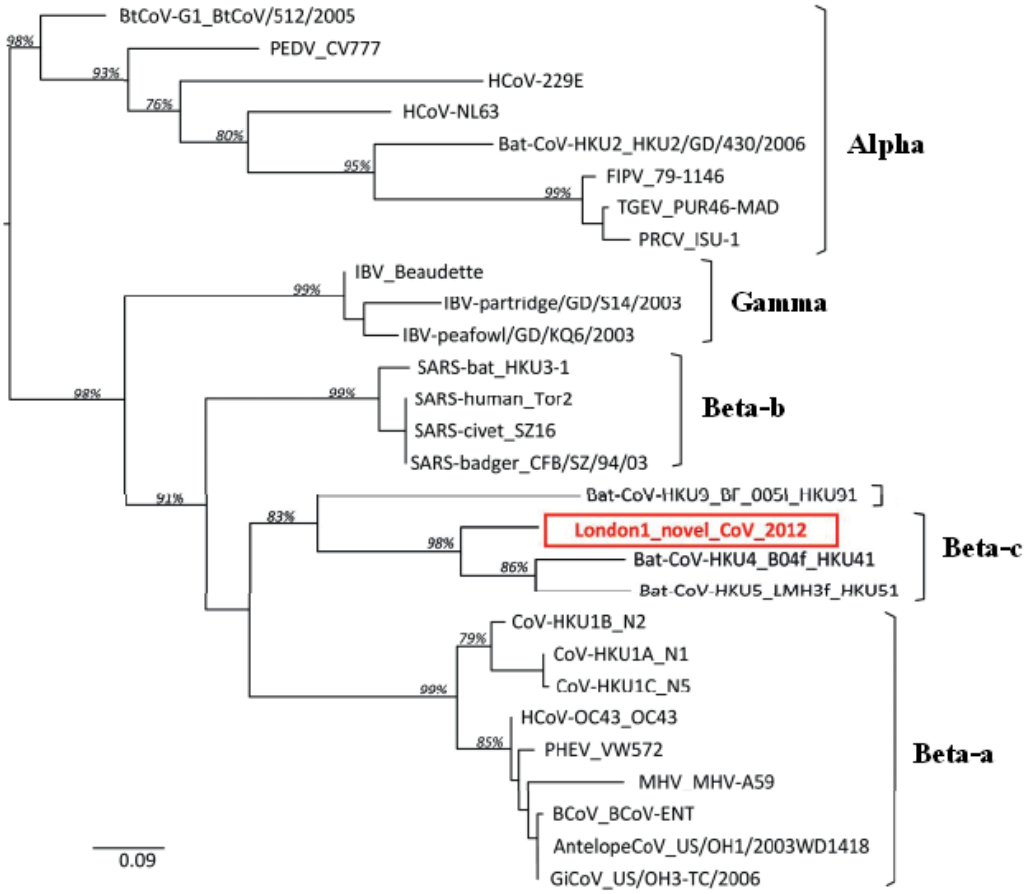

Figure 2: Phylogenetic tree of partial sequences from the polymerase gene (nsp12) of coronaviruses [Modified from Bermingham *et al*, 2012]

Coronaviruses can attach to host cellular receptors by the spike proteins on their surface [Blau *et al*, 2001]. CD13 (human aminopeptidase N) is the cellular receptor for HCoV-229E [Yeager *et al*, 1992] whereas angiotensin-converting enzyme 2 (ACE2) is the entry receptor for HCoV-NL63 and SARS-CoV [Hofmann *et al*, 2005]. The receptors for HCoV-OC43 and HCoV-HKU1 are still unknown [Wevers *et al*, 2009]. Internalization into host cells occurs by direct fusion with the plasma membrane or by endocytosis. Post-translational proteolytic processes are important regulatory mechanisms. Polyproteins are then cleaved by viral proteases, facilitating assembly of subunit protein complexes that are responsible for replication and transcription [Pyrc *et al*, 2004]. There is little information on the host response to coronavirus replication. Humoral immune responses are detectable following natural infection, but the role of cell-mediated immunity is largely unknown [Callow *et al*, 1990; Schmidt *et al*, 1981]. Coronaviruses have diverse animal hosts ranging from mammalian (including humans) to avian species. They also have a high frequency of recombination along with high mutation rates which may allow them to adapt to new hosts and ecological reservoirs. Transmission occurs through fecal-oral secretions and excretions. The viruses are fairly fragile and survive outside the body for only around 24 hours. They are easily destroyed by the usual detergents and cleaning agents.

According to epidemiological studies in adults, coronaviruses were estimated to cause ~15% of adult common colds [McIntosh *et al*, 1970]. Coronaviruses were found to cause epidemics every 2 to 3 years, with re-infections being common [Monto, 1974]. All ages are susceptible for viral infection. Coronaviruses were found associated with respiratory illnesses, usually in the upper respiratory tract, but occasionally causing pneumonia. In temperate climates, HCoV-OC43 and HCoV-229E are transmitted primarily during the winter. The elderly are also prone to these infections and are a cause of hospitalization [Falsey *et al*, 1997; Falsey *et al*, 2002]. In Hong Kong, coronaviruses were detected in 2.1% of patients admitted to the hospital with signs and symptoms of acute respiratory illness. Of the 87 infected patients, 13 were positive for HCoV-HKU1, 17 were positive for HCoV-NL63, 53 were positive for HCoV-OC43, and 4

were positive for 229E. HCoV-HKU1 and HCoV-OC43 peaked in the winter months. Upper respiratory tract illness was the most common presentation for HCoV-HKU1 infections. HCoV-NL63 infections occurred in early summer and fall but not in winter [Esper *et al*, 2006]. HCoV was identified in 5.4% of specimens from 279 hospitalized adult patients with lower respiratory tract infections [Garbino *et al*, 2006]. The most frequently identified isolates were HCoV-OC43 in 12, followed by HCoV-229E in 7, HCoV-NL63 in 6, and HCoV-HKU1 in 4 specimens. Many patients had high-risk underlying conditions.

Polyomaviruses

Polyomaviruses are small (40–50 nanometers in diameter) DNA viruses belonging to the *Polyomaviridae* family. The family name *Polyomaviridae* derives from the original observation that the first virus member of this family could induce multiple (poly) tumors (oma) in mice. They are non-enveloped icosahedral particles containing a circular double stranded DNA genome of approximately 5000 base pairs in length (Table 1). The genome can be divided into three functional regions: the early region encodes regulatory proteins involved in viral DNA replication and gene expression, the late region encodes the capsid proteins, and the non-coding region triggers the origin of replication and transcription control elements [Imperiale *et al*, 2007]. They can infect various host species such as birds, rodents and primates. Currently, 9 human polyomaviruses have been identified.

Table 1: Comparison of genome organization and coding regions of the human polyomaviruses [Van Ghelue *et al*., 2012]

HPyV	Accession number	Genome	LT-ag	st-ag	Agnoprotein	VP1	VP2	VP3
JCV	NC_001699	5130	688	172	71	354	344	225
BKV	NC_001538	5153	695	172	66	362	351	232
KI	NC_009238	5040	641	191	Absent	378	400	257
WU	NC_009539	5229	648	194	Absent	369	415	272
MCPyV	NC_010277	5387	817	186	Absent	423	241	196
HPyV6	NC_014406	4926	669	190	Absent	387	336	215
HPyV7	NC_014407	4952	671	193	Absent	380	329	209
TSPyV	NC_014361	5232	698/692	199	Absent	376	313	195
HPyV9	NC_015150	5026	680	189	Absent	371	352	233

The early human polyomaviruses: JC polyomavirus (JCPyV) and BK polyomavirus (BKPyV) were isolated four decades ago from the brain of a Hodgkin lymphoma patient with the initials J.C. who suffered from progressive multifocal leukoencephalopathy (PML) [Padgett *et al*, 1971] and from the urine of a kidney transplant recipient with the initials B.K., respectively [Gardner *et al*, 1971]. JCPyV is the etiological agent of PML, whereas BKPyV is associated with urinary tract pathologies in transplant patients [Jiang *et al*, 2009; Brew *et al*, 2010]. Both viruses have oncogenic potentials in animal models and cell culture, and viral DNA/RNA/proteins can be detected in human tumors [Gjoerup *et al*, 2010]. Recently, several novel human polyomavirus (HPyV) have been identified. In 2007, the KI polyomavirus (KIPyV) and WU polyomavirus (WUPyV) were detected and characterized in nasopharyngeal aspirates by researchers at the Karolinska Institute and at the Washington University, respectively [Allander *et al*, 2007; Gaynor *et al*, 2007]. In 2008, Merkel cell polyomavirus (MCPyV) was discovered in Merkel cell carcinoma (MCC) [Feng *et al*, 2008]. The presence of this virus has since then been confirmed in 80% of MCC examined, and MCPyV is considered as a causative factor for MCC [Chang *et al*, 2012]. In 2010, the novel HPyV6 and HPyV7 from skin swabs of healthy individuals were isolated. Seroprevalence was 69% for HPyV6 and 35% for HPyV7 in 95 individuals tested [Schowalter *et al*, 2010]. HPyV6 and HPyV7 have not been clearly associated with any human disease. Another new HPyV was identified in a boy suffering from trichodysplasia spinulosa (TS), a rare skin disease characterized by the development of follicular papules and keratin spines known as spicules [van der Meijden *et al*, 2010]. Complete sequencing of the viral genome confirmed that this virus is a new HPyV, and thus it was called TS-associated polyomavirus (TSPyV) [van der Meijden et al, 2010]. For the moment, HPyV9 is the last member to join the family of HPyV. Viral DNA sequences were amplified from the serum of a kidney transplant patient using degenerate primers against conserved regions of VP1 gene in the PyV [Scuda et al., 2011].

Recently, 4 human polyomaviruses including KIPyV, WUPyV, MCPyV and HPyV9 were detected in the respiratory tract specimens of patients with respiratory symptoms [Allander *et al*., 2007; Gaynor *et al*., 2007; Goh *et al*., 2009; Babakir-Mina *et*

al.,2010; Csoma *et al*., 2012]. KIPyV DNA was detected in 6/637 (1%), 24/951 (2.5%), and 1/222 (0.45%) nasopharyngeal specimens, respectively [Allander *et al*., 2007; Bialasiewicz *et al*., 2007; Babakir-Mina *et al*., 2008]. WUPyV DNA was amplified in 43/2135 (2%) nasopharyngeal aspirates [Gaynor *et al*., 2007]. MCPyV DNA was detected at a variable frequency in 3 of 140 (2.1%) and 27 of 635 nasopharyngeal aspirates (NPAs) (4.25%), respectively [Kantola *et al*., 2009; Goh *et al*., 2009]; two of 106 (1.9%) nasal swabs [Kantola *et al*., 2009], and seven (1.3%) of 526 respiratory tract samples from Australian patients with upper respiratory symptoms [Bialasiewicz *et al*., 2009]. Finally, MCPyV DNA was amplified in 15 (17.24%) of 87 lower respiratory tract samples from hospitalized Italian patients with lower respiratory tract symptoms [Babakir-Mina *et al*., 2010]. HPyV9 DNA was detected in 2 (2%) of 100 respiratory samples from pregnant women as well as 2 (2%) of 100 respiratory samples obtained from non-pregnant women [Csoma *et al*., 2012]. The presence of KIPyV, WUPyV, MCPyV and HPyV9 in the respiratory tract raises questions about the mode of transmission and respiratory pathogenicity of this newly described polyomavirus. Further studies are needed before the role of these new polyomaviruses as respiratory pathogens can be confirmed

Therefore, it is important to study and identify these novel viruses in Thailand. The epidemiology and molecular characterization of these newly described viruses will help us to understand the roles of these novel virus strains in respiratory disease and to develop better intervention strategies. The present study describes the epidemiology and molecular characterization of human coronavirus and human polyomaviruses in nasopharyngeal swabs and nasopharyngeal suctions of Thai patients with respiratory tract infection during 2012-2013

วิธีการทดลอง **(Methodology)**

The protocol for this study was approved by the Institutional Review Board (IRB No. 388/56 and 457/56), Faculty of Medicine, Chulalongkorn University and followed the International guidelines for human research protection established by the Declaration of Helsinki.

Clinical samples

Patient identifiers including personal information (name, sex, age,) and the hospitalization number were removed from these samples to protect patient privacy. The study were collected samples from patients with influenza-like illness. Nasopharyngeal swabs (NPS) were collected from patients presenting upper respiratory tract infections to the Bangpakok 9 International Hospital and Chum Phae Hospital (Khon Kaen, Thailand) from January 2012 to December 2013. Nasopharyngeal aspirates (NPA) were collected from patients presenting lower respiratory tract infections admitted to King Chulalongkorn Memorial Hospital and Chon Buri Hospital. All samples were collected into the viral transport medium and tested at the Center of Excellence in Clinical Virology, Faculty of Medicine, Chulalongkorn University. Symptoms, history of illness, results of clinical examination and laboratory investigations, and demographic data were recorded for each patient using a standardized form.

RNA extraction and cDNA synthesis

Viral RNA was extracted from 200 µL of NP swab sample using HiYield™ Viral Nucleic Acid Extraction Kit (RBC Bioscience, Taipei, Taiwan). The eluted RNAs were stored immediately at -70°C until use and subsequently reverse transcription (RT) was carried out with random hexamers and ImProm-II™ Reverse Transcriptase (Promega, Madison, WI) according to the manufacturer's instruction. Briefly, RNAs (5 µl) was incubated with 10 µM random hexamer primers (6 µl) at 70°C for 5 minutes, chilled on ice for 5 minutes, and mixed with 12.5-15 µl of ImProm-II ™ Reverse Transcriptase. The first strand cDNA synthesis was extended for 2 hours at 42°C. Reverse transcriptase was then heat-inactivated at 70°C for 15 minutes. The cDNA was immediately used for amplification or stored at -20°C. All the specimens were positive for GAPDH which served as an internal control.

Coronavirus Detection

A panel of respiratory viruses commonly found in the respiratory tract was used to determine the specificity of the semi-nested RT-PCR. Nucleic acids were extracted from samples for detection of influenza A virus [subtype H1N1 (pandemic 2009), H3N2], influenza B virus, respiratory syncytial virus (RSV), human parainfluenza (HPIVs) and human adenovirus (HAdV) only these respiratory viruses were screened. This study develop method to amplify the HCoV was used to determine of the semi-nested reverse transcription polymerase chain reaction (semi-nested RT-PCR) assay targeting the RNA-dependent RNA polymerase (RdRp) gene for HCoVs screening and N gene for detection of MERS-CoV infection was described previously [Corman *et al*., 2012]. The details of the primers are shown in Table 2. In addition to the primers, each PCR mixture (25 µl) contained cDNA and Perfect *Taq*Plus Master Mix kit (5 prime GmbH, Hamburg, Germany). The mixtures were amplified by a thermocycler (Mastercycler® Personal; Eppendorf AG, Hamburg, Germany) by applying the following conditions: initial denaturation at 94°C for 3 min, followed by 40 cycles each at 94°C for 30 seconds, 55-58°C for 30 seconds, and 72°C for 40 seconds. The final extension step was at 72°C for 7 min. The amplified products were detected using a 2% agarose gel electrophoresis stained with ethidium bromide. The amplification of the RdRp gene yields a 530-bp product for the first PCR and a 454 bp product for the second PCR, while the amplification of the N gene yields a 310-bp product for the first PCR and a 263-bp product for the second PCR.

HCoV genotyping using S gene amplification

After classifying HCoV genotype by BLAST analysis of the RdRp gene, positive samples were amplified by nested RT-PCR with the spike (S) gene genotype-specific primers (Table 2) [Suwannakarn *et al*., 2014]. The first PCR reaction mixture contained 1 µl of cDNA and second PCR reaction contained 1 µl of the first PCR product. The reaction volume also contained 0.5 µM forward and reverse primers and nuclease free water in a final volume of 25 µl. Both rounds of PCR were performed under the following conditions: denaturation at 94°C for 3 min, followed by 40 amplification cycles

consisting of denaturation at 94°C for 30 sec, primer annealing at 50°C for 30 sec followed by extension at 72°C for 90 sec, and a final extension at 72°C for 7 min.

Detection of HPyV by semi-nested PCR amplification

DNA was extracted from 100 µL of NP suction using a HiYield^{TM} Viral Nucleic Acid Extraction kit (Real Genomics, USA), according to manufacturer protocol**.** Semi-nested PCR amplification within LTAg of HPyV was performed using specific primers (Table 3). The PCR reaction mixture comprised 1 µl of DNA, 2.5 µl of 10xPCR buffer minus Mg, 0.5 µl of 10 mM dNTPs mixture, 0.75 µl of 50 mM $MgCl_2$, 0.5 µM of each primer, and 19.25 µl of distilled water for a final volume of 25 µl. Thermal profiles are described, as follows: initial denaturation at 94^{o}C for 3 minutes; followed by, 40 amplification cycles consisting of 94^{o}C for 30 seconds, 55^{o}C for 30 seconds, and 72^{o}C for 1.30 minutes; and, a final extension at 72^{o}C for 7 minutes. Positive and negative controls were included in each run to ensure suitable detections.

Gel electrophoresis and nucleotide sequencing

PCR products were separated by 2% agarose gel electropholysis and then visualized by ethidium bromide staining under UV transillumination. The PCR amplified products were then purified using HiYield^{TM} Gel Extraction (RBC Bioscience, Taiwan). Nucleotide sequencing was then performed by First BASE Laboratories Sdn Bhd, Selangor, Malaysia.

Nucleotide sequences analysis

Nucleotide sequences were analyzed using the BLAST analysis tool (http://www.ncbi.nlm.gov/BLAST). Complete genome sequences were assembled using the contig assembly program (CAP) and aligned using ClustalW software, and implemented using the BioEdit Sequence Alignment Editor (version 7.0.4.1).

Phylogenetic analysis

Phylogenetic trees were constructed by neighbor-joining (NJ) method with bootstrap (1000) and Tamura-Nei nucleotide substitution model implemented in Molecular Evolutionary Genetics Analysis (MEGA) program version 5.2 (http://www.mybiosoftware.com/phylogenetic-analysis/2334).

Table 2. Primers for amplification of CoV.

Gene	Primer	Genotype	Sequence (5' to 3')*	PCR Application
RdRp	SP6-CoV_16053_F	Pan CoV	ATTTAGGTGACACTATAGGGTTGGGAY TAYCCTAARTGTGA	First & second round
	CoV-16594_R		TAYTATCARAAYAATGTCTTTATGTC	First round
	CoV-Pan_16510_R		TGATGATGGNGTTGTBTGYTATAA	Second round
S	HCoV-S229E_F1	229E	GTGGGTGCACTACCTAAGAC	First round
	HCoV-S229E_R1		CGTGGTTGAACAGCAATTATAGAACC	
	HCoV-S229E_F2		GAGTTTGTTATTTCACGCACAGGAC	Second round
	HCoV-S229E_R2		CCATCTGCACAAACGCCAAAAC	
	HCoV-SHKU1_F1	HKU1	TCACCTCTTAATTGGGAACGTA	First round
	HCoV-SHKU1_R1		CATTAGAACAAGTGGTGCCAC	
	HCoV-SHKU1_F2		GATTTGCAGTTGGGCAGTTCTGG	Second round
	HCoV-SHKU1_R2		AAAGGCATCAGGACTACAAA	
	HCoV-SNL63_F1	NL63	GACACCACAATACCTTTTGG	First round
	HCoV-SNL63_R1		CTGGTTGGTTACATGGTGTCAC	
	HCoV-SNL63_F2		CATGTTAGCACTTTTGTGGGT	Second round
	HCoV-SNL63_R2		CCACCAGCAAGTGACTGGTTTG	
	HCoV-SOC43_F1	OC43	GTCGGTGCCCTCTCCATTAAATT	First round
	HCoV-SOC43_R1		GGCCGCAGAAACACGAC	
	HCoV-SOC43_F2		AATATGAGCAGCCTGATGTC	Second round
	HCoV-SOC43_R2		CCGAAATAGCAATGCTGGTTC	
N	NSeq-Fwd	MERS	CCTTCGGTACAGTGGAGCCA	First round
	NSeq-Fnest		TGACCCAAAGAATCCCAACTAC	Second round
	NSeq-Rev		GATGGGGTTGCCAAACACAAAC	First & second round

Table 3. Primers for amplification of HPyV.

Primer Name	Types of HPyV	Sequence (5' to 3')	PCR Application
KI/WU_4337F	KI / WU	CATTATTAACWCCTTTACARAATAA	First round
KI/WU_4390F		AAGTTATTAAYAGCACTAACTCTATG	Second round
SP6 KI/WU_4585R		GATTTAGGTGACACTATAGTGTCWCAWGCTGTATTTAGTAATA	First & second round
HPyV9_4180F	HPyV9	GTTTAATAACAGCTTTACAATGAAT	First round
HpyV9_4233F		AAATGTTTTACAGCAGAAACTCTA	Second round
SP6_HpyV9_4443R		GATTTAGGTGACACTATAGTAAGTCATGCTATCTATAGTAATA	First & second round
MCPyV _4180F	MCPyV	CAAATCTAAGAGATTCCCTGGA	First round
MCPyV _4231F		AAGAATTCTTCAAAGTGGAACCA	Second round
SP6_MCPyV_4443R		GATTTAGGTGACACTATAGCCTCAATAAGAATATTGAGCAG	First & second round

ผลการทดลอง (Results)

Prevalence of HCoV Infections

To examine the proportion of respiratory illness associated with viral infections, clinical samples from NPS (n=5,196) and NPA (n=637) were obtained between January 2012 and December 2013 (Figure 3). Samples were collected from patients diagnosed with influenza-like illness. During this two-year period, it was observed that respiratory illness peaked between July and October, which coincided with the rainy season. Among the 5,833 samples analyzed, only these respiratory viruses were screened influenza A virus was detected in 637 patients (10.92%), influenza B virus was detected in 206 patients (3.53%), respiratory syncytial virus A was detected in 201 patients (3.45%), respiratory syncytial virus B was detected in 91 patients (1.56%), and adenovirus was detected in 78 patients (1.33%). Forty-six samples (0.79%) tested positive for HCoV by RT-PCR. Co-infection with other respiratory viruses was not observed in these HCoV-positive samples.

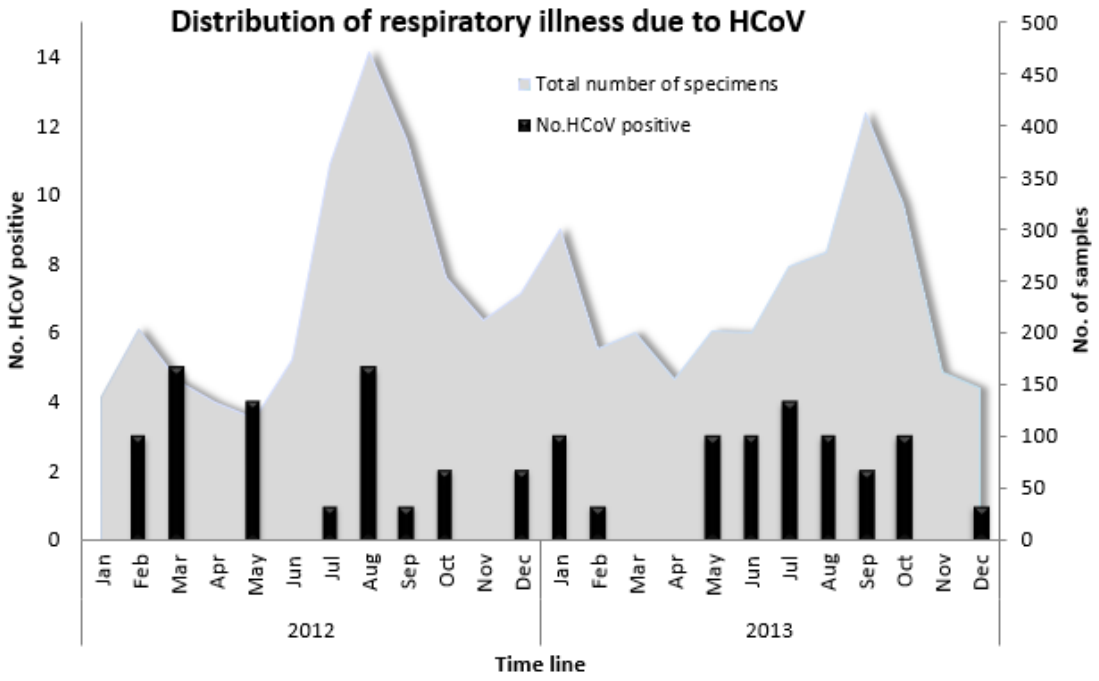

Figure 3. Seasonal distribution of HCoV infection from January 2012 to December 2013. Gray peaks represent the total number of specimens examined (right scale). Black bars represent the number of cases positive for HCoV (left scale).

Amongst the HCoV-positive cases, 56.52% were male and 43.48% were female (gender ratio 1.3:1) (Table 4). HCoV infection was detected in all age groups, and the mean age of HCoV infected patients was 21.37 years (min. = 4 mo., max. = 93 yr., mean =27.04). On an annual basis, the percentage of HCoV infection per year was 0.81% (23/2,838) in 2012 and 0.77% (23/2,995) in 2013. There were no seasonal peaks associated with HCoV and no positive cases were found in the typically dry months of April and November during both years.

Table 4. Demographic characteristics of participants

Characteristic	Specimens	
	No. specimens	Positive HCoV (%)
Gender		
Male, n (%)	2,935 (50.31)	26 (56.52)
Female, n (%)	2,898 (49.69)	20 (43.48)
Age(y)		
Median	11	8.5
Mode	1	1
Mean (SD)	19.57 (19.93)	21.37 (27.04)
Age group		
0-5 y (%)	2,197 (37.67)	25 (54.35)
6-10 y (%)	732 (12.55)	2 (4.35)
11-15 y (%)	538 (9.22)	6 (13.04)
16-30 y (%)	866 (14.85)	3 (6.25)
31-60 y (%)	1,102 (18.89)	3 (6.25)
>60 y (%)	397 (6.82)	7 (15.22)
Provinces		
Bangkok, n (%)	3,292 (56.45)	17 (36.96)
Khon Kaen, n (%)	2,408 (41.29)	28 (60.87)
Chon Buri, n (%)	132 (2.26)	1 (2.17)

Numbers in parentheses indicate the percentages of positive infection in total samples.

The majority of HCoV (25/46 or 54%) were detected mainly in young children between the ages of 0-5 years (Figure 4, hatched bar), followed by 15% in the elderly aged over 60 years. Approximately 80% of the positive samples (37/46) were from the NS, while 20% (9/46) were from the NPA. Age-stratification of both positive NS and NPA samples revealed that 46% (Figure 4, white bar) and 89% (black bar) were in the 0-5 year age group, respectively. Finally, all samples were negative when tested for MERS-CoV N gene.

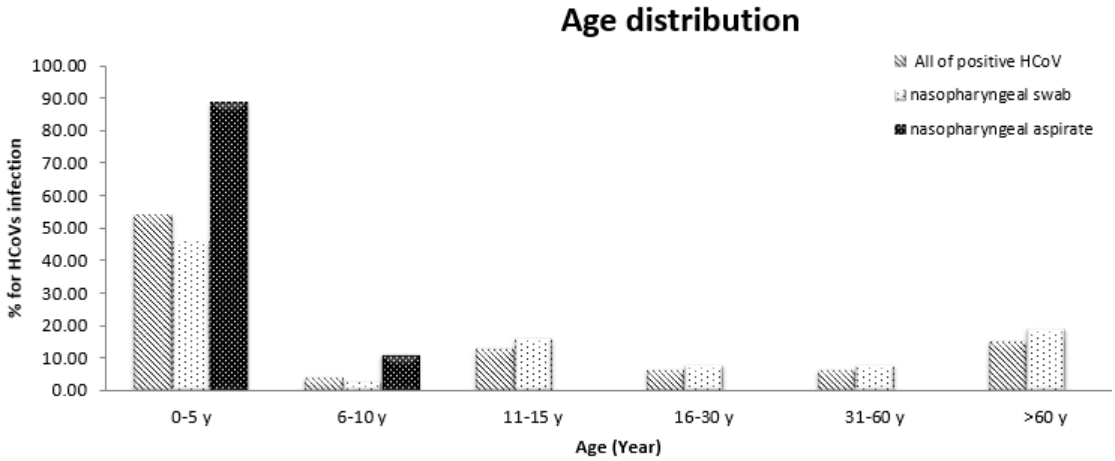

Figure 4. Age distribution of HCoV infection. Highest rate was detected among patients between 0-5 years old. Hatched bars represent the percentage of HCoV positive cases from the total number of specimens examined. White and black bars denote the percentage of positive results from nasopharyngeal swabs and aspirates, respectively.

To further differentiate the 46 samples of HCoV identified among the 5,833 samples, the S gene was sequenced. Analysis showed that these HCoV strains belonged to one of the four HCoV species. Among them, 19 (0.32%) were positive for HCoV-HKU1, 19 (0.32%) were positive for HCoV-NL63, 5 patients (0.09%) were positive for CoV-229E, and 3 (0.05%) were positive for HCoV-OC43. Therefore, relative to all HCoV-positive samples, the predominant genotypes were 41.3% for both HCoV-HKU1 and HCoV-NL63 (19/46) while other two minor strains were 11% HCoV-229E (5/46) and 6.5% HCoV-OC43 (3/46). NL63 and HKU1 appeared sporadically during the study period in which most cases were detected mainly in March 2012 and July 2013, respectively (Figure 5).

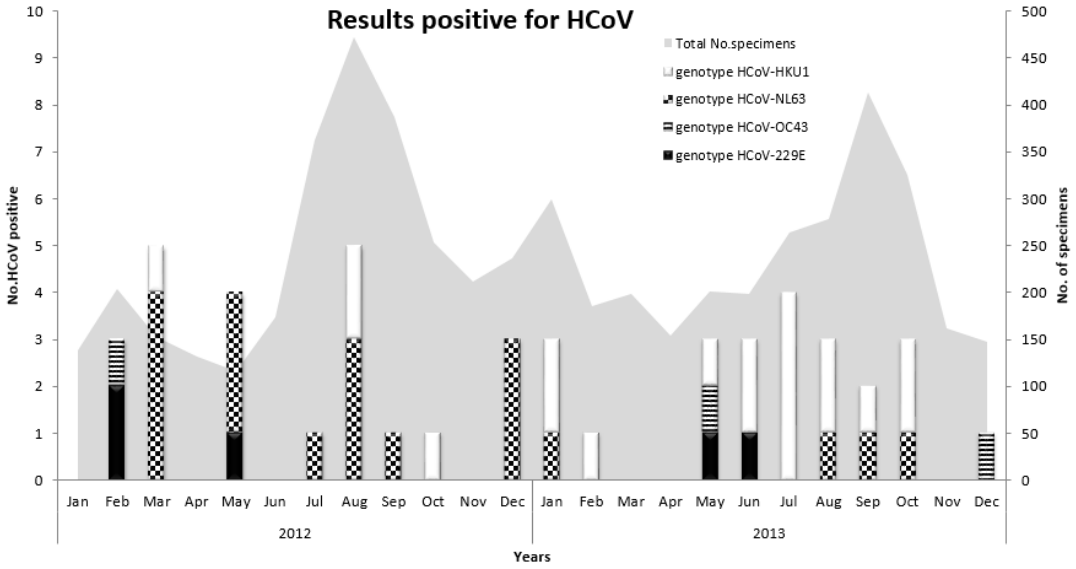

Figure 5. HCoV-positive samples obtained from patients during January 2012 to December 2013. Relative to the total number of specimen examined (gray peaks, right scale), 4 strains of coronaviruses (HKU1, NL63, OC43, and 229E) were found throughout the year (bars, left scale).

Clinical Characteristics of HCoV Infections

Clinical characteristics of the HCoV-infected patients are shown in Table 5. Of the 46 HCoV-positive patients, 38 (82.61%) had upper respiratory tract infection (URTI). These are illnesses ARE caused by an acute infection which involves the upper respiratory tract such as the nose, sinuses, pharynx or larynx. The remaining 8 (17.39 %) had lower respiratory tract infections (LRTI) as defined by pneumonia, bronchiolitis, and acute infection of the pulmonary parenchyma. The most common clinical manifestations were fever (body temperature greater than 38 ºC) and rhinorrhea. Several patients experienced tachypnea as defined by The World Health Organization (age-related definitions of tachypnea are as follows: younger than two months: >60 breaths/min, two to twelve months: >50 breaths/min, one to five years: >40 breaths/min and ≥ five years: >20 breaths/min). Some patients experienced hypoxemia, which refers to the oxygen saturation (SpO2) level below 95 percent. For signs of respiratory distress, they include retractions (subcostal, intercostal, suprasternal), nasal flaring, and grunting. Abnormal breath sound refers to the crepitation, rhonchi and wheezing.

Table 5. Clinical characteristics of patients with human coronavirus (HCoV) infection.

Characteristic	Number of positive HCoV (%)			
	HCoV-229E	HCoV-OC43	HCoV-NL63	HCoV-HKU1
Total no. of patients	5	3	19	19
URTI	5 (100)	2 (66.67)	16 (84.21)	15 (78.95)
LRTI	0	1 (33.33)	3 (15.79)	4 (21.05)
Clinical symptom				
Fever	5 (100)	3 (100)	18 (94.74)	16 (84.21)
Cough	2 (40)	2 (66.67)	11 (57.89)	10 (52.63)
Sputum	0	1 (33.33)	5 (26.32)	2 (10.53)
Rhinorrhea	4 (80)	2 (66.67)	16 (84.21)	17 (89.47)
Vomiting	3 (60)	0	10 (52.63)	12 (63.16)
Tachypnea	0	1 (33.33)[a]	6 (31.58)	7 (36.84) [a]
Hypoxemia	1 (20)	1 (33.33) [a]	5 (26.32)	5 (26.32)
Signs of respiratory distress	0	1 (33.33) [a]	6 (31.58)	7 (36.84) [a]
Abnormal breath sounds	0	1 (33.33) [a]	6 (31.58)	7 (36.84) [a]

The numbers in parentheses indicate the percentages of positive infection in total samples.

Molecular characterization of HCoV genotypes

To assess the relationship among the strains identified, the S gene of HCoV-positive samples was sequenced to determine changes to the surface protein, which represents the antigenic determinant of the virus and correlates to strain evolution. Then phylogenetic trees were constructed based on the alignment analysis of the S gene (Figure 6). The HCoV-NL63 strains isolated in this study were related closely to NL63-Amsterdam 496 and NL63-DEN/2009/15, which belong to clade B [Dominguez *et al*., 2012].

Although HCoV-HKU1 can be divided into clade A, B and C, phylogenetic analysis showed that the HCoV-HKU1 samples from this study belonged to clades A and B (Figure 6). Furthermore, the S gene shared ˜99.6% identity with the other group A HCoV-HKU1 isolates [Pyrc *et al*., 2010]. Comparison of the HCoV-229E strains in GenBank and HCoV-229E identified in this study yielded five cluster groups (Figure 6). Based on the nucleotide sequence, the CU isolates clustered together with the 229E-N04 strain of the Shanghai variant isolated in 2008. Finally, 3 isolates identified as HCoV-OC43 belonged to clades C and B.

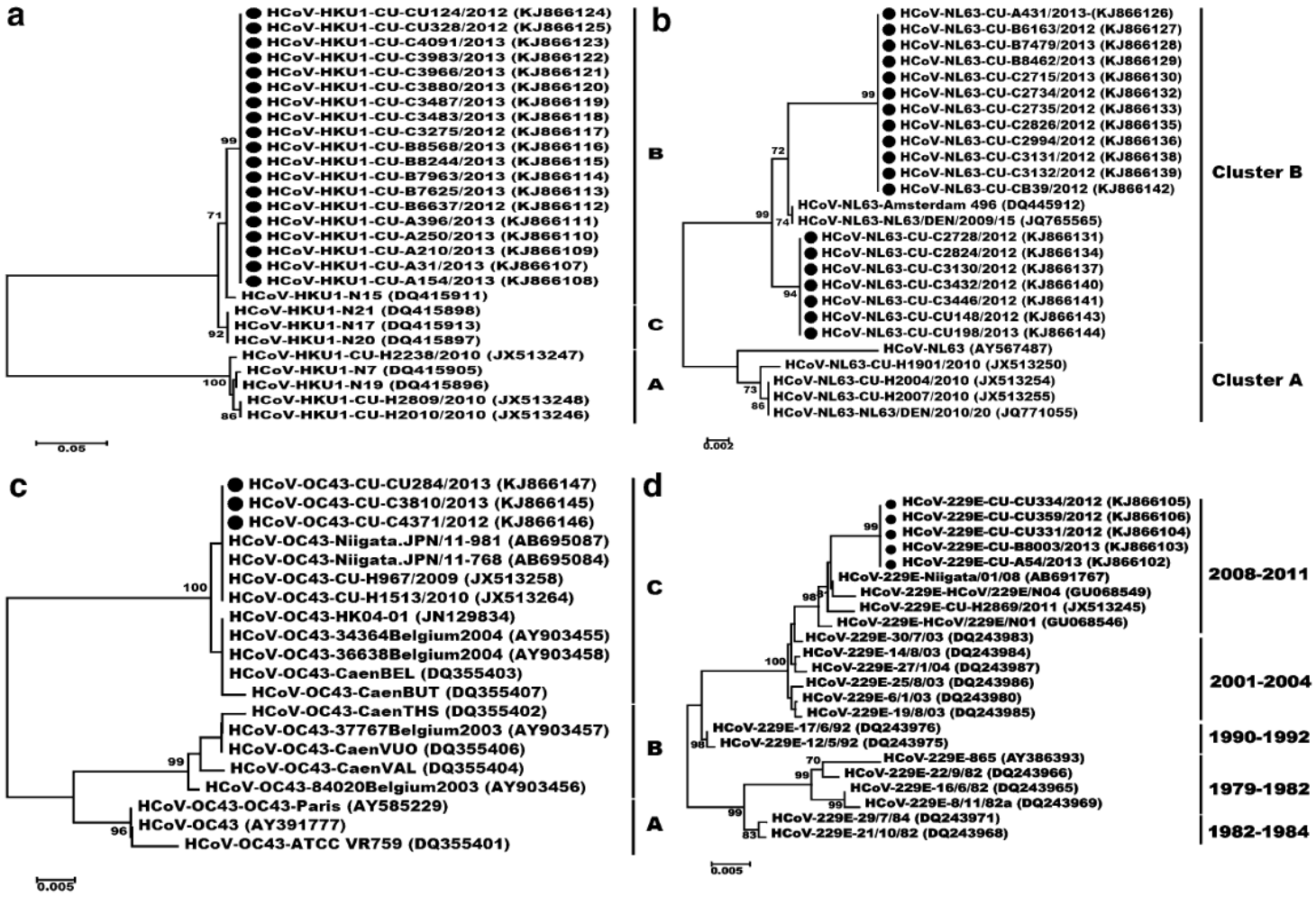

Figure 6. Phylogenetic trees of the S gene for 4 HCoV species. Phylogenetic trees were constructed based on nucleotide sequences of PCR products corresponding to the partial S gene of OC43, 229E, NL63, and HKU1, analyzed by MEGA 6.06 software using the distance method and the neighbor-joining algorithm with Kimura 2 parameters. Black dots indicate the isolates identified in this study. The node clusters were supported by bootstrap values > 80%.

Detection of HPyV

HPyV was detected by using semi-nested PCR and then characterized by whole genome sequencing. The nucleotides and deduced amino acid sequences were analyzed by multiple sequences alignment and phylogenetic tree. The result revealed that 0.16% (1/614) was positive for WU polyomavirus (WUPyV) whereas KIPyV, HPyV9 and MCPyV were not detected in this study. BLAST analysis confirmed that this positive sample was closely related to WUPyV. This sample was assigned as WUPyV isolate CU_Chonburi 3 and the complete genome was further characterized. Other samples were negative for HPyV, but were positive for GAPDH internal control; a result indicating appropriate sample collections and DNA extraction processes.

Complete genome analysis of WU polyomavirus

The genome of WUPyV (isolate CU_Chonburi 3) was closely related to the reference sequence of WUPyV (NC_009539), with 99% similarity. The genomes were then further compared by using the SimPlot software program (Figure 7). The result revealed that WUPyV (CU_Chonburi 3) was slightly different from WUPyV (NC_009539), as follows: non-coding region (positions 100-350); VP2 (positions 850-1,000); LTAg (positions 3,500-3,700); and, STAg (positions 4,650-4,800). The complete genome of WUPyV (CU_Chonburi 3) was then aligned with several WUPyV whole genome sequences from several countries, including Australia, USA, Germany, China, and Thailand during the timeframe of 2007-2011. Table 5 describes several nucleotide variations within non-coding regions, to include positions 37, 67, 73, 95, 130, 152, 173, 177, 180, 181, 206, 275, 293, 294, 350, 451, 499, 4522, and 5211. Table 6 illustrates amino acid changes in VP1 (position S347T); VP2 (positions L40V, G120R, Y121I, P123R, G127S, L137F, Q287R, and A327V); LTAg (positions Q357P, V369E, E377K, D378V, A381T, R382E, R383G, and D389G); and, STAg (positions R139S, K141E, R148K, and W153C).

Table 5. Nucleotide variations within non-coding regions of WU polyomavirus

Isolate name	**Country**	**Year**	**Nucleotide variations within non-coding regions** (Position refers to NC_009539 WU Ref strain)																	**Accession no.**
			37	67	73	95	130	152	173	177	180	181	206	275	293	294	350	451	499	4522	5211	
WU Ref strain	Australia	2007	g	g	g	g	c	g	c	c	g	g	a	a	t	a	c	c	c	a	g	NC_009539
S5	USA	2007	g	g	g	g	c	g	c	c	g	g	a	a	t	a	c	c	c	**g**	**a**	EF444554
CU-295	Thailand	2008	g	g	g	g	c	g	c	c	g	g	a	a	t	a	c	c	c	**g**	**a**	EU358768
CU-302	Thailand	2008	g	g	g	g	c	g	c	c	g	g	a	a	t	a	c	c	c	**g**	g	EU358769
CLFF	China	2008	g	g	g	g	c	g	c	c	g	g	a	a	t	a	c	c	c	a	g	EU296475
GD-WU709	China	2009	g	g	g	g	c	g	c	c	g	g	a	a	t	a	c	c	c	**g**	**a**	GQ926980
Rochester-7029	USA	2009	g	g	g	g	c	g	c	c	g	g	a	a	t	a	c	c	c	**g**	**a**	FJ794068
Wuerzburg	Germany	2009	g	g	g	g	c	g	c	c	g	g	a	a	t	a	c	c	c	**g**	**a**	EU711058
O91	Australia	2010	g	g	g	g	c	g	c	c	g	g	a	a	t	a	c	c	c	**g**	**a**	GU296363
MN2726	Australia	2010	g	g	g	g	c	g	c	c	a	g	a	a	t	a	c	c	c	**g**	**a**	GU296405
O3	Australia	2010	g	g	g	g	c	g	c	c	g	g	a	a	t	a	c	c	c	**g**	**a**	GU296408
FZ18	China	2011	g	g	g	g	c	g	c	c	g	g	a	a	t	a	c	c	c	**g**	**a**	FJ890981
CU_Chonburi 3	Thailand	2013	**c**	**c**	**a**	**c**	**a**	**t**	**a**	**a**	**t**	**a**	**c**	**g**	**g**	**g**	**a**	**t**	**t**	**g**	**t**	KJ725828

Table 6. Amino acid changes in VP1, VP2, LTAg, and STAg of WU polyomavirus

Isolate name	Country	Year	**Amino acid changes** (Position refers to NC_009539 WU Ref strain)																				Accession no.
			VP1	**VP2**								**LTAg**								**STAg**			
			347	40	120	121	123	127	137	287	327	357	369	377	378	381	382	383	389	139	141	148	153	
WU Ref strain	Australia	2007	S	L	G	Y	P	G	L	Q	A	Q	V	E	D	A	R	R	D	R	K	R	W	NC_009539
S5	USA	2007	S	L	G	Y	P	G	L	Q	A	Q	V	E	G	A	R	R	D	R	K	R	W	EF444554
CU-295	Thailand	2008	S	L	G	Y	P	G	L	Q	A	Q	V	E	D	A	R	R	D	R	K	R	W	EU358768
CU-302	Thailand	2008	S	L	G	Y	P	G	L	Q	A	Q	V	E	D	A	R	R	D	R	K	R	W	EU358769
CLFF	China	2008	S	L	G	Y	P	G	L	Q	A	Q	V	E	D	A	R	R	D	R	K	R	W	EU296475
GD-WU709	China	2009	S	L	G	Y	P	G	L	Q	A	Q	V	E	D	A	R	R	D	R	K	R	W	GQ926980
Rochester-7029	USA	2009	S	L	G	Y	P	G	L	Q	A	Q	V	E	D	A	R	R	D	R	K	R	W	FJ794068
Wuerzburg	Germany	2009	**T**	L	G	Y	P	G	L	**E**	A	Q	V	E	D	A	R	R	D	R	K	**K**	W	EU711058
O91	Australia	2010	**T**	L	G	Y	P	G	L	Q	A	Q	V	E	D	A	R	R	D	R	K	**K**	W	GU296363
MN2726	Australia	2010	S	L	G	Y	P	G	L	Q	A	Q	V	E	D	A	R	R	D	R	K	R	W	GU296405
O3	Australia	2010	**T**	L	G	Y	P	G	L	Q	A	Q	V	E	D	A	R	R	D	R	K	R	W	GU296408
FZ18	China	2011	**T**	L	G	Y	P	G	L	Q	A	Q	V	E	D	A	R	R	D	R	K	R	W	FJ890981
CU_Chonburi 3	Thailand	2013	**T**	**V**	**R**	**I**	**R**	**S**	**F**	**R**	**V**	P	E	K	**V**	**T**	**E**	**G**	**G**	**S**	**E**	**K**	**C**	KJ725828

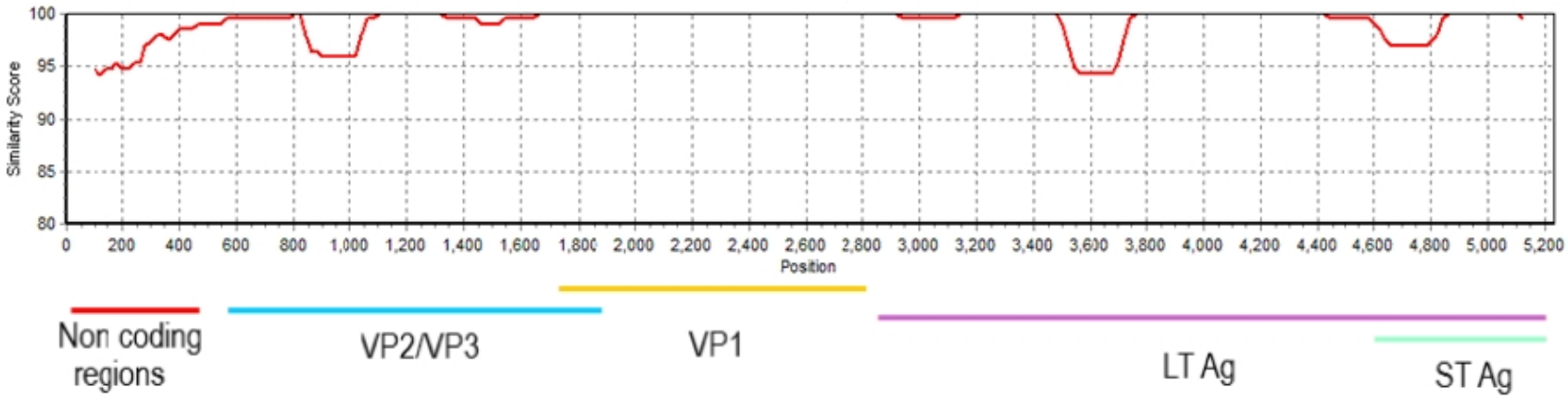

Figure 7. Similarity plot of complete genome sequences between WUPyV (CU_Chonburi 3) and WUPyV reference sequence (NC_009539)

Phylogenetic analysis

Phylogenetic trees were constructed based on analysis of nucleotide sequences within VP1, VP2, LTAg, and STAg. (Figure 8) The phylogenetic tree of the VP1 gene (Figure 8A) demonstrated that WUPyV (isolate CU_Chonburi 3) was closely related to previously described WUPyV, such as WUPyV reference sequence (NC 009539), isolate MN 2726 from Australia in 2010 (GU296405), and isolate CLFF from China in 2008 (EU296475). Conversely, phylogenetic trees obtained from the analysis of VP2 (Figure 8B), LTAg (Figure 8C), and STAg (Figure 8D), revealed that WUPyV (isolate CU_Chonburi 3) was quite unrelated to other strains of WUPyV.

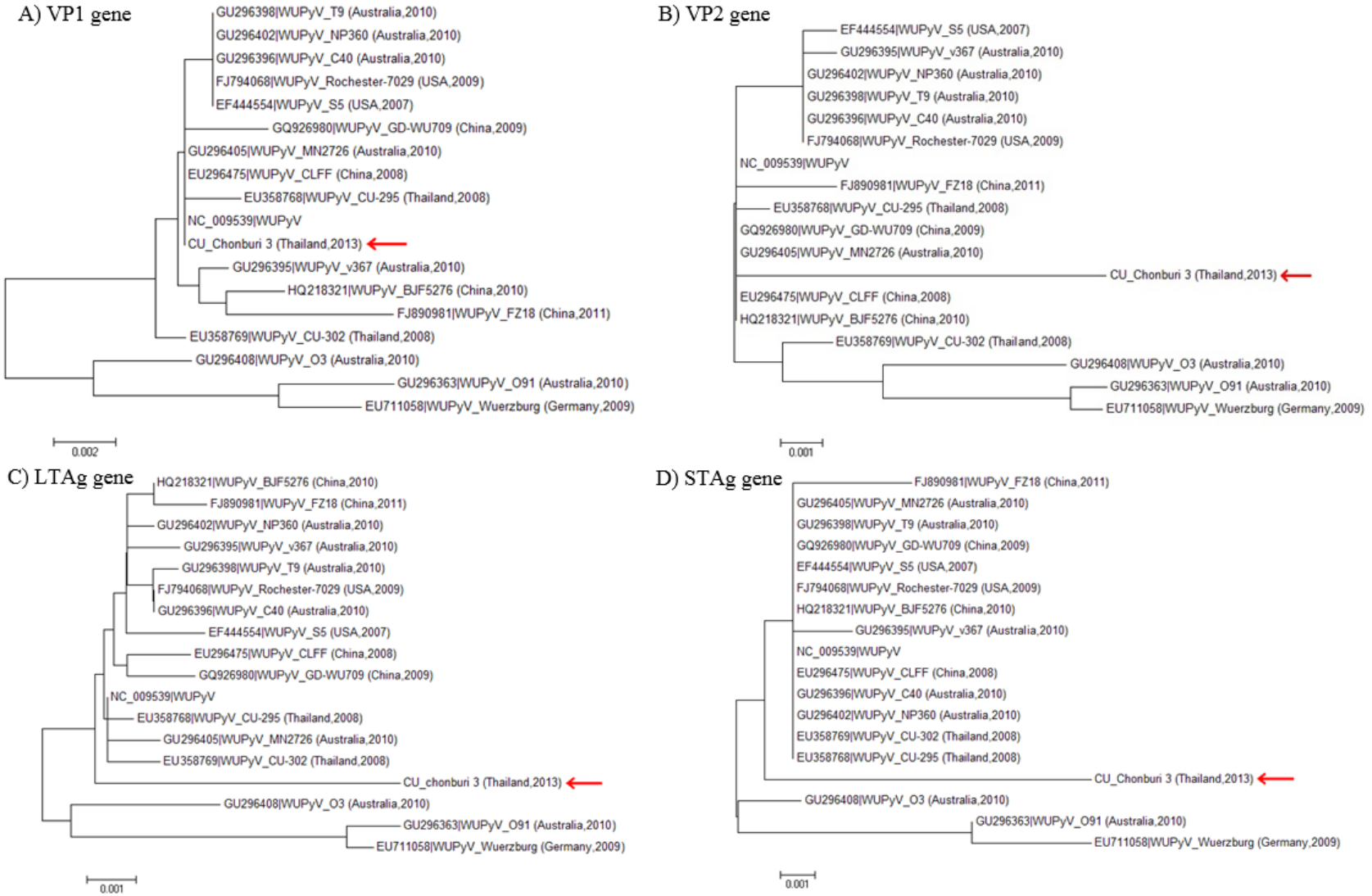

Figure 8. Phylogenetic analysis of WUPyV based on (A) VP1, (B) VP2, (C) LTAg, and (D) STAg genes.

บทวิจารณ์ (DISCUSSION)

Due to the awareness of MERS-CoV and other novel human coronavirus infections worldwide, this study aimed to characterize the circulation and prevalence of HCoV in Thailand from January 2012 to December 2013. The two types of specimens examined consist of 5,833 nasopharyngeal swabs and aspirate samples collected anonymously through the influenza surveillance project and viruses identified for acute respiratory tract infections using RT-PCR. From these samples, 0.79% (46/5,833) of the patients with influenza-like illness was positive for HCoV.

The prevalence of HCoV infection found in this study was lower than that of previous studies, in which detection of HCoV ranged from 2.1% to 5.7% [Gorse *et al*., 2009; Lau *et al*., 2006; Bellei *et al*., 2008; Pierangeli *et al*., 2007]. On the other hand, the rate of HCoV positive samples found in this study was more similar to the level of infection in countries such as mainland China (1%) [Ren *et al*., 2011] and United Kingdom (0.85%) [Gaunt *et al*., 2010]. Several factors may account for this disparity: (1) the subjects recruited in this study were adult patients whereas those in some other studies were mainly hospitalized children [Talbot et al., 2009; McIntosh et al., 1974] or adults with underlying diseases [Dare et al., 2007], (2) the viral infection rate obtained from nasopharyngeal swab used in this study may be lower than that of nasopharyngeal aspirates [Lau et al., 2006; Talbot et al., 2009], (3) differences in the study time frame and geographical area [Dominguez et al., 2009], and (4) differences in the techniques used for testing, such as the highly sensitive real-time PCR [Gaunt et al., 2010].

Although previous reports in Hong Kong and mainland Chinese population showed that HCoV-OC43 was the predominant strain found [Ren et al., 2011], only a few HCoV-OC43 infections were detected in the Thai population examined. A larger proportion of HCoV-NL63 and HCoV-HKU1 infections were also found. These differences may reflect our different geographical regions in which the samples were gathered (Khon Kaen, Chon Buri, and Bangkok), different years of collection (2012-2013) and the alternating pattern of viral seasonality in our study. This study indicates that in Thailand, HCoV-NL63 and HCoV-HKU1 infections peaked every other year, while HCoV-OC43 and HCoV-229E appeared less often. Furthermore, HCoV-NL63 was

found mainly in 2012 and HCoV-HKU1 was found mainly in 2013, and only a few cases of HCoV-229E and HCoV-OC43 appeared in the rainy season and winter season in 2012 and 2013. Previous studies conducted in Thailand also demonstrated annual fluctuations in the predominance of HCoV strains [Dare et al., 2007]. Previous reports have shown that the infections by 229E and OC43 strains are highest during the winter–spring seasons and can recur every 2–4 years [McIntosh et al., 1967; Shao et al., 2007; Monto and Lim, 1974]. Furthermore, comparing current PCR data from other parts of the world, the prevalence of the different HCoVs also appears to vary by year and location [Vabret et al., 2008; Gorse et al., 2009; Dominguez et al., 2009]. For instance, in France there was a relatively equal prevalence of HCoV-NL63 and HCoV-HKU1 [Vabret et al., 2008].

We found that HCoV was detected mainly in young patients between the ages of 0 -5 years (54.35%). HCoV infections elicited common symptoms such as fever, cough, sputum, rhinorrhea, headache, vomiting, muscle pain and sore throat. These symptoms were similar to those in other reports of HCoV infections [Ren et al., 2011; Dominguez et al., 2009]. However, the clinical presentations were slightly different among on each subtype of HCoV. In this study, vomiting was more common in HCoV-229E, NL63 and HKU1-positive patients but not in those infected by OC43 strains. Sputum production was also absent in HCoV-229E infections. During the study period, lower respiratory tract infections were found in individuals infected by HCoV-OC43, HKU1 and NL63, but not in those with HCoV-229E infections. Tachypnea, hypoxemia, abnormal breath sounds and signs of respiratory distress occurred less often in HCoV-229E infections. These clinical features associated with coronavirus infection appear to be similar to those observed with other respiratory viruses, such as RSV, parainfluenza virus and human metapneumovirus. Symptoms of upper respiratory tract infection such as rhinorrhea, sputum, and of lower respiratory tract infection such as tachypnea and abnormal breath sounds were frequently observed in our patients.

The simultaneous screening for common respiratory viruses allowed us to investigate co-infection of HCoV infected patients with other viral pathogens. Although co-infection with RSV and other pathogens has been previously described

[Theamboonlers et al., 2007], we did not find co-infection of HCoV-infected patients with other viral pathogens. It may be that HCoV and the other viral pathogens do not share a similar seasonal circulation. Additionally, the possibility of viral coinfection with bacteria cannot be ruled out. Nevertheless, confirmation of the underlying mechanism of co-infection will require good clinical sampling and further longitudinal studies conducted over several years.

Previous characterization of the genetic variation and evolution of HCoVs have utilized the whole viral genome, partial spike, the RdRp, or nucleocapsid gene. Here, the phylogenetic study of HCoVs was performed based on the sequences of partial spike gene. The S gene contains two subdomains: S1 region comprises the receptor binding site while the S2 region is essential for membrane fusion [Zheng et al., 2006]. Phylogenetic analysis using the S gene may be more discriminating than the RdRp gene [Lau et al., 2006]. Lau and co-workers [Lau et al., 2011] divided the human coronavirus subtype HCoV-OC43 into four sub-genotypes of A, B, C and D with genotype D most likely arising from recombination. Five Belgium strains from 2003 and Caen strain formed another cluster, clade B, while the other Niigata.JPN strains and isolate CU strain formed the third cluster, clade C. Only three samples isolated from this study were of the strain HCoV-OC43. Phylogenetic analysis showed that the two HCoV-OC43 samples isolated in this study were closely related to the clade C Niigata.JPN and isolate CU strains and one sample was closely related with genotype B, most likely Belgium 2003 strain.

Ten HCoV-HKU1 samples belonged to clade A and nine samples to clade B. None of the isolates in this study identified with clade C similar to a previous study [Lee et al., 2013]. For HCoV-NL63, genotypes A and B were identified previously in European clinical specimens [Fouchier et al., 2004]. Here, all 19 HCoV-NL63 isolates could be classified into clade B. Meanwhile, the genetic pattern of HCoV-229E appeared to be changing over time. Previously, the most recent isolates of HCoV-229E were assigned to the 2001-2004 cluster [Chibo and Birch, 2006]. However, isolates in this study formed a novel HCoV-229E cluster designated as 2008-2013 clade and whose sequences are most closely related to the recent strains in GenBank.

In summary, this study reports a large-scale, detailed analysis of the prevalence and clinical presentations of different HCoV infections in Thai patients for two years from 2012 to 2013. Although this study did not explain the factors contributing to the prevalence of HCoV, it demonstrated the distribution of HCoVs during this period. The results from this study should help to improve our understanding of the pathogenesis of HCoVs and provide information for evaluating the disease burden in the clinics and influence disease control policies. However, given that the study population was limited and the number of HCoV-positive samples studied was low, future investigations are needed to characterize the infections of the various HCoVs in patients more thoroughly including the types of sample used for HCoV detection. More importantly, vigilant surveillance and prevention of HCoV infection in early childhood will serve to minimize the overall hospitalization and morbidity in this vulnerable age group.

หนังสืออ้างอิง (References)

Allander T, Andreasson K, Gupta S, Bjerkner A, Bogdanovic G, Persson MA, Dalianis T, Ramqvist T, Andersson B. Identification of a third human polyomavirus. J Virol. 2007 Apr; 81(8):4130-6.

Babakir-Mina M, Ciccozzi M, Dimonte S, Farchi F, Valdarchi C, Rezza G, Perno CF, Ciotti M. Identification of the novel KI polyomavirus in the respiratory tract of an Italian patient. J Med Virol. 2008 Nov; 80(11):2012-4.

Babakir-Mina M, Ciccozzi M, Lo Presti A, Greco F, Perno CF, Ciotti M. Identification of Merkel cell polyomavirus in the lower respiratory tract of Italian patients. J Med Virol. 2010 Mar; 82(3):505-9.

Balboni A, Battilani M, Prosperi S. The SARS-like coronaviruses: the role of bats and evolutionary relationships with SARS coronavirus. New Microbiol. 2012 Jan; 35(1):1-16.

Bellei N, Carraro E, Perosa A, Watanabe A, Arruda E, Granato C. Acute respiratory infection and influenza-like illness viral etiologies in Brazilian adults. J Med Virol. 2008; 80:1824-1827.

Bermingham A, Chand MA, Brown CS, Aarons E, Tong C, Langrish C, et al. Severe respiratory illness caused by a novel coronavirus, in a patient transferred to the United Kingdom from the Middle East, September 2012. Euro Surveill. 2012 Oct 4; 17(40):20290.

Bialasiewicz S, Whiley DM, Lambert SB, Wang D, Nissen MD, Sloots TP. A newly reported human polyomavirus, KI virus, is present in the respiratory tract of Australian children. J Clin Virol. 2007 Sep; 40(1):15-8.

Blau DM, Holmes KV. Human coronavirus HCoV-229E enters susceptible cells via the endocytic pathway. Adv Exp Med Biol. 2001; 494:193–198.

Brew BJ, Davies NW, Cinque P, Clifford DB, Nath A. Progressive multifocal leukoencephalopathy and other forms of JC virus disease. Nat Rev Neurol. 2010 Dec; 6(12):667-79.

Callow KA, Parry HF, Sergeant M, Tyrrell DA. The time course of the immune response to experimental coronavirus infection of man. Epidemiol Infect. 1990; 105(2):435–446.

Chang Y, Moore PS. Merkel cell carcinoma: a virus-induced human cancer. Annual Review of Pathology. 2012; 7:123-44.

Chibo D, Birch C. Analysis of human coronavirus 229E spike and nucleoprotein genes demonstrates genetic drift between chronologically distinct strains. J Gen Virol. 2006; 87:1203-1208.

Corman VM, Muller MA, Costabel U, Timm J, Binger T, Meyer B, Kreher P, Lattwein E, Eschbach-Bludau M, Nitsche A, Bleicker T, Landt O, Schweiger B, Drexler JF, Osterhaus AD, Haagmans BL, Dittmer U, Bonin F, Wolff T, Drosten C. Assays for laboratory confirmation of novel human coronavirus (hCoV-EMC) infections. Euro Surveill. 2012; 17:pii, 20334.

Csoma E, Sápy T, Mészáros B, Gergely L. Novel human polyomaviruses in pregnancy: Higher prevalence of BKPyV, but no WUPyV, KIPyV and HPyV9. J Clin Virol. 2012;55(3):262-5.

Dare RK, Fry AM, Chittaganpitch M, Sawanpanyalert P, Olsen SJ, Erdman DD. Human coronavirus infections in rural Thailand: a comprehensive study using real-time reverse-transcription polymerase chain reaction assays. J Infect Dis. 2007; 196:1321-1328.

Dominguez SR, Robinson CC, Holmes KV. Detection of four human coronaviruses in respiratory infections in children: a one-year study in Colorado. J Med Virol. 2009; 81:1597-1604.

Dominguez SR, Sims GE, Wentworth DE, Halpin RA, Robinson CC, Town CD, Holmes KV. Genomic analysis of 16 Colorado human NL63 coronaviruses identifies a new genotype, high sequence diversity in the N-terminal domain of the spike gene and evidence of recombination. J Gen Virol. 2012; 93:2387-2398.

Esper F, Weibel C, Ferguson D, Landry ML, Kahn JS. Coronavirus HKU1 infection in the United States. Emerg Infect Dis. 2006; 12(5):775–779.

Falsey AR, McCann RM, Hall WJ, Criddle MM, Formica MA, Wycoff D, Kolassa JE. The "common cold" in frail older persons: impact of rhinovirus and coronavirus in a senior daycare center. J Am Geriatr Soc. 1997 Jun; 45(6):706-11.

Falsey AR, Walsh EE, Hayden FG. Rhinovirus and coronavirus infection-associated hospitalizations among older adults. J Infect Dis. 2002; 185(9):1338–1341.

Fauquet CM, Mayom A, Maniloff J, Desselberger U, Ball LA (Virus Taxonomy) ed.VIII Amsterdam: Elsevier academic press., 937-955.

Feng H, Shuda M, Chang Y, Moore PS. Clonal integration of a polyomavirus in human Merkel cell carcinoma. Science. 2008 Feb 22; 319(5866):1096-100.

Fouchier RA, Hartwig NG, Bestebroer TM, Niemeyer B, de Jong JC, Simon JH, Osterhaus AD. A previously undescribed coronavirus associated with respiratory disease in humans. Proc Natl Acad Sci U S A. 2004; 101:6212-6216.

Garbino J, Crespo S, Aubert JD, Rochat T, Ninet B, Deffernez C, Wunderli W, Pache JC, Soccal PM, Kaiser L. A prospective hospital-based study of the clinical impact of non-severe acute respiratory syndrome (Non-SARS)-related human coronavirus infection. Clin Infect Dis. 2006 Oct 15; 43(8):1009-15.

Gardner SD, Field AM, Coleman DV, Hulme B. New human papovavirus (B.K.) isolated from urine after renal transplantation. Lancet. 1971 Jun 19; 1(7712):1253-7.

Gaunt ER, Hardie A, Claas EC, Simmonds P, Templeton KE. Epidemiology and clinical presentations of the four human coronaviruses 229E, HKU1, NL63, and OC43 detected over 3 years using a novel multiplex real-time PCR method. J Clin Microbiol. 2010; 48:2940-2947.

Gaynor AM, Nissen MD, Whiley DM, Mackay IM, Lambert SB, Wu G, Brennan DC, Storch GA, Sloots TP, Wang D. Identification of a novel polyomavirus from patients with acute respiratory tract infections. PLoS Pathog. 2007 May 4; 3(5):e64.

Gjoerup O, Chang Y. Update on human polyomaviruses and cancer. Advances in Cancer Research. 2010; 106: 1–51.

Goh S, Lindau C, Tiveljung-Lindell A, Allander T. Merkel cell polyomavirus in respiratory tract secretions. Emerg Infect Dis. 2009 Mar; 15(3):489-91.

Gorse GJ, O'Connor TZ, Hall SL, Vitale JN, Nichol KL. Human coronavirus and acute respiratory illness in older adults with chronic obstructive pulmonary disease. J Infect Dis. 2009; 199:847-857.

Hofmann H, Pyrc K, van der Hoek L, Geier M, Berkhout B, Pohlmann S. Human coronavirus NL63 employs the severe acute respiratory syndrome coronavirus receptor for cellular entry. Proc Natl Acad Sci U S A. 2005; 102(22): 7988–7993.

Imperiale MJ, Major E. Polyomaviruses. In Fields Virology, 5th edition, Knipe DM, Howley PM, Griffin DE, Lamb RA, Martin MA, Roizman B, Straus SE (eds). Lippincott Williams and Wilkins: Philadelphia. 2007; 2263–2298.

Jiang M, Abend JR, Johnson SF, Imperiale MJ. The role of polyomaviruses in human disease. Virology. 2009 Feb 20; 384(2):266-73.

Kantola K, Sadeghi M, Lahtinen A, Koskenvuo M, Aaltonen LM, Möttönen M, Rahiala J, Saarinen-Pihkala U, Riikonen P, Jartti T, Ruuskanen O, Söderlund-Venermo M,

Hedman K. Merkel cell polyomavirus DNA in tumor-free tonsillar tissues and upper respiratory tract samples: implications for respiratory transmission and latency. J Clin Virol. 2009 Aug; 45(4):292-5.

Lau SK, Lee P, Tsang AK, Yip CC, Tse H, Lee RA, So LY, Lau YL, Chan KH, Woo PC, Yuen KY. Molecular epidemiology of human coronavirus OC43 reveals evolution of different genotypes over time and recent emergence of a novel genotype due to natural recombination. J Virol. 2011; 85:11325-11337.

Lau SK, Woo PC, Yip CC, Tse H, Tsoi HW, Cheng VC, Lee P, Tang BS, Cheung CH, Lee RA, So LY, Lau YL, Chan KH, Yuen KY. Coronavirus HKU1 and other coronavirus infections in Hong Kong. J Clin Microbiol. 2006; 44:2063-2071.

McIntosh K, Chao RK, Krause HE, Wasil R, Mocega HE, Mufson MA. Coronavirus infection in acute lower respiratory tract disease of infants. J Infect Dis. 1974; 130:502-507.

McIntosh K, Dees JH, Becker WB, Kapikian AZ, Chanock RM. Recovery in tracheal organ cultures of novel viruses from patients with respiratory disease. Proc Natl Acad Sci U S A. 1967; 57:933-940.

McIntosh K, Kapikian AZ, Turner HC, Hartley JW, Parrott RH, Chanock RM. Seroepidemiologic studies of coronavirus infection in adults and children. Am J Epidemiol. 1970; 91(6): 585–592.

Monto AS, Lim SK. The Tecumseh study of respiratory illness. VI. Frequency of and relationship between outbreaks of coronavirus infection. J Infect Dis. 1974; 129:271-276.

Monto AS. Medical reviews: coronaviruses. Yale J Biol Med. 1974; 47(4):234–251.

Padgett BL, Walker DL, ZuRhein GM, Eckroade RJ, Dessel BH. Cultivation of papova-like virus from human brain with progressive multifocal leucoencephalopathy. Lancet. 1971 Jun 19;1(7712):1257-60.

Pierangeli A, Gentile M, Di Marco P, Pagnotti P, Scagnolari C, Trombetti S, Lo Russo L, Tromba V, Moretti C, Midulla F, Antonelli G. Detection and typing by molecular techniques of respiratory viruses in children hospitalized for acute respiratory infection in Rome, Italy. J Med Virol. 2007; 79:463-468.

Pyrc K, Jebbink MF, Berkhout B, van der Hoek L. Genome structure and transcriptional regulation of human coronavirus NL63. Virol J. 2004; 1:7

Pyrc K, Sims AC, Dijkman R, Jebbink M, Long C, Deming D, Donaldson E, Vabret A, Baric R, van der Hoek L, Pickles R. Culturing the unculturable: human

coronavirus HKU1 infects, replicates, and produces progeny virions in human ciliated airway epithelial cell cultures. J Virol. 2010; 84:11255-11263.

Ren L, Gonzalez R, Xu J, Xiao Y, Li Y, Zhou H, Li J, Yang Q, Zhang J, Chen L, Wang W, Vernet G, Paranhos-Baccala G, Wang Z, Wang J. Prevalence of human coronaviruses in adults with acute respiratory tract infections in Beijing, China. J Med Virol. 2011; 83:291-297.

Schmidt OW. Antigenic characterization of human coronaviruses 229E and OC43 by enzyme-linked immunosorbent assay. J Clin Microbiol. 1984; 20(2):175–180.

Schowalter RM, Pastrana DV, Pumphrey KA, Moyer AL, Buck CB. Merkel cell polyomavirus and two previously unknown polyomaviruses are chronically shed from human skin. Cell Host Microbe. 2010 Jun 25; 7(6):509-15.

Scuda N, Hofmann J, Calvignac-Spencer S, Ruprecht K, Liman P, Kühn J, Hengel H, Ehlers B. A novel human polyomavirus closely related to the african green monkey-derived lymphotropic polyomavirus. J Virol. 2011 May; 85(9):4586-90.

Shao X, Guo X, Esper F, Weibel C, Kahn JS. Seroepidemiology of group I human coronaviruses in children. J Clin Virol. 2007; 40:207-213.

Suwannakarn K, Chieochansin T, Vichiwattana P, Korkong S, Theamboonlers A, Poovorawan Y. Prevalence and genetic characterization of human coronaviruses in southern Thailand from July 2009 to January 2011. Southeast Asian J Trop Med Public Health. 2014; 45:326-336.

Talbot HK, Crowe JE, Jr., Edwards KM, Griffin MR, Zhu Y, Weinberg GA, Szilagyi PG, Hall CB, Podsiad AB, Iwane M, Williams JV. Coronavirus infection and hospitalizations for acute respiratory illness in young children. J Med Virol. 2009; 81:853-856.

Theamboonlers A, Samransamruajkit R, Thongme C, Amonsin A, Chongsrisawat V, Poovorawan Y. Human coronavirus infection among children with acute lower respiratory tract infection in Thailand. Intervirology. 2007; 50:71-77.

Vabret A, Dina J, Gouarin S, Petitjean J, Tripey V, Brouard J, Freymuth F. Human (non-severe acute respiratory syndrome) coronavirus infections in hospitalised children in France. J Paediatr Child Health. 2008; 44:176-181.

van der Meijden E, Janssens RW, Lauber C, Bouwes Bavinck JN, Gorbalenya AE, Feltkamp MC. Discovery of a new human polyomavirus associated with trichodysplasia spinulosa in an immunocompromized patient. PLoS Pathog. 2010 Jul 29; 6(7):e1001024.

Van Ghelue M, Khan MT, Ehlers B, Moens U. Genome analysis of the new human polyomaviruses. Rev Med Virol. 2012 Nov; 22(6):354-77.

Wevers BA, van der Hoek L. Recently discovered human coronaviruses. Clin Lab Med. 2009; 29(4):715–724.

Yeager CL, Ashmun RA, Williams RK, Cardellichio CB, Shapiro LH, Look AT, Holmes KV. Human aminopeptidase N is a receptor for human coronavirus 229E. Nature. 1992 Jun 4; 357(6377):420-2.

Zheng Q, Deng Y, Liu J, van der Hoek L, Berkhout B, Lu M. Core structure of S2 from the human coronavirus NL63 spike glycoprotein. Biochemistry. 2006; 45:15205-15215.

Output จากโครงการวิจัยที่ได้รับทุนจาก สกว.

1. ผลงานตีพิมพ์ในวารสารวิชาการนานาชาติ

1: Soonnarong R, Thongpan I, Payungporn S, Vuthitanachot C, Vuthitanachot V, Vichiwattana P, Vongpunsawad S, Poovorawan Y. Molecular epidemiology and characterization of human coronavirus in Thailand, 2012-2013. Springerplus. 2016 Aug 26;5(1):1420. [สถานะ published]

2: Jinato T, Chuaypen N, Poomipak W, Praianantathavorn K, Makkoch J, Kiatbumrung R, Jampoka K, Tangkijvanich P, Payungporn S. Original Research: Analysis of hepatic microRNA alterations in response to hepatitis B virus infection and pegylated interferon alpha-2a treatment. Exp Biol Med (Maywood). 2016 Oct;241(16):1803-10. [สถานะ published]

3: Makkoch J, Poomipak W, Saengchoowong S, Khongnomnan K, Praianantathavorn K, Jinato T, Poovorawan Y, Payungporn S. Human microRNAs profiling in response to influenza A viruses (subtypes pH1N1, H3N2, and H5N1). Exp Biol Med (Maywood). 2016 Feb;241(4):409-20. [สถานะ published]

4: Khlaiphuengsin A, T-Thienprasert NP, Tangkijvanich P, Posuwan N, Makkoch J, Poovorawan Y, Payungporn S. Human miR-5193 Triggers Gene Silencing in Multiple Genotypes of Hepatitis B Virus. Microrna. 2015;4(2):123-30. [สถานะ published]

5: Khongnomnan K, Makkoch J, Poomipak W, Poovorawan Y, Payungporn S. Human miR-3145 inhibits influenza A viruses replication by targeting and silencing viral PB1 gene. Exp Biol Med (Maywood). 2015 Dec;240(12):1630-9. [สถานะ published]

6: Chanchaem P, Poovorawan Y, Payungporn S. Complete genome characterization and phylogenetic analysis of WU polyomavirus in Thai pediatric patients with respiratory tract infections in 2013. J Med Assoc Thai. 2015 Jan;98 Suppl 1:S29-35. [สถานะ published]

2. การนำผลงานวิจัยไปใช้ประโยชน์ เชิงวิชาการ โดยมีการสร้างบัณฑิต และพัฒนานักวิจัยดังนี้

- นายกฤษฎา คงนมนาน หลักสูตร วท.ม. ชีวเคมีทางการแพทย์ จุฬาฯ
- นางสาวอภิชญา คล้ายพึ่งสินธุ์ หลักสูตร วท.ม. ชีวเคมีทางการแพทย์ จุฬาฯ
- นางสาวรพีพรรณ สูณรงค์ หลักสูตร วท.ม. ชีวเคมีทางการแพทย์ จุฬาฯ
- นางสาวปรางวลัย จันทร์แจ่ม หลักสูตร วท.ม. วิทยาศาสตร์การแพทย์ จุฬาฯ
- นางสาวธนัญญา จินาโต หลักสูตร วท.ม. วิทยาศาสตร์การแพทย์ จุฬาฯ
- นางสาวจาริกา มากคช นักวิจัยหลังปริญญาเอก คณะแพทยศาสตร์ จุฬาฯ

ภาคผนวก

Reprints ผลงานวิจัยระดับนานาชาติ

Soonnarong *et al. SpringerPlus (2016) 5:1420*
DOI 10.1186/s40064-016-3101-9

SpringerPlus

RESEARCH Open Access

Molecular epidemiology and characterization of human coronavirus in Thailand, 2012–2013

Rapeepun Soonnarong[1], Ilada Thongpan[2], Sunchai Payungporn[1], Chanpim Vuthitanachot[3], Viboonsuk Vuthitanachot[3], Preeyaporn Vichiwattana[2], Sompong Vongpunsawad[2] and Yong Poovorawan[2*]

Abstract

Background: Coronavirus causes respiratory infections in humans. To determine the prevalence of human coronavirus (HCoV) infection among patients with influenza-like illness, 5833 clinical samples from nasopharyngeal swabs and aspirates collected between January 2012 and December 2013 were examined.

Results: HCoV was found in 46 (0.79 %) samples. There were 19 (0.32 %) HCoV-HKU1, 19 (0.32 %) HCoV-NL63, 5 (0.09 %) HCoV-229E, and 3 (0.05 %) HCoV-OC43. None of the sample tested positive for MERS-CoV. The majority (54 %) of the HCoV-positive patients were between the ages of 0 and 5 years. HCoV was detected throughout the 2-year period and generally peaked from May to October, which coincided with the rainy season. Phylogenetic trees based on the alignment of the spike (*S*) gene sequences suggest an emergence of a new clade for HCoV-229E.

Conclusions: The data in this study provide an insight into the prevalence of the recent circulating HCoVs in the region.

Keywords: Human coronavirus (HCoV), Epidemiology, Respiratory tract infection (RTI), Thailand

Background

Human coronavirus (HCoV) is an enveloped positive-strand RNA virus with ~27–32 kb genome. Its genome contains five major open reading frames (Orfs) encoding the replicase polyproteins (Orf 1a and Orf 1b), spike (S), envelope (E), membrane (M), and nucleocapsid (N) proteins (Hilgenfeld and Peiris 2013). HCoV belongs to the order *Nidovirales*, family *Coronaviridae* and the genus *Coronavirus* (Lai and Cavanagh 1997). Virions are pleomorphic with diameters between 60 and 220 nm. There are four genera of coronaviruses (*Alpha-*, *Beta-*, *Gamma-* and *Deltacoronavirus*) based on serologic and phylogenetic characterization. Among the five recognized human coronaviruses, HCoV strains 229E and NL63 are alphacoronaviruses, while HCoV strains OC43, HKU1, and SARS (responsible for the severe acute respiratory syndrome) are betacoronaviruses (Gaunt et al. 2010; Gonzalez et al. 2003; Drosten et al. 2003). In addition, a novel genotype of coronavirus was identified in Saudi Arabia in 2012, later referred to as MERS-CoV (for the Middle East respiratory syndrome coronavirus), which was isolated from the sputum of a 60-year-old man in Saudi Arabia who presented acute pneumonia and renal failure with a fatal outcome (Hilgenfeld and Peiris 2013; Zaki et al. 2012). It was subsequently found to be most closely related to the bat betacoronavirus HKU4 and HKU5 (Gonzalez et al. 2003). Fortunately, the conserved structure and function of the polymerase made it possible to develop a PCR assay based on the polymerase gene region to accurately differentiate new coronaviruses as was done with MERS-CoV and other novel coronaviruses (Rota et al. 2003; Moës et al. 2005).

HCoVs are recognized as one of the most frequent causes of upper respiratory tract infection in elderly adults leading to acute pneumonia and renal failure (Memish et al. 2013; Gorse et al. 2009). HCoV infection

*Correspondence: yong.p@chula.ac.th
[2] Center of Excellence in Clinical Virology, Department of Pediatrics, Faculty of Medicine, Chulalongkorn University, Bangkok, Thailand
Full list of author information is available at the end of the article

is thought to participate in the exacerbations of chronic obstructive pulmonary disease, congestive heart failure, and other chronic diseases necessitating emergency care and long-term hospitalization. In addition to respiratory syncytial virus, parainfluenza virus, adenovirus, and influenza virus, HCoVs are also known to cause the common cold especially among children (Moës et al. 2005; Lu et al. 2012). Furthermore, HCoVs are associated with mild to severe upper and lower respiratory tract illness and can cause more serious respiratory diseases in children, the elderly and people with underlying conditions (McIntosh et al. 1974; van Elden et al. 2004).

The study of coronaviruses has sometimes been difficult due to limitations in cell culture and serology. Thus, epidemiological and viral prevalence data are valuable in investigating the emergence of HCoV infection. Using reverse-transcription polymerase chain reaction (RT-PCR) and phylogenetic analysis, we characterized HCoVs identified in Thai patients with respiratory tract infection between 2012 and 2013.

Methods

Clinical samples

This study was approved by the Faculty of Medicine of Chulalongkorn University (IRB 388/56). A total of 5833 clinical samples from patients with influenza-like illness were obtained between January 2012 and December 2013 for routine testing of respiratory viruses as part of an epidemiological surveillance (Auksornkitti et al. 2014; Prachayangprecha et al. 2013; Sriwanna et al. 2013). From these, 5196 nasopharyngeal swabs (NPS) were collected from patients with upper respiratory tract infections who sought treatment at the Bangpakok 9 International Hospital and Chum Phae Hospital (Khon Kaen, Thailand). Additionally, 637 nasopharyngeal aspirates (NPA) were collected from patients with lower respiratory tract infections who were admitted to King Chulalongkorn Memorial Hospital and Chon Buri Hospital. All samples were stored in the viral transport medium (prepared according to The World Health Organization guideline). Patient identifiers were removed and all samples were anonymous, although data on demographics, symptoms, history of illness, results of clinical examination and laboratory investigations were retained for analysis.

Coronavirus detection

Viral DNA/RNA was extracted using HiYield Viral Nucleic Acid Extraction Kit (RBC Bioscience, Taipei, Taiwan, ROC). Complementary DNA was synthesized with random hexameric primers and ImProm-II (Promega, Madison, WI, USA) according to the manufacturer's instructions. HCoV was identified using the semi-nested RT-PCR to amplify the RNA-dependent RNA polymerase (*RdRp*) gene of HCoV and the *N* gene of MERS-CoV as previously described (Corman et al. 2012; Kon et al. 2012). For controls, a panel of viral nucleic acid extracted from samples previously tested positive for influenza A virus [subtype H1N1 (pandemic 2009), H3N2], influenza B virus, respiratory syncytial virus (RSV), human parainfluenza virus (HPIV) and human adenovirus was used to determine the specificity of the HCoV semi-nested RT-PCR. PCR was performed using the Perfect*Taq*^{TM} Plus Master Mix kit (5 PRIME, Hamburg, Germany) and primers (Table 1) in 25 μL reaction volume under the following conditions: initial denaturation at 94 °C for 3 min, 40 cycles of 94 °C for 30 s, 55–58 °C for 30 s, 72 °C for 40 s, and a final extension at 72 °C for 7 min. Expected amplicons for RdRp and N were ~450 and ~260 bp, respectively. All the specimens were positive for GAPDH, which served as an internal control.

To identify the types of HCoVs (HCoV-229E, HCoV-NL63, HCoV-OC43, and HCoV-HKU1), the *S* gene was genotyped using nested RT-PCR. Amplification condition was the same as above except that the annealing temperature was 50 °C. Amplicons were agarose gel-purified using the Expin Gel SV kit (GeneAll, Seoul, Korea) and DNA sequencing was performed by First BASE Laboratories (Seri Kembangan, Selangor, Malaysia).

Sensitivity of semi-nested RT-PCR for coronavirus detection

PCR products from the amplification of HCoV-229E, HCoV-NL63, HCoV-OC43, HCoV-HKU1 and MERS-CoV were cloned into pGEM-T Easy Vector System (Promega, CA, USA) according to the manufacturer's instructions. RNA transcripts from these five coronaviruses were used as standards to validate assay sensitivity. The sensitivity of the semi-nested RT-PCR assay was established for each coronavirus by testing transcripts of known concentrations from serial dilution.

Sequence and phylogenetic analysis

Nucleotide sequences of the *RdRp* and *S* genes were edited using Chromas Lite (version 2.1.1) and compared to the HCoV reference strains available in GenBank using the Basic Local Alignment Search Tool (BLAST) program (www.ncbi.nlm.nih.gov/Blast.cig). Multiple alignments of the nucleotide sequences utilized Clustal W in BioEdit (version 7.0.9). Phylogenetic trees were constructed using the neighbor-joining method and the Kimura two-parameter distance model (MEGA version 6.06) and evaluated by 1000 bootstrap pseudo-replicates.

Nucleotide sequences

The nucleotide sequences of the *RdRp* gene (accession numbers KJ866056–KJ866101) and the *S* gene (accession

Table 1 Sequences of primers used to identify HCoVs in this study

Gene	Primer	Genotype	Sequence (5′–3′)[a]	PCR application
RdRp	SP6-CoV_16053_F		ATTTAGGTGACACTATAGGGTTGGGAY TAYCCTAARTGTGA	First and second round
	CoV-16594_R		TAYTATCARAAYAATGTCTTTATGTC	First round
	CoV-Pan_16510_R		TGATGATGGNGTTGTBTGYTATAA	Second round
S	HCoV-S229E_F1	229E	GTGGGTGCACTACCTAAGAC	First round
	HCoV-S229E_R1	229E	CGTGGTTGAACAGCAATTATAGAACC	
	HCoV-S229E_F2	229E	GAGTTTGTTATTTCACGCACAGGAC	Second round
	HCoV-S229E_R2	229E	CCATCTGCACAAACGCCAAAAC	
	HCoV-SHKU1_F1	HKU1	TCACCTCTTAATTGGGAACGTA	First round
	HCoV-SHKU1_R1	HKU1	CATTAGAACAAGTGGTGCCAC	
	HCoV-SHKU1_F2	HKU1	GATTTGCAGTTGGGCAGTTCTGG	Second round
	HCoV-SHKU1_R2	HKU1	AAAGGCATCAGGACTACAAA	
	HCoV-SNL63_F1	NL63	GACACCACAATACCTTTTGG	First round
	HCoV-SNL63_R1	NL63	CTGGTTGGTTACATGGTGTCAC	
	HCoV-SNL63_F2	NL63	CATGTTAGCACTTTTGTGGGT	Second round
	HCoV-SNL63_R2	NL63	CCACCAGCAAGTGACTGGTTTG	
	HCoV-SOC43_F1	OC43	GTCGGTGCCCTCTCCATTAAATT	First round
	HCoV-SOC43_R1	OC43	GGCCGCAGAAACACGAC	
	HCoV-SOC43_F2	OC43	AATATGAGCAGCCTGATGTC	Second round
	HCoV-SOC43_R2	OC43	CCGAAATAGCAATGCTGGTTC	
N	NSeq-Fwd	MERS	CCTTCGGTACAGTGGAGCCA	First round
	NSeq-Fnest	MERS	TGACCCAAAGAATCCCAACTAC	Second round
	NSeq-Rev	MERS	GATGGGGTTGCCAAACACAAAC	First and second round

[a] Y = (C/T) and R = (A/G)

numbers KJ866102–KJ866147) identified in this study were deposited in the GenBank database.

Results

Sensitivity and specificity of semi-nested RT-PCR assays for coronavirus detection

Serial dilutions of coronavirus RNA transcripts (HCoV-229E, HCoV-NL63, HCoV-OC43, HCoV-HKU1, and MERS-CoV) were tested using semi-nested RT-PCR. RNA transcripts for all virus types were detectable at ≤10 copies per reaction, or <400 copies/mL of sample. To evaluate detection specificity and possible cross-reactivity, nucleic acid from 18 different types of respiratory viruses were tested. All assay results were negative, and no false positive was observed.

Prevalence of HCoV infection

Among the 5833 samples analyzed, 637 (10.9 %) were positive for influenza A virus, 206 (3.5 %) were positive for influenza B virus, 201 (3.4 %) were positive for respiratory syncytial virus A, 91 (1.6 %) were positive for respiratory syncytial virus B, and 78 (1.3 %) were positive for adenovirus (Table 2). More importantly, 46 samples (0.79 %) tested positive for HCoV. Co-infection with other respiratory viruses was not observed in the HCoV-positive samples. All samples were negative when tested for MERS-CoV *N* gene.

Table 2 Identification of viruses in the samples obtained from 5833 patients hospitalized for acute respiratory tract infection

Viruses	Number of samples tested positive (%)
HCoV-229E	5 (0.09)
HCoV-OC43	3 (0.05)
HCoV-NL63	19 (0.32)
HCoV-HKU1	19 (0.32)
Influenza A virus	637 (10.9)
Influenza B virus	206 (3.5)
Adenovirus	78 (1.3)
Respiratory syncytial virus A	201 (3.4)
Respiratory syncytial virus B	91 (1.6)

Amongst the HCoV-positive samples, 56.5 % were from men and 43.5 % were from women (gender ratio 1.3:1) (Table 3). HCoV infection was detected in all age groups, and the mean age of HCoV-infected patients was 21.37 years (min. = 4 months, max. = 93 years, mean = 27.04 years). The percentage of HCoV infection per year was 0.81 % (23/2838) in 2012 and 0.77 %

Table 3 Demographic characteristics of individuals with respiratory tract infection

Characteristic	Specimens	
	No. specimens	Positive HCoV (%)
Gender		
Male [n (%)]	2935 (50.3)	26 (56.5)
Female [n (%)]	2898 (49.7)	20 (43.5)
Age (years)		
Median	11	8.5
Mode	1	1
Mean (SD)	19.57 (19.9)	21.37 (27.0)
Age group		
0–5 [years (%)]	2197 (37.7)	25 (54.3)
6–10 [years (%)]	732 (12.5)	2 (4.3)
11–15 [years (%)]	538 (9.2)	6 (13.0)
16–30 [years (%)]	866 (14.8)	3 (6.5)
31–60 [years (%)]	1102 (18.9)	3 (6.5)
>60 [years (%)]	397 (6.8)	7 (15.2)
Provinces		
Bangkok [n (%)]	3292 (56.4)	17 (37.0)
Khon Kaen [n (%)]	2408 (41.3)	28 (60.9)
Chon Buri [n (%)]	132 (2.3)	1 (2.2)

Numbers in parentheses indicate the percent of positive infection from total samples

(23/2995) in 2013. There were no seasonal peaks associated with HCoV and no positive samples were identified in the typically dry months of April and November during both years (Fig. 1).

The majority of HCoV (25/46 or 54 %) were detected mainly in young children between the ages of 0–5 years and 15 % in the elderly aged over 60 years (Fig. 2). Approximately 80 % of the positive samples (37/46) were isolated from the NPS samples, while the rest (9/46) were from the NPA samples. Furthermore, 46 % (17/37) of all positive NPS and 89 % (8/9) of all positive NPA samples belonged to the 0–5 year age group.

To further differentiate the 46 HCoV-positive samples, the *S* gene was sequenced. Analysis showed that these HCoV strains belonged to one of the four HCoV species (Table 2; Fig. 3). In all, 19 (0.32 %) were positive for HCoV-HKU1, 19 (0.32 %) were positive for HCoV-NL63, 5 patients (0.09 %) were positive for HCoV-229E, and 3 (0.05 %) were positive for HCoV-OC43. Relative to all HCoV-positive samples, therefore, the predominant genotypes were 41.3 % for both HCoV-HKU1 and HCoV-NL63 (19/46), followed by 11 % HCoV-229E (5/46) and 6.5 % HCoV-OC43 (3/46). Interestingly, HCoV-NL63 and HCoV-HKU1 appeared sporadically during the study period and were detected mainly in March 2012 and July 2013, respectively.

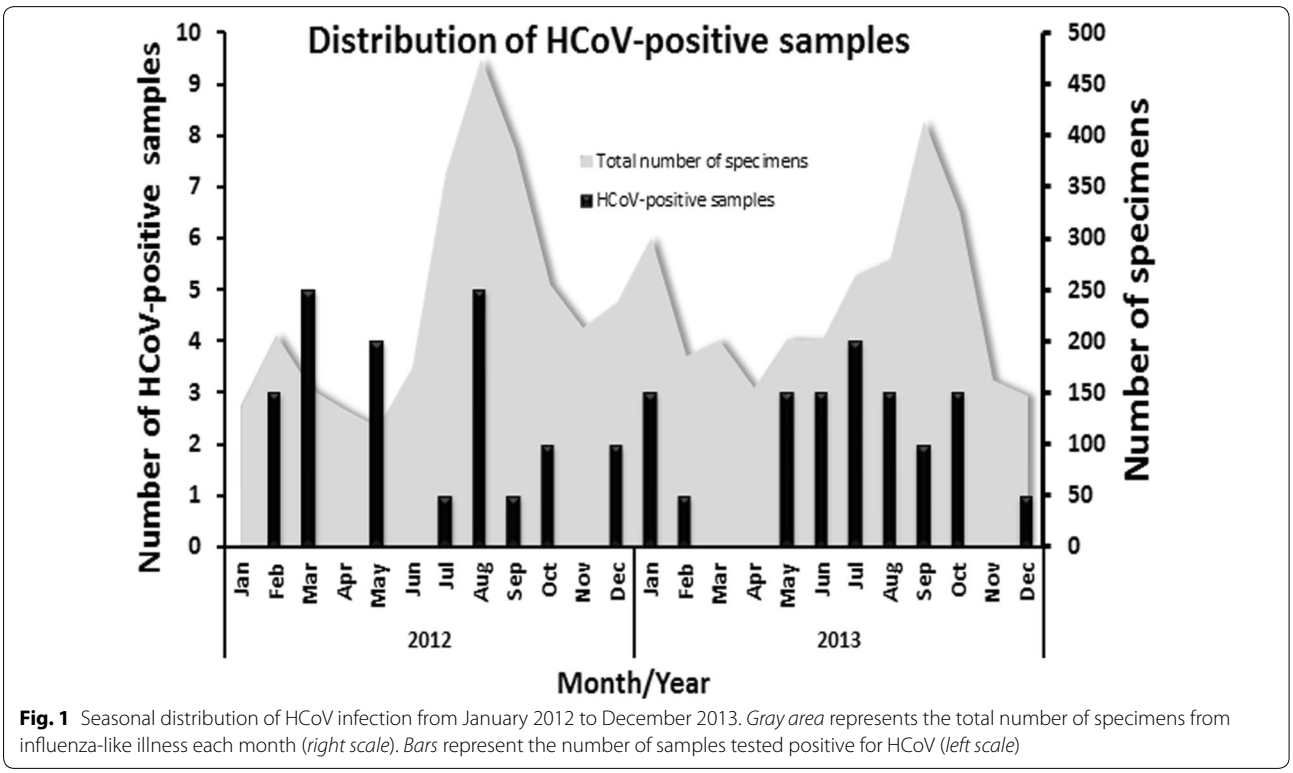

Fig. 1 Seasonal distribution of HCoV infection from January 2012 to December 2013. *Gray area* represents the total number of specimens from influenza-like illness each month (*right scale*). *Bars* represent the number of samples tested positive for HCoV (*left scale*)

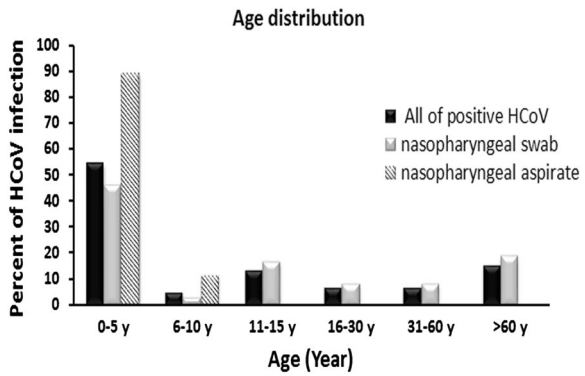

Fig. 2 Age distribution of HCoV infection. Percentage of HCoV-positive samples were derived from different age groups (*black bars*). Positive samples tested from nasopharyngeal swab and aspirate from each age group are indicated by *gray* and *hatched bars*, respectively

Clinical characteristics of HCoV infections

Of the 46 HCoV-positive samples, 38 (82.6 %) were derived from patients with acute infections involving the upper respiratory tract such as the nose, sinuses, pharynx or larynx (Table 4). The remaining 8 (17.4 %) were from patients with lower respiratory tract infections. The most common clinical manifestations were fever and rhinorrhea, although several patients experienced tachypnea and hypoxemia.

Molecular characterization of different HCoVs

To assess the relationship among the strains identified, partial nucleotide sequences of the *S* gene from HCoV-positive samples were subjected to phylogenetic analysis (Fig. 4). This region was examined as it represents the antigenic determinant of the virus and correlates with strain evolution. HCoV-HKU1 strains identified in this study formed a single cluster (~99.6 % sequence identity) within clade B together with the strain identified on mainland China. Meanwhile, HCoV-NL63 strains clustered in two different groups within the same clade. Their sequences were genetically closest to the isolates from The Netherlands and U.S.A. Three HCoV-OC43 strains grouped together with previous viruses characterized in Japan in clade C. Finally, although the 5 HCoV-229E identified in this study appeared to cluster into a new group, they demonstrated nearest genetic resemblance to strains from Japan and China.

Discussion

Due to the awareness of MERS-CoV and other novel human coronavirus infections worldwide, this study aimed to characterize possible circulation and prevalence of HCoV in Thailand in a 2-year period. The HCoV prevalence of 0.79 % found in this study was lower than that from previous reports, which ranged from 2.1 to 5.7 % (Bellei et al. 2008; Dominguez et al. 2009; Gorse

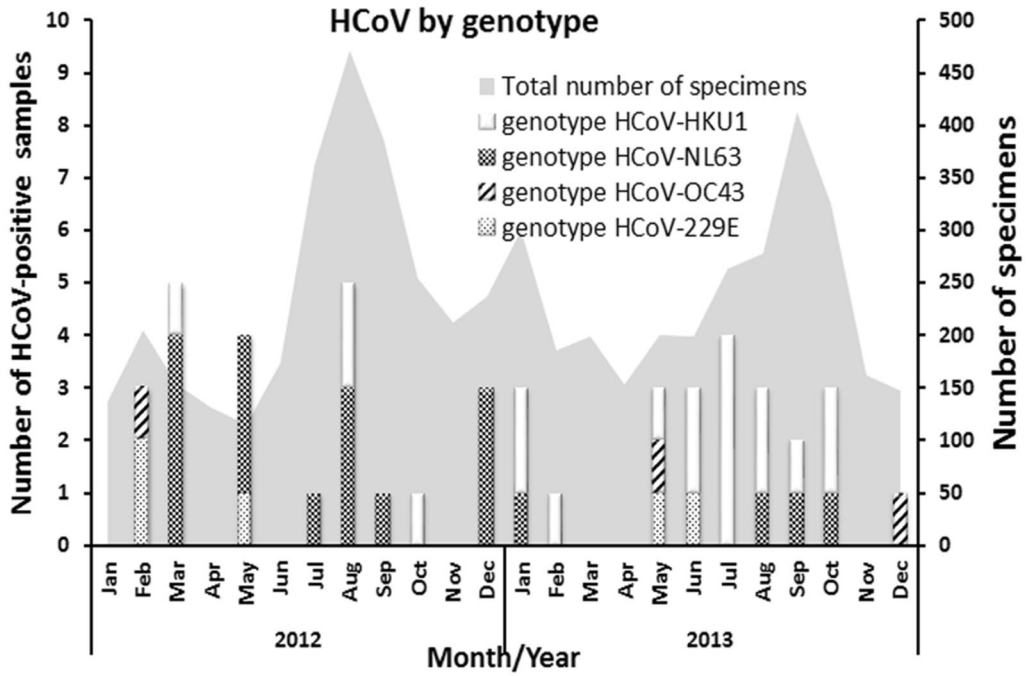

Fig. 3 HCoV-positive samples identified by species. The total number of specimens examined is shown in *gray* (*right scale*), while the strains of HCoVs (HKU1, NL63, OC43, and 229E) identified each month are indicated as *bars* (*left scale*)

Table 4 Clinical characteristics of patients with HCoV infection

Characteristic	HCoV-positive individuals (%)[a]			
	HCoV-229E	HCoV-OC43	HCoV-NL63	HCoV-HKU1
Total no. of patients	5	3	19	19
URTI	5	2	16 (84 %)	15 (79 %)
LRTI	0	1	3 (16 %)	4 (21 %)
Clinical symptom				
Fever	5	3	18 (95 %)	16 (84 %)
Cough	2	2	11 (58 %)	10 (53 %)
Sputum	0	1	5 (26 %)	2 (11 %)
Rhinorrhea	4	2	16 (84 %)	17 (89 %)
Vomiting	3	0	10 (53 %)	12 (63 %)
Tachypnea[b]	0	1	6 (32 %)	7 (37 %)
Hypoxemia[c]	1	1	5 (26 %)	5 (26 %)
Respiratory distress[d]	0	1	6 (32 %)	7 (37 %)
Abnormal breathing sound[e]	0	1	6 (32 %)	7 (37 %)

URTI upper respiratory tract infection, *LRTI* lower respiratory tract infection (pneumonia, bronchiolitis, and acute infection of the pulmonary parenchyma)

[a] Percent of HCoV-positive individuals with such symptoms

[b] Age-related definition of tachypnea by The World Health Organization for individuals <2 months (>60 breaths/min), 2–12 months (>50 breaths/min), 1–5 years (>40 breaths/min) and ≥5 years (>20 breaths/min)

[c] Oxygen saturation (SpO2) level below 95 %

[d] Including retractions (subcostal, intercostal, suprasternal), nasal flaring, and grunting

[e] Crepitation, rhonchi, and wheezing

et al. 2009; Pierangeli et al. 2007). However, the rate of HCoV-positive samples found in this study was similar to the level of infection reported in countries such as mainland China (1 %) (Ren et al. 2011) and United Kingdom (0.85 %) (Gaunt et al. 2010). Several factors may account for this disparity: (1) the subjects included in this study were adult patients whereas other studies examined mainly hospitalized children (Talbot et al. 2009) or adults with underlying diseases (Dare et al. 2007), (2) the viral infection rate obtained from NPS used in this study may be lower than that of NPA (Lau et al. 2006; Talbot et al. 2009), (3) differences in the study time frame and geographical area, (4) natural varying of yearly distribution of HCoV species, and (5) differences in the techniques used for testing, such as conventional versus real-time PCR.

Although a previous study in southern Thailand found that HCoV-OC43 was the predominant strain (Suwannakarn et al. 2014), very few HCoV-OC43 infections were detected in this study. Yearly fluctuation in the predominance of HCoV strains in Thailand has been documented (Dare et al. 2007). The majority of HCoVs detected in this study was HCoV-NL63 and HCoV-HKU1. HCoV-NL63 was found mainly in 2012 and HCoV-HKU1 in 2013, while HCoV-OC43 and HCoV-229E were sporadic and less frequent.

HCoV infections elicited common symptoms such as fever, cough, headache, vomiting, muscle pain and sore throat. Upper respiratory tract infection such as rhinorrhea, sputum, and lower respiratory tract infection such as tachypnea and abnormal breath sounds were frequently observed in our patients similar to past observations (Ren et al. 2011; Dominguez et al. 2009). However, clinical presentations were slightly different among each subtype of HCoV. In this study, vomiting was more common in HCoV-229E, HCoV-NL63 and HCoV-HKU1-positive patients but not in those infected by HCoV-OC43. Lower respiratory tract infections were associated with individuals with HCoV-OC43, HCoV-NL63, and HCoV-HKU1, but not in those with HCoV-229E. Tachypnea, hypoxemia, abnormal breathing sound and signs of respiratory distress also occurred less often for HCoV-229E. These clinical features were very similar to those observed with other respiratory viruses, such as RSV, HPIV, and human metapneumovirus.

The simultaneous screening for common respiratory viruses allowed us to investigate possible co-infection of HCoV with other viral pathogens. Although parainfluenza viruses, enteroviruses, and human metapneumovirus were not tested, co-infection of HCoV with RSV was never observed (Theamboonlers et al. 2007). It may be that HCoV and other respiratory viruses do not share the same seasonal circulation. The possibility of viral coinfection with bacteria, however, cannot be ruled out. Nevertheless, confirmation of the mechanism of co-infection will require good clinical sampling and further longitudinal studies conducted over several years.

Previous characterization of the genetic variation and evolution of HCoV have utilized the whole viral genome, *S*, *RdRp*, or *N* gene. Here, the phylogenetic analysis of HCoV was performed based on the sequences of partial spike gene because the *S* gene may be more discriminating than the *RdRp* gene (Lau et al. 2006, 2011). While phylogenetic grouping of HCoV-HKU1, HCoV-NL63, and HCoV-OC43 were characterized by clades or clusters, HCoV-229E strains were typically subdivided by the year of emergence. HCoV-229E strains collectively appeared to form a new cluster similar to but distinct from previous strains in the phylogenetic tree.

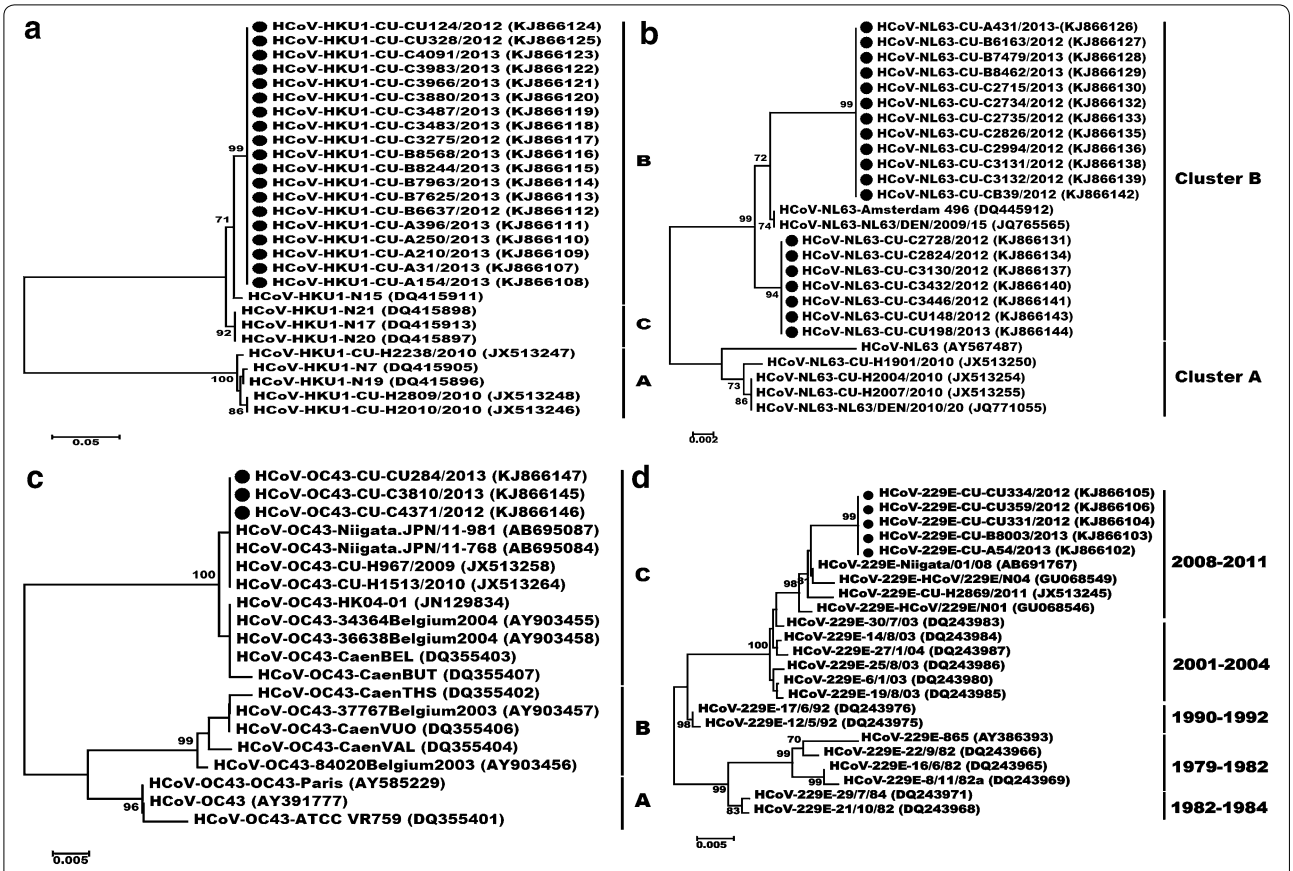

Fig. 4 Phylogenetic analyses of the *S* genes of 4 HCoV species. Phylogenetic trees were constructed based on the partial nucleotide sequences of the *S* gene of HCoV-HKU1 (**a**), HCoV-NL63 (**b**), HCoV-OC43 (**c**), and HCoV-229E (**d**) with MEGA 6.06 software using the distance method and the neighbor-joining algorithm with Kimura 2 parameters. Phylogenetic clusters are indicated to the right of the trees. CU designation is given to each of the 46 clinical isolates examined in this study (*black dots*). The node clusters were supported by bootstrap values >70 %

Conclusions

In summary, this study surveyed the prevalence and clinical presentations of different HCoV infections in Thai patients from 2012 to 2013. Although the numbers of HCoV-positive samples were low, we detected four species of HCoV and phylogenetically characterized their diversity. These viruses appeared to continue to cause infections globally, thus accurate and timely diagnosis will be essential. The assay described in this study can be used to assist in the rapid and accurate detection of emerging HCoV infection.

Abbreviations

HCoV: human coronavirus; NPA: nasopharyngeal aspirate; NPS: nasopharyngeal swab; RSV: respiratory syncytial virus; RT-PCR: reverse-transcription polymerase chain reaction.

Authors' contributions

RS, IT and PV performed the experiments. SP and YP designed the research study. CV and VV collected the samples. RS, SV, and YP wrote the manuscript. All authors read and approved the final manuscript.

Author details

[1] Department of Biochemistry, Faculty of Medicine, Chulalongkorn University, Bangkok, Thailand. [2] Center of Excellence in Clinical Virology, Department of Pediatrics, Faculty of Medicine, Chulalongkorn University, Bangkok, Thailand. [3] Chum Phae Hospital, Khon Kaen, Thailand.

Competing interests

The authors declare that they have no competing interests.

Availability of data and materials

The dataset supporting the conclusions of this article is available within this manuscript.

Ethics approval and consent

This study was approved by the Faculty of Medicine, Chulalongkorn University (IRB 388/56).

Funding

This work was supported by the Bureau of General Communicable Disease, Department of Disease Control (DDC), Ministry of Public Health; The National Research Council of Thailand (NRCT); the Thailand Research Fund (TRF: RSA5680031); The Research Chair Grant from the National Science and Technology Development Agency; Chulalongkorn University Centenary Academic Development Project (CU56-HR01); Ratchadaphiseksomphot Endowment Fund of Chulalongkorn University (RES560530093); The Outstanding Professor of Thailand Research Fund (DPG5480002); and The Center of Excellence in

Clinical Virology of Chulalongkorn University (GCE 58-014-30-004); King Chulalongkorn Memorial Hospital; the 100th Anniversary Chulalongkorn University Fund for doctoral scholarship awarded to Ilada Thongpan; The National Blood Center, Thai Red Cross; MK Restaurant Company; and The Siam Cement Group.

Received: 12 May 2016 Accepted: 18 August 2016
Published online: 26 August 2016

References

Auksornkitti V, Kamprasert N, Thongkomplew S, Suwannakarn K, Theamboonlers A, Samransamruajkij R, Poovorawan Y (2014) Molecular characterization of human respiratory syncytial virus, 2010–2011: identification of genotype ON1 and a new subgroup B genotype in Thailand. Arch Virol 159(3):499–507

Bellei N, Carraro E, Perosa A, Watanabe A, Arruda E, Granato C (2008) Acute respiratory infection and influenza-like illness viral etiologies in Brazilian adults. J Med Virol 80(10):1824–1827

Corman VM, Muller MA, Costabel U, Timm J, Binger T, Meyer B, Kreher P, Lattwein E, Eschbach-Bludau M, Nitsche A, Bleicker T, Landt O, Schweiger B, Drexler JF, Osterhaus AD, Haagmans BL, Dittmer U, Bonin F, Wolff T, Drosten C (2012) Assays for laboratory confirmation of novel human coronavirus (hCoV-EMC) infections. Euro Surveill 17(49):20334

Dare RK, Fry AM, Chittaganpitch M, Sawanpanyalert P, Olsen SJ, Erdman DD (2007) Human coronavirus infections in rural Thailand: a comprehensive study using real-time reverse-transcription polymerase chain reaction assays. J Infect Dis 196(9):1321–1328

Dominguez SR, Robinson CC, Holmes KV (2009) Detection of four human coronaviruses in respiratory infections in children: a one-year study in Colorado. J Med Virol 81(9):1597–1604

Drosten C, Gunther S, Preiser W, van der Werf S, Brodt HR, Becker S, Rabenau H, Panning M, Kolesnikova L, Fouchier RA, Berger A, Burguiere AM, Cinatl J, Eickmann M, Escriou N, Grywna K, Kramme S, Manuguerra JC, Muller S, Rickerts V, Sturmer M, Vieth S, Klenk HD, Osterhaus AD, Schmitz H, Doerr HW (2003) Identification of a novel coronavirus in patients with severe acute respiratory syndrome. N Engl J Med 348(20):1967–1976

Gaunt ER, Hardie A, Claas EC, Simmonds P, Templeton KE (2010) Epidemiology and clinical presentations of the four human coronaviruses 229E, HKU1, NL63, and OC43 detected over 3 years using a novel multiplex real-time PCR method. J Clin Microbiol 48(8):2940–2947

Gonzalez JM, Gomez-Puertas P, Cavanagh D, Gorbalenya AE, Enjuanes L (2003) A comparative sequence analysis to revise the current taxonomy of the family Coronaviridae. Arch Virol 148(11):2207–2235

Gorse GJ, O'Connor TZ, Hall SL, Vitale JN, Nichol KL (2009) Human coronavirus and acute respiratory illness in older adults with chronic obstructive pulmonary disease. J Infect Dis 199(6):847–857

Hilgenfeld R, Peiris M (2013) From SARS to MERS: 10 years of research on highly pathogenic human coronaviruses. Antivir Res 100(1):286–295

Kon M, Watanabe K, Tazawa T, Watanabe K, Tamura T, Tsukagoshi H, Noda M, Kimura H, Mizuta K (2012) Detection of human coronavirus NL63 and OC43 in children with acute respiratory infections in Niigata, Japan, between 2010 and 2011. Jpn J Infect Dis 65(3):270–272

Lai MM, Cavanagh D (1997) The molecular biology of coronaviruses. Adv Virus Res 48:1–100

Lau SK, Woo PC, Yip CC, Tse H, Tsoi HW, Cheng VC, Lee P, Tang BS, Cheung CH, Lee RA, So LY, Lau YL, Chan KH, Yuen KY (2006) Coronavirus HKU1 and other coronavirus infections in Hong Kong. J Clin Microbiol 44(6):2063–2071

Lau SK, Lee P, Tsang AK, Yip CC, Tse H, Lee RA, So LY, Lau YL, Chan KH, Woo PC, Yuen KY (2011) Molecular epidemiology of human coronavirus OC43 reveals evolution of different genotypes over time and recent emergence of a novel genotype due to natural recombination. J Virol 85(21):11325–11337

Lu R, Yu X, Wang W, Duan X, Zhang L, Zhou W, Xu J, Xu L, Hu Q, Lu J, Ruan L, Wang Z, Tan W (2012) Characterization of human coronavirus etiology in Chinese adults with acute upper respiratory tract infection by real-time RT-PCR assays. PLoS ONE 7(6):e38638

McIntosh K, Chao RK, Krause HE, Wasil R, Mocega HE, Mufson MA (1974) Coronavirus infection in acute lower respiratory tract disease of infants. J Infect Dis 130(5):502–507

Memish ZA, Zumla AI, Al-Hakeem RF, Al-Rabeeah AA, Stephens GM (2013) Family cluster of Middle East respiratory syndrome coronavirus infections. N Engl J Med 368:2487–2494

Moës E, Vijgen L, Keyaerts E, Zlateva K, Li S, Maes P, Pyrc K, Berkhout B, van der Hoek L, Van Ranst M (2005) A novel pancoronavirus RT-PCR assay: frequent detection of human coronavirus NL63 in children hospitalized with respiratory tract infections in Belgium. BMC Infect Dis 5:6

Pierangeli A, Gentile M, Di Marco P, Pagnotti P, Scagnolari C, Trombetti S, Lo Russo L, Tromba V, Moretti C, Midulla F, Antonelli G (2007) Detection and typing by molecular techniques of respiratory viruses in children hospitalized for acute respiratory infection in Rome, Italy. J Med Virol 79(4):463–468

Prachayangprecha S, Makkoch J, Suwannakarn K, Vichaiwattana P, Korkong S, Theamboonlers A, Poovorawan Y (2013) Epidemiology of seasonal influenza in Bangkok between 2009 and 2012. J Infect Dev Ctries 7(10):734–740

Ren L, Gonzalez R, Xu J, Xiao Y, Li Y, Zhou H, Li J, Yang Q, Zhang J, Chen L, Wang W, Vernet G, Paranhos-Baccala G, Wang Z, Wang J (2011) Prevalence of human coronaviruses in adults with acute respiratory tract infections in Beijing, China. J Med Virol 83(2):291–297

Rota PA, Oberste MS, Monroe SS, Nix WA, Campagnoli R, Icenogle JP, Penaranda S, Bankamp B, Maher K, Chen MH, Tong S, Tamin A, Lowe L, Frace M, DeRisi JL, Chen Q, Wang D, Erdman DD, Peret TC, Burns C, Ksiazek TG, Rollin PE, Sanchez A, Liffick S, Holloway B, Limor J, McCaustland K, Olsen-Rasmussen M, Fouchier R, Gunther S, Osterhaus AD, Drosten C, Pallansch MA, Anderson LJ, Bellini WJ (2003) Characterization of a novel coronavirus associated with severe acute respiratory syndrome. Science 300(5624):1394–1399

Sriwanna P, Chieochansin T, Vuthitanachot C, Vuthitanachot V, Theamboonlers A, Poovorawan Y (2013) Molecular characterization of human adenovirus infection in Thailand, 2009–2012. Virol J 10:193

Suwannakarn K, Chieochansin T, Vichiwattana P, Korkong S, Theamboonlers A, Poovorawan Y (2014) Prevalence and genetic characterization of human coronaviruses in southern Thailand from July 2009 to January 2011. Southeast Asian J Trop Med Public Health 45:326–336

Talbot HK, Crowe JE Jr, Edwards KM, Griffin MR, Zhu Y, Weinberg GA, Szilagyi PG, Hall CB, Podsiad AB, Iwane M, Williams JV, Network NVS (2009) Coronavirus infection and hospitalizations for acute respiratory illness in young children. J Med Virol 81(5):853–856

Theamboonlers A, Samransamruajkit R, Thongme C, Amonsin A, Chongsrisawat V, Poovorawan Y (2007) Human coronavirus infection among children with acute lower respiratory tract infection in Thailand. Intervirology 50(2):71–77

van Elden LJ, van Loon AM, van Alphen F, Hendriksen KA, Hoepelman AI, van Kraaij MG, Oosterheert JJ, Schipper P, Schuurman R, Nijhuis M (2004) Frequent detection of human coronaviruses in clinical specimens from patients with respiratory tract infection by use of a novel real-time reverse-transcriptase polymerase chain reaction. J Infect Dis 189:652–657

Zaki AM, van Boheemen S, Bestebroer TM, Osterhaus AD, Fouchier RA (2012) Isolation of a novel coronavirus from a man with pneumonia in Saudi Arabia. N Engl J Med 367(19):1814–1820

Original Research

Analysis of hepatic microRNA alterations in response to hepatitis B virus infection and pegylated interferon alpha-2a treatment

Thananya Jinato[1], Natthaya Chuaypen[2,3], Witthaya Poomipak[1], Kesmanee Praianantathavorn[2], Jarika Makkoch[2], Rattanaporn Kiatbumrung[2], Kanisa Jampoka[2], Pisit Tangkijvanich[2,3] and Sunchai Payungporn[1,2,3]

[1]Systems Biology Center, Research Affairs, Faculty of Medicine, Chulalongkorn University, Bangkok 10330, Thailand; [2]Department of Biochemistry, Faculty of Medicine, Chulalongkorn University, Bangkok 10330, Thailand; [3]Research Unit of Hepatitis and Liver Cancer, Faculty of Medicine, Chulalongkorn University, Bangkok 10330, Thailand
Corresponding author: Sunchai Payungporn. Email: sp.medbiochemcu@gmail.com

Abstract

Interferons play important roles in defense mechanisms against viral infection, and thus interferon therapy has been a standard treatment in chronic hepatitis B patients. Interferons signaling pathways promote interferon-inducible genes including microRNAs. In this research, we aimed to determine microRNAs expression profiles *in vitro* and *in vivo*. For *in vitro* model, Huh7 cells were transfected with or without hepatitis B virus plasmid for 6 h, and then treated with 100 ng of pegylated-interferon alpha-2a for 24 h. *In vivo*, we defined microRNAs expression profiles in pair-liver tissues of chronic hepatitis B patients in comparison between before and after treatment of pegylated-interferon alpha-2a for 48 weeks. Cellular small RNAs were extracted followed by library preparation. To determine microRNAs expression profiles, the next-generation sequencing was carried out on MiSeq platform (Illumina®). *In vitro* analysis demonstrated that microRNAs can be classified into up-regulated and down-regulated microRNAs in response to hepatitis B virus, interferon, and combination of hepatitis B virus and interferon. Moreover, *in vivo* analysis revealed microRNAs profiles in non-responders, responders without hepatitis B surface antigen clearance, and responders with hepatitis B surface antigen clearance. The target genes of the candidate microRNAs were determined in terms of roles in cellular pathways and immune response, which might be related to treatment in chronic hepatitis B patients. Results revealed that two down-regulated microRNAs including miR-185-5p and miR-186-5p were correlated in both *in vitro* and *in vivo* studies. These two microRNAs might be represented as specific hepatic microRNAs responding to hepatitis B virus and pegylated-interferon alpha-2a treatment, which may remarkable and attractive for further study involving in the association of their target genes and prediction of pegylated-interferon alpha-2a response. Interestingly, microRNAs expression patterns might be useful for understanding the response mechanism and serve as biomarkers for prediction of pegylated-interferon alpha-2a treatment response in patients with chronic hepatitis B.

Keywords: microRNA, hepatitis B virus, interferon, next-generation sequencing

***Experimental Biology and Medicine* 2016; 241: 1803–1810. DOI: 10.1177/1535370216647184**

Introduction

Hepatitis B virus (HBV) is the main cause of acute or chronic liver disease which up to 70–90% of patient can lead to cirrhosis and hepatocellular carcinoma (HCC), according to 50% of HCC patients have presence of HBV infection.[1,2] Almost 360 million people worldwide have chronic hepatitis infection with HBV, and 0.5 to 1.2 million people die each year from HBV-related liver disease. Prevalence of this disease depends on prevalence rates of HBV that can be varied by geographical regions and nationality population.[3] During HBV infection, host genome was integrated by HBV DNA and produced viral proteins such as HBx, hepatitis B surface antigen (HBsAg), and HBeAg. These viral proteins can trigger cancer-related genes, motivate several signaling pathways including genetic instability, inflammatory, and host immune responses, which will lead to hepatocyte injury and then transform to HCC.[4]

Currently, anti-viral drugs have been used in the treatment of HBV infection. First of all, a nucleos(t)ide analog affects the inhibition of viral polymerase and also viral production. The second type of drugs is an interferon (IFN) alpha, which can be called as immunomodulatory

drug triggering host immune responses and leads to inhibition of viral proliferation.[5] For the treatment of HBV patients, IFN alpha was the first permitted drug to use since 1980s.[5,6] IFN alpha was attached with polyethylene glycol (PEG) to improve pharmacological advantages such as more resistance to protease activity and less renal clearance leading to extension of drug circulation time.[7] Treatment with IFN provides better treatment response without drug resistant occur. Furthermore, IFN treatment can show the definite duration of therapy.[5,8] However, there are various side-effects of IFN treatment such as flu-like symptoms, headache, nausea, fatigue, weight and hair loss.[9] Furthermore, the Peg-IFN alpha treatment response rate is just 32–36% with high cost of treatment.[10,11] Prediction of Peg-IFN alpha response in HBV-infected patients will be useful for personalized medicine or alternative treatments.

Small (18–24 nt in lengths) non-coding RNAs called microRNAs (miRNAs) play an important role in gene silencing via the mechanism of RNA interference pathway, which leads to the degradation or translational repression of mRNA target after matching the complement sequences between miRNAs itself and target mRNA.[12] Approximately 30% of human genes can be regulated by miRNAs.[13] From the previous studies, many evidences suggested that various cellular pathways and events such as cell development, differentiation, and cell immunity can be regulated by miRNAs.[14] Besides, miRNAs can be used as outstanding biomarkers of cancer prognosis and diagnosis, because they are easily detected and measured in human serum and plasma. The risen possibility at present is to find the unique miRNA patterns in serum and plasma that can be useful for performing non-invasive disease markers.[15]

The first aim of this research is to determine differential expression of miRNA profiling in Huh7 cells in response to HBV and Peg-IFN alpha-2a treatment. Second, to investigate hepatic miRNAs expression profiles in chronic hepatitis B (CHB) patients between before and after treatment with Peg-IFN alpha-2a. Finally, to compare miRNAs expression profiles in CHB patients treated with Peg-IFN alpha-2a between responders and non-responders.

Materials and methods

Patients and sample collection

Pair-liver tissue samples of pre-and post-treatment with Peg-IFNs alpha-2a were collected from patients with chronic HBV infection who were admitted in King Chulalongkorn Memorial Hospital, Thailand. Before treatment, all patients share similar pattern of disease including CHB (>6 months), infected with HBV genotype C, and positive for HBeAg with baseline characteristics as shown in Table 1. All patients were continuously treated with 180 μg/week of Peg-IFNs alpha-2a (Hoffmann-La Roche Ltd) for 48 weeks. After treatment, the patients were selected and classified into responders ($n=6$) and non-responders ($n=4$). The responders were defined by serum HBV DNA level (<2000 IU/mL) at 48 weeks post-treatment.[16] The responders were further separated into the responders with HBsAg clearance ($n=3$) and the responders without HBsAg clearance ($n=3$). The HBsAg clearance was defined by HBsAg seroconversion (HBsAg loss and positive for anit-HBsAg) at 48 weeks post-treatment.[16] Exclusion criteria consisted of cancer progression and coinfection with HCV or HIV.

Plasmids and cell lines

The HCC cell lines (Huh7) and the plasmid expressing the HBV genome were generously provided by Prof. Yasuhito Tanaka, Nagoya City University Graduate School of Medical Sciences, Japan). The HBV plasmid was constructed by adding a full-length genome of HBV DNA genotype C (accession no. AB246345) into the pUC19 vector as described previously.[17] These plasmids were propagated in *E. coli* (DH5α) competent cells by heat shock transformation method.[18]

Transfection of HBV plasmid

Huh7 cell line was cultured and maintained at 37°C, 5% CO_2 humidified incubator in Dulbecco's Modified Eagle's Medium (Thermo Scientific) with 10% heat inactivated (56°C, 30 min) fetal bovine serum (Thermo Scientific) and 1% antibiotic-antimycotic (Gibco®). Cell cultures were divided into four different conditions in triplicates including mock infection, HBV expression plasmids transfection,

Table 1 Baseline characteristics of patients with chronic hepatitis B (CHB)

Clinical data	Responders		Non-responders ($n=4$)	*P*
	With HBsAg clearance ($n=3$)	Without HBsAg clearance ($n=3$)		
Mean age, years (±SD)	25.67 ± 5.68	28.0 ± 4.00	25.0 ± 5.41	0.745
Gender (male/female)	2/1	1/2	2/2	0.785
Mean HBV DNA before Peg-IFN treatment, Log_{10} IU/ml (± SD)	8.34 ± 0.07	7.47 ± 0.46	7.88 ± 0.39	0.055
Mean HBsAg before Peg-IFN treatment, Log_{10} IU/ml (±SD)	4.7 ± 0.00	3.5 ± 1.04	4.5 ± 0.22	0.460
Mean ALT, U/L (±SD)	71.0 ± 25.16	63.0 ± 12.52	76.0 ± 13.62	0.610

HBV: hepatitis B virus; IFN: interferon.

Peg-IFNs alpha-2a treatment, and combined transfection of HBV expression plasmids and Peg-IFNs alpha-2a treatment. For transfection, the cells were seeded into 6-mm Petri dish (TPP) at a density of 7×10^5 cells/dish in medium without antibiotic-antimycotic and were incubated for 24 h. After the cells reached approximately 80% confluence, 3 μg of the HBV plasmid was diluted with Opti-MEM I reduced serum medium (Gibco®) and then transfected into cells by using 7.5 μL of Lipofectamine™ 2000 (Invitrogen) following the manufacturer's guidelines. In IFN treatment condition, the cell cultures were treated with 100 ng of Peg-IFNs alpha-2a after 6 h of HBV transfection and then followed by 24-h incubation.

Isolation of miRNAs

Total miRNAs in cell cultures and clinical liver tissues were extracted by miRNA purification kit (Norgen) and the concentration of small RNA was quantitated by Qubit® BR RNA Assay kit (Invitrogen) following the manufacturer's protocol.

Library preparation and next-generation sequencing

Small RNA libraries preparation begins with at least 100 ng/sample of total small RNAs using NEBNext® Multiplex Small RNA Library Prep Set for Illumina® (New England Biolabs). Briefly, small RNA was ligated with 3′ SR adaptor, and 5′ SR adaptor was then reverse transcribed into a cDNA library. After that, the cDNA library obtained from each sample was amplified by PCR with different indexes (distinctive 6 base-labeled). The size-selection of DNA library was performed through 3% agarose gel electrophoresis. The specific product size of DNA library (the length of miRNA with adaptors approximately 147 bp) was extracted by QIAquick gel extraction kit (QIAGEN). The DNA libraries were quantified by KAPA SYBR FAST qPCR Master Mix (2 ×) (Kapa Biosystems) according to the manufacturer's recommendation. DNA libraries with different indexes were pooled together with equal concentration to make a 2 nM master DNA library. After that the DNA library was denatured by NaOH and then diluted using HT1 buffer in order to yield 10 pM DNA library which is suitable for next-generation sequencing (NGS). The NGS was performed using MiSeq® v2 reagent kit (Illumina®) carried out on MiSeq platform (Illumina®) according to Illumina's instructions manual.

MicroRNA expression profiling

The CLC genomic workbench version 8 (http://www.clcbio.com/) was used for data processing and analysis of miRNA expression profiles. Low-quality reads (Q-score < 30) and adapter sequences were trimmed. The pass filtered reads (Q-score ≥ 30) were aligned with human genomic DNA (hg19), mature and precursor human miRNA (from miRbase), and contaminant RNA (human tRNA, rRNA, and mRNA). The sequencing reads which matched to the miRNA database but not contaminant RNA were considered as miRNA. The miRNAs were identified and counted based on the number of reads matched to the miRbase (www.mirbase.org/). Fold change between control and cases was calculated by $\log_2$ of normalized expression in case divided by normalized expression in control. Fold changes higher than 2 were considered as the significant difference. For miRNA profiling *in vivo*, candidate miRNAs were selected based on similar expression profiles (up-regulated or down-regulated) observed in the same group (responders with HBsAg clearance, responders without HBsAg clearance or non-responders). RNAhybrid (https://bibiserv2.cebitec.uni bielefeld.de/rnahybrid) was used for prediction of hybridization pattern between miRNA and their target genes.

Results

Analysis of miRNAs profiling by NGS

In cell culture model, miRNAs collected from the triplicate wells of each group were pooled together and used for preparation of four DNA libraries, including mock, Peg-IFN alpha-2a treatment, HBV transfection and HBV and Peg-IFN alpha-2a combination. In CHB patients, miRNAs extracted from 10 pair-liver biopsy of pre-treatment (week 0) and post-treatment (week 48) with Peg-IFN alpha-2a were used to construct 20 DNA libraries for individual sample. All 24 DNA libraries were pooled with equal concentration and subjected to run at the same time on MiSeq platform. The DNA library obtained from each sample was identified by different indexes. The results obtained from NGS yielded raw data 18,598,911 total reads. After trimming of low-quality reads (Q-score < 30) and adapter sequences, the passed filter reads (Q-score ≥ 30) were 17,761,014 reads (97.37% of total reads). Average reads per index were 740,042 reads. High-quality filtered reads were achieved and used for further analysis. The miRNAs were identified and counted based on the number of reads matched to the miRbase (www.mirbase.org/).

MiRNAs in Huh7 cells responding to Peg-IFN-alpha 2a and HBV

The miRNAs profiles obtained from a mock control were served as a baseline calibrator in order to compare with other groups including Peg-IFN alpha-2a treatment, HBV transfection and HBV and Peg-IFN alpha-2a combination. The expression levels of each miRNA in cell cultures were calculated and classified into up-regulated (>2-fold increase) and down-regulated (<2-fold decrease) as shown in Table 2. In Peg-IFN-alpha 2a-treated cells, four miRNAs were up-regulated, while six miRNAs were down-regulated. There were 13 up-regulated miRNAs, but only one down-regulated miRNA was observed in HBV-transfected group. For the cells transfected with HBV and treated with Peg-IFN-alpha 2a, seven miRNAs were up-regulated whereas four miRNAs were down-regulated.

Common miRNAs in Huh7 cells responding to Peg-IFN-alpha 2a and HBV

For the characterization of miRNAs which is commonly expressed among groups and those exclusively expressed

Table 2 Up-regulated and down-regulated miRNAs in Huh7 cells responding to Peg-IFN-alpha-2a treatment and HBV transfection

Peg-IFN-alpha-2a treatment		HBV transfection		HBV and Peg-IFN-alpha-2a	
miRNAs	**Fold change**	**miRNAs**	**Fold change**	**miRNAs**	**Fold change**
miR-574-5p	3.25	let-7g-5p	3.27	let-7g-5p	3.07
miR-455-5p	2.25	miR-4791	3.10	miR-574-5p	3.07
let-7e-5p	2.25	miR-574-5p	2.90	miR-374b-5p	2.99
miR-885-5p	2.25	let-7a-5p	2.83	miR-217	2.51
miR-331-3p	−2.07	miR-20a-5p	2.74	miR-23b-3p	2.31
miR-143-3p	−2.14	miR-1180-3p	2.68	miR-4791	2.31
miR-99b-3p	−2.39	miR-27b-5p	2.42	let-7a-5p	2.26
miR-1303	−2.66	miR-502-3p	2.42	miR-450b-5p	−2.01
miR-660-5p	−2.66	miR-130b-5p	2.42	miR-185-5p	−3.01
miR-16-2-3p	−2.88	miR-15b-5p	2.10	miR-186-5p	−3.34
		miR-374b-5p	2.10	miR-16-2-3p	−3.82
		miR-19b-3p	2.10		
		miR-3607-3p	2.10		
		miR-92b-3p	−2.23		

HBV: hepatitis B virus; IFN: interferon.

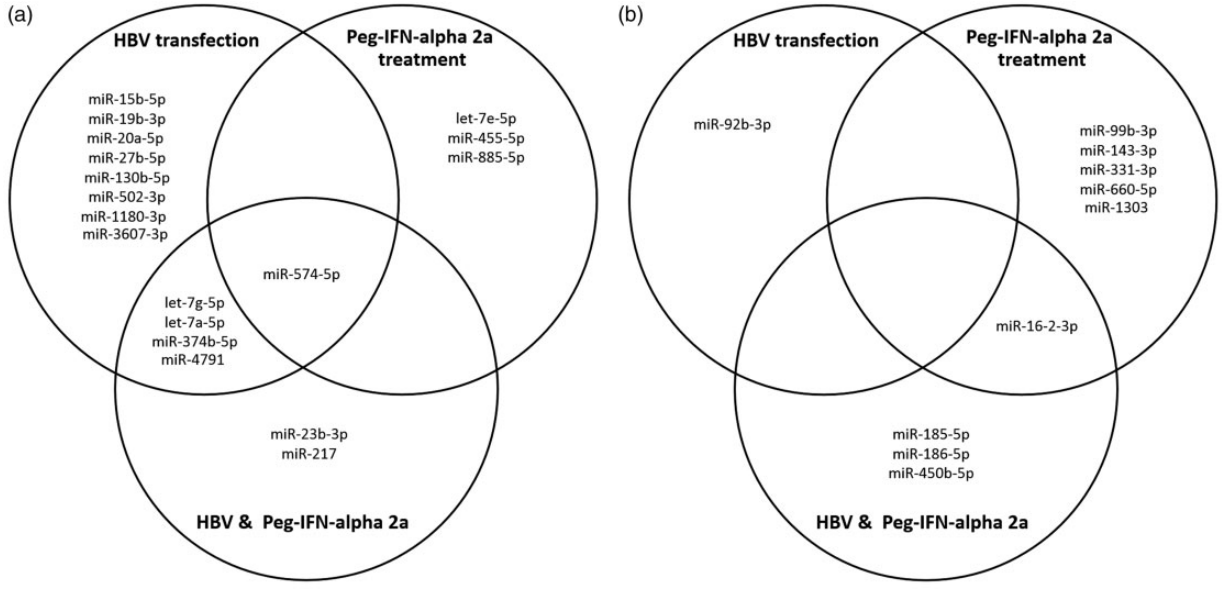

Figure 1 Venn diagram representing unique and common miRNAs which significantly expressed (fold changed > 2) in Huh7 cells culture model. Cells were divided into four groups including mock control, HBV transfected, Peg-IFN alpha-2a treated, and combination of HBV and Peg-IFN alpha-2a. (a) The up-regulated miRNAs in each group compared with mock control. (b) The down-regulated miRNAs in each group compared with mock control

in each group of interest, Venn diagram was used to distinguish all miRNAs into three groups as shown in Figure 1. The results revealed miR-574-5p in the center of Venn diagram which was found to be up-regulated in all the three groups. In addition, up-regulated miRNAs observed between HBV transfected group and combination of HBV and Peg-IFN alpha-2a group were let-7g-5p, let-7a-5p, 374b-5p and miR-4791. These miRNAs possibly expressed when the cell infected with HBV and involved with endogenous IFNs response in the cell which enough to induced miRNAs in this group. The miRNA expression in cells treated with Peg-IFN alpha-2a between with and without HBV transfection revealed that only miR-16-2-3p was down-regulated which probably resulted from treatment with IFNs.

Hepatic miRNAs profiling in CHB treated with Peg-IFN alpha-2a

MiRNA profiles were determined in pair-liver tissue samples obtained from 10 patients with CHB during pre- and post-treatment (48 weeks) with Peg-IFNs alpha-2a. The miRNA expression profiles were compared between pre-treatment and post-treatment in each individual patient. Then the patients were classified based on the outcomes

of the treatment including responders without HBsAg clearance ($n=3$), responders with HBsAg clearance ($n=3$) and non-responders ($n=4$). Therefore, miRNA profiles were compared among patients within the same group in order to determine the consensus miRNA expression patterns which might be useful as predictive biomarkers for the outcomes of treatment. The results revealed that all of the consensus miRNAs observed from patients within the same group were down-regulated. For responders without HBsAg clearance revealed the decrease of 5 miRNAs (let-7d-5p, let-7f-5p, miR-155-5p, miR-181a-5p and miR-423-5p). The reduction of six miRNAs expression in responders with HBsAg clearance such as miR-183-5p, miR-185-5p, miR-186-5p, miR-199b-5p, miR-422a and miR-424-5p is influenced by the treatment of Peg-IFN alpha-2a, whereas non-responders showed a decline of miR-145-5p and miR-199a-5p. There is no overlapping miRNA expression pattern observed among patients in different groups as shown in Figure 2.

Target genes of candidate miRNAs

Our study focused on differential expression pattern of miRNAs exclusively expressed in Huh7 cell line transfected with HBV and treated with Peg-IFN alpha-2a (*in vitro* analysis) and miRNAs profiles in responders with HBsAg clearance (*in vivo* analysis). Target genes of candidate miRNAs were identified based on data obtained from previous studies. Prediction of hybridization patterns between miRNAs and 3′-UTR of mRNA targets as well as minimum free energy (MFE) was performed by RNAhybrid (Table 3).

Discussion

Currently, cell culture models have been used for studying the mechanism of cancer cells. HepG2, HepG2.2.15 and Huh7 cell lines have been favored for representing HCC cells. However, previous studies demonstrated that the

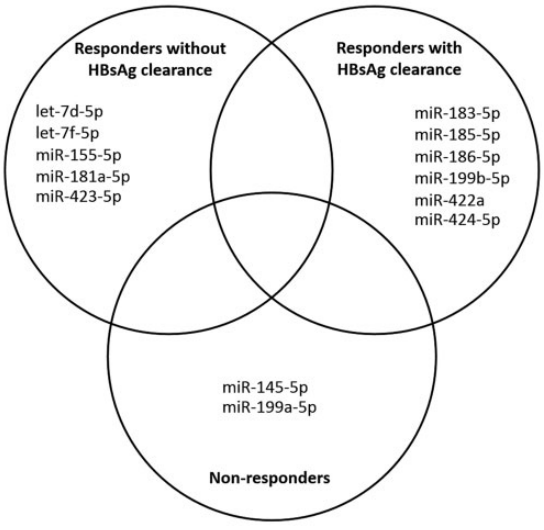

Figure 2 Venn diagram representing consensus of down-regulated miRNAs observed among groups of CHB patients after treated with Peg-IFN alpha-2a for 48 weeks including responders without HBsAg clearance, responders with HBsAg clearance, and non-responders

expression level of IFN-α mRNA in Huh7 cells was more than those found in HepG2 cells,[32] meaning that Huh7 cells could respond to IFN better than HepG2 cells. Moreover, a previous study found that the HepG2 cells completely lacked primary response genes of IFN pathway.[33] Therefore, Huh7 cell culture would be more suitable than HepG2 cells for being a model to investigate the effect of Peg-IFN alpha-2a in this study. The result found that Huh7 could respond to HBV transfection and Peg-IFN alpha-2a treatment as differential miRNAs expression. MiRNAs expression in each group would affect the related target genes by the regulation of cellular gene expression. The HBV plasmid was used instead of HBV infection due to the fact that the HBV still lacks effective cell culture system in a laboratory. Therefore, 6-h HBV plasmid transfection was used to mimic HBV acute hepatitis B infection, but it could not represent CHB infection.

For miRNAs responding to HBV, a previous report found that miR-15b promotes HBV replication and expression of HBx protein which leads to repression of the miR-15b expression in long-term events.[34] However, this study found the up-regulation of miR-15b, which might be due to the acute phase (6 h) of HBV plasmid transfection. There were some studies about miRNAs expression in response to Peg-IFN alpha treatment. Cheng *et al*. studied the effect of IFN alpha-2b to miRNAs expression level in Huh7 cells by incubating with 1 ng/ml of IFN alpha-2b for 12 h and quantified miRNAs expression by *Taq*Man miRNA profiling. The study of Cheng and colleagues found up-regulation of let-7e, miR-455-5p and down-regulation of miR-1303 which similar to those found in our study. In contrast, miR-143, miR-99b, miR-331, miR-660 and miR-885-5p showed different expression levels between our study and the previous report.[35] The variations might be due to different doses of IFN and measuring time of the miRNA expression.

In combined treatment group (HBV and Peg-IFN alpha-2a), our study found that miR-23b-3p and miR-217 were up-regulated while miR-185-5p, miR-186-5p and miR-450b-5p were down-regulated. Putative target genes of these candidate miRNAs were predicted by RNAhybrid and confirmed by previous researches. In up-regulated miRNAs, miR-23b-3p has been found in targeting the 3′ UTR of SMAD family member 3 (Smad3), leading to down-regulation of transforming growth factor-beta1 (TGF-β)/bone morphogenetic protein signaling-induced apoptosis[19,20] and association with cell proliferation, migration and differentiation.[36,37] MiR-217 was reported as a biomarker for pancreatic injury.[38] Previous study has shown that miR-217 can target oncogenes or tumor suppressor genes. As in breast cancer, miR-217 can promote cell proliferation through targeting dachshund family transcription factor 1.[27] However, miR-217 acts as a tumor suppressor gene by targeting Kirsten rat sarcoma viral oncogene homolog in pancreatic ductal adenocarcinoma.[28]

In down-regulated miRNAs, marginal zones B and B1 cell-specific protein (Mzb1) and Burton tyrosine kinase (BTK) are target genes of miR-185, which are related with T cells and B-cell developments. In DN3 cells and Jurkat T cells, there was the up-regulation of miR-185

Table 3 Hybridization patterns between candidate miRNAs and target genes.

MiRNAs	Target genes	Hybridization pattern	MFE (kcal/mol)	Biological process	References
miR-23b-3p	SMAD3	target 5' A UA C 3' GUG CCCU CAAUGUGAU CAU GGGA GUUACACUA miRNA 3' C UA CC 5'	−21.6	Cell proliferation, apoptosis	Rogler *et al*.[19]; Yuan *et al*.[20]
miR-183-5p	PTEN	target 5' U UAA AAG A 3' GUG UC GCCAGUGCUA CAC AG UGGUCACGGU miRNA 3' U UUA A AU 5'	−25.9	Cell proliferation	Sarver *et al*.[21]
	PDCD4	target 5' G UUUUGUA 3' CUACC AGUGCCAUG GAUGG UCACGGUAU miRNA 3' UCACUUAA 5'	−22.9	Apoptosis	Li *et al.*[22]
miR-185-5p	MZB1	target 5' U U U GACGG 3' GGGGC UGC CU UCUCCA CCUUG ACG GA AGAGGU miRNA 3' GU AAG 5'	−23.5	T-cells and B-cells development	Belkaya *et al.*[23]
	BTK	target 5' C CCUGGA G G C 3' UUAGGAGC GCCUUU U CUCC AGUCCUUG CGGAAA A GAGG miRNA 3' A G U 5'	−27.8	T-cells and B-cells development	Flach *et al.*[24]
miR-186-5p	AKAP12/Gravin	target 5' U CU CU UAUC A 3' GCUU GAAA GGAG AUUCUUU CGGG UUUU CCUC UAAGAAA miRNA 3' U U C 5'	−19.1	Cell proliferation	Goeppert *et al.*[25]
miR-199b-5p	KIT	target 5' AACCA UU A 3' GGA AGU U GCACUGG UCU UCA A UGUGACC miRNA 3' CUUG A G UU C 5'	−19.1	Erythropoiesis	Li *et al.*[26]
miR-217	DACH1	target 5' A GGAA AUUA U G 3' CAA GGU UG AUGCAGUA GUU UCA AC UACGUCAU miRNA 3' AG AG AGG 5'	−20.3	Cell proliferation	Zhang *et al.*[27]
	KRAS	target 5' C UGA U 3' CCA CUUGAUGCAGU GGU GGACUACGUCA miRNA 3' A UAGUCAA U 5'	−23.6	Cell proliferation	Zhao *et al.*[28]
miR-422a	CD3G	target 5' A C U A 3' CCU CUG C CCUGGGUUCA GGA GAC G GGAUUCAGGU miRNA 3' C A U CA 5'	−25.6	T-cells recognition	Alashti and Minuchehr *et al.*[29]
miR-424-5p	WEE1	target 5' U U A 3' GUGAAUU GCUGCU UACUUAA CGACGA miRNA 3' AAGUUUUG C 5'	−22.1	Cell proliferation	Chen *et al.*[30]
miR-450b-5p	PAX6	target 5' AU GU UAUG A 3' CAG GAA U UGCAAAA GUC CUU A ACGUUUU miRNA 3' AUAA GU UA 5'	−14.9	Cell development	Shalom-Feuerstein *et al.*[31]

AKAP12/AKAP250/Gravin: A kinase anchor protein 12; BTK: Burton tyrosine kinase; CD3G: CD3g molecule; gamma; DACH1: Dachshund family transcription factor 1; KRAS: Kirsten rat sarcoma viral oncogene homolog; Mzb1: Marginal zone B and B1 cell-specific protein; MFE: minimum free energy; PAX6: Paired box 6; PTEN: phosphatase and tensin homolog; PDCD4: programmed cell death 4; SMAD3: SMAD family member 3; v-kit Hardy-Zuckerman 4 feline sarcoma viral oncogene homolog (KIT); Wee1: WEE1 G2 checkpoint kinase.

leading to Mzb1 down-regulation and calcium responses effect in T-cell receptor (TCR), B-cell antigen receptor (BCR) and development of plasma cell.[24] Moreover, previous studies have found that BTK has a function in BCR cell signaling connected to Erk phosphorylation which is essential in follicular B-cell development regulated by miR-185.[39,40] One target gene of miR-186 is a kinase anchor protein 12 (AKAP12/AKAP250/Gravin), which acts as a tumor suppressor gene by the decrease of cyclin D1 expression and also inhibits cell signaling of protein kinase A and protein kinase C through ERK2 and actin cytoskeleton.[25] Prior study revealed that down-regulation of Gravin expression was found in HCC and other cancers[25,41,42] and also related to virulence of HCC progression.[25] MiR-450b-5p was found to target the pairbox 6 (Pax6) gene, which is important in fate decision of epidermal cell development[31] including pancreatic β-cell function.

In CHB patients, there were several significantly down-regulated miRNAs after treatment with Peg-IFN alpha-2a. In non-responders, down-regulation of miR-145-5p and miR-199a-5p were observed. MiR-145-5p was known as a tumor suppressor miRNA by regulating histone deacetylase 2 in liver cells.[43,44] Down-regulation of MiR-199a-5p was induced by cisplatin leading to drug resistance through activating autophagy in liver cancer cell.[45] Moreover, a study found that miR-199a-5p could target discoidin domain receptor tyrosine kinase 1 and affected the increase of cell invasion in HCC.[46]

The results obtained from CHB patients treated with Peg-IFN alpha-2a showed that down-regulation of let-7d-5p, let-7f-5p, miR-155-5p, miR-181a-5p and miR-423-5p were found in responders without HBsAg clearance group whereas down-regulation of miR-183-5p, miR-185-5p, miR-186-5p, miR-199b-5p, miR-422a and miR-424-5p were observed in responders with HBsAg clearance

group. Generally, miR-183 acts as a potent oncogene by targeting tumor suppressor genes such as EGR1 and PTEN.[21] MiR-183 significantly up-regulates in HCC, targeting the programmed cell death 4 inducing cell growth and cancer development.[22] In this study, miR-183-5p was down-regulated in responders with HBsAg clearance which implied that the decrease of miR-183-5p might be a potential marker for treatment responsiveness in CHB patients. MiR-199b-5p was identified as a positive regulator of human erythropoiesis by targeting c-Kit expression.[26] CD3G is one of cluster of differentiation 3 (CD3) subunits assembled in TCR complexes targeted by miR-422a.[29] CD3 subunits interact with TCR to form a CD3-TCR complex to play a key part in cell recognition events.[47] MiR-424-5p targeted Wee1 kinase, similar to miR-128, leading to cell cycle arrest.[30] Target genes of miR-185-5p and miR-186-5p were explained above.

Comparisons of miRNAs expression profiling between Huh7 cell (*in vitro*) and liver tissues of CHB patients (*in vivo*) were performed in order to determine the hepatic miRNAs in response to HBV and Peg-IFN alpha-2a treatment. Results revealed that two down-regulated miRNAs including miR-185-5p and miR-186-5p were correlated in both *in vitro* and *in vivo*. This implied that these two miRNAs might be represented as specific hepatic miRNAs responding to HBV and Peg-IFN alpha-2a treatment. Thus, miR-185-5p and miR-186-5p may remarkable for further study involving in the association of their target genes and trends to predict Peg-IFN alpha-2a response. Other uncorrelated miRNAs observed between *in vitro* and *in vivo* might be due to several factors. Firstly, miRNAs observed in liver tissues of CHB patients were affected from various cell types (hepatic stellate cells, kupffer cells, liver sinusoids and endothelial cells), whereas miRNAs observed in Huh7 cells were expressed from only hepatic cells. Secondly, miRNAs in liver tissues might be affected by circulating miRNAs and various stimulants (hormones, cytokines and xenobiotics) from other tissues, while miRNAs in cell culture were homogenously obtained from Huh7 cells. In addition, HBV plasmid transfection in cell culture represented as an acute HBV infection, whereas HBV infection in CHB patients was in chronic stage. Moreover, the IFN treatment in Huh7 cells was a single dose short-term treatment (24 h), but CHB patients were treated with multiple doses in long-term treatment (48 weeks).

In conclusion, miRNAs expression patterns might be useful as biomarkers for prediction of Peg-IFN alpha-2a treatment response in CHB patients. However, this study has some limitations in terms of small clinical sample sizes and invasive sample collections. The small sample sizes are limited by the difficulty to obtain pair-liver tissue samples (before and after treatments). Moreover, liver tissue collections from CHB patients are done by invasive methods which implied that hepatic miRNAs are not suitable for biomarkers. Therefore, large sample sizes and non-invasive sample collection (serum or plasma miRNAs) should be further studied in order to identify suitable serum or plasma miRNAs as a biomarker for prediction of Peg-IFN alpha-2a treatment response in CHB patients.

Authors' contributions: TJ analyzed the miRNA profiling and drafted the manuscript. NC assisted with liver tissues collection and cell culture. WP carried out the NGS process and data processing. KP performed NGS libraries preparation. JM assisted with data analysis and revised the manuscript. RK and KJ assisted with sample processing and libraries preparation. PT provided liver tissue samples and clinical data. SP designed the study, analyzed data, revised the manuscript, and coordinated the project.

ACKNOWLEDGEMENTS

We would like to gratefully acknowledge the Department of Biochemistry and Research affairs, Faculty of Medicine, Chulalongkorn University for the research facilities. This study was kindly supported by the Research Unit of Hepatitis and Liver Cancer, Chulalongkorn University. Funding was supported by a Joint Research Program between Thailand and Japan (NRCT-JSPS); the National Research Council of Thailand Grant under the Research University Network (RUN) initiative; the Thailand Research Fund (TRF: RSA5680031); Ratchadapiseksompotch Fund (Faculty of Medicine, Chulalongkorn University); the Research Chair Grant, the National Science and Technology Development Agency (NSTDA); National Research University Project; Office of Higher Education Commission; Chulalongkorn Academic Advancement into Its Second Century Project; The Scholarship from the Graduate School, Chulalongkorn University to commemorate 72nd Anniversary of his Majesty King Bhumibol Adulyadej and the 90th Anniversary Chulalongkorn University Fund (Ratchadaphiseksomphot Endowment Fund) are gratefully acknowledged.

DECLARATION OF CONFLICTING INTERESTS

The author(s) declared no potential conflicts of interest with respect to the research, authorship, and/or publication of this article.

REFERENCES

1. Hagymasi K, Tulassay Z. Epidemiology, risk factors and molecular pathogenesis of primary liver cancer. *Orv Hetil* 2008;**149**:541–8
2. El-Serag HB, Rudolph KL. Hepatocellular carcinoma: epidemiology and molecular carcinogenesis. *Gastroenterology* 2007;**132**:2557–76
3. Kew MC. Epidemiology of chronic hepatitis B virus infection, hepatocellular carcinoma, and hepatitis B virus-induced hepatocellular carcinoma. *Pathol Biol (Paris)* 2010;**58**:273–7
4. Neuveut C, Wei Y, Buendia MA. Mechanisms of HBV-related hepatocarcinogenesis. *J Hepatol* 2010;**52**:594–604
5. Zhang Y, Wu Y, Ye S, Wang T, Zhao R, Chen F, Abe K, Jin X. The response to interferon is influenced by hepatitis B virus genotype in vitro and in vivo. *Virus Res* 2013;**171**:65–70
6. Poynard T, Bedossa P, Chevallier M, Mathurin P, Lemonnier C, Trepo C, Couzigou P, Payen JL, Sajus M, Costa JM. A comparison of three interferon alfa-2b regimens for the long-term treatment of chronic non-A, non-B hepatitis. Multicenter Study Group. *N Engl J Med* 1995;**332**:1457–62
7. Kang JS, Deluca PP, Lee KC. Emerging PEGylated drugs. *Expert Opin Emerg Drugs* 2009;**14**:363–80
8. Cooksley WG. Do we need to determine viral genotype in treating chronic hepatitis B? *J Viral Hepat* 2010;**17**:601–10
9. Sleijfer S, Bannink M, Van Gool AR, Kruit WH, Stoter G. Side effects of interferon-alpha therapy. *Pharm World Sci* 2005;**27**:423–31
10. Lau GK, Piratvisuth T, Luo KX, Marcellin P, Thongsawat S, Cooksley G, Gane E, Fried MW, Chow WC, Paik SW, Chang WY, Berg T, Flisiak R, McCloud P, Pluck N; Peginterferon Alfa-2a H-PCHBSG. Peginterferon

Alfa-2a, lamivudine, and the combination for HBeAg-positive chronic hepatitis B. *N Engl J Med* 2005;**352**:2682–2695
11. Janssen HL, van Zonneveld M, Senturk H, Zeuzem S, Akarca US, Cakaloglu Y, Simon C, So TM, Gerken G, de Man RA, Niesters HG, Zondervan P, Hansen B, Schalm SW, Group HBVS; Rotterdam Foundation for Liver R. Pegylated interferon alfa-2b alone or in combination with lamivudine for HBeAg-positive chronic hepatitis B: a randomised trial. *Lancet* 2005;**365**:123–9
12. Rodriguez A, Griffiths-Jones S, Ashurst JL, Bradley A. Identification of mammalian microRNA host genes and transcription units. *Genome Res* 2004;**14**:1902–10
13. Lewis BP, Burge CB, Bartel DP. Conserved seed pairing, often flanked by adenosines, indicates that thousands of human genes are microRNA targets. *Cell* 2005;**120**:15–20
14. Tang Y, Luo X, Cui H, Ni X, Yuan M, Guo Y, Huang X, Zhou H, de Vries N, Tak PP, Chen S, Shen N. MicroRNA-146A contributes to abnormal activation of the type I interferon pathway in human lupus by targeting the key signaling proteins. *Arthritis Rheum* 2009;**60**:1065–75
15. Mitchell PS, Parkin RK, Kroh EM, Fritz BR, Wyman SK, Pogosova-Agadjanyan EL, Peterson A, Noteboom J, O'Briant KC, Allen A, Lin DW, Urban N, Drescher CW, Knudsen BS, Stirewalt DL, Gentleman R, Vessella RL, Nelson PS, Martin DB, Tewari M. Circulating microRNAs as stable blood-based markers for cancer detection. *Proc Natl Acad Sci USA* 2008;**105**:10513–8
16. Terrault NA, Bzowej NH, Chang KM, Hwang JP, Jonas MM, Murad MH. AASLD guidelines for treatment of chronic hepatitis B. *Hepatology* 2016;**63**:261–83
17. Sugiyama M, Tanaka Y, Kato T, Orito E, Ito K, Acharya SK, Gish RG, Kramvis A, Shimada T, Izumi N, Kaito M, Miyakawa Y, Mizokami M. Influence of hepatitis B virus genotypes on the intra- and extracellular expression of viral DNA and antigens. *Hepatology* 2006;**44**:915–24
18. Froger A, Hall JE. Transformation of plasmid DNA into *E. coli* using the heat shock method. *J Vis Exp* 2007;**6**:253
19. Rogler CE, Levoci L, Ader T, Massimi A, Tchaikovskaya T, Norel R, Rogler LE. MicroRNA-23b cluster microRNAs regulate transforming growth factor-beta/bone morphogenetic protein signaling and liver stem cell differentiation by targeting Smads. *Hepatology* 2009;**50**:575–84
20. Yuan B, Dong R, Shi D, Zhou Y, Zhao Y, Miao M, Jiao B. Down-regulation of miR-23b may contribute to activation of the TGF-beta1/Smad3 signalling pathway during the termination stage of liver regeneration. *FEBS letters* 2011;**585**:927–34
21. Sarver AL, Li L, Subramanian S. MicroRNA miR-183 functions as an oncogene by targeting the transcription factor EGR1 and promoting tumor cell migration. *Cancer research* 2010;**70**:9570–9580
22. Li J, Fu H, Xu C, Tie Y, Xing R, Zhu J, Qin Y, Sun Z, Zheng X. miR-183 inhibits TGF-beta1-induced apoptosis by downregulation of PDCD4 expression in human hepatocellular carcinoma cells. *BMC Cancer* 2010;**10**:354
23. Belkaya S, Murray SE, Eitson JL, de la Morena MT, Forman JA, van Oers NS. Transgenic expression of microRNA-185 causes a developmental arrest of T cells by targeting multiple genes including Mzb1. *J Biol Chem* 2013;**288**:30752–62
24. Flach H, Rosenbaum M, Duchniewicz M, Kim S, Zhang SL, Cahalan MD, Mittler G, Grosschedl R. Mzb1 protein regulates calcium homeostasis, antibody secretion, and integrin activation in innate-like B cells. *Immunity* 2010;**33**:723–35
25. Goeppert B, Schmezer P, Dutruel C, Oakes C, Renner M, Breinig M, Warth A, Vogel MN, Mittelbronn M, Mehrabi A, Gdynia G, Penzel R, Longerich T, Breuhahn K, Popanda O, Plass C, Schirmacher P, Kern MA. Down-regulation of tumor suppressor A kinase anchor protein 12 in human hepatocarcinogenesis by epigenetic mechanisms. *Hepatology* 2010;**52**:2023–33
26. Li Y, Bai H, Zhang Z, Li W, Dong L, Wei X, Ma Y, Zhang J, Yu J, Sun G, Wang F. The up-regulation of miR-199b-5p in erythroid differentiation is associated with GATA-1 and NF-E2. *Mol Cells* 2014;**37**:213–9
27. Zhang Q, Yuan Y, Cui J, Xiao T, Jiang D. MiR-217 Promotes tumor proliferation in breast cancer via targeting DACH1. *J Cancer* 2015;**6**:184–91
28. Zhao WG, Yu SN, Lu ZH, Ma YH, Gu YM, Chen J. The miR-217 microRNA functions as a potential tumor suppressor in pancreatic ductal adenocarcinoma by targeting KRAS. *Carcinogenesis* 2010;**31**:1726–33
29. Asghari Alashti F, Minuchehr Z. MiRNAs which target CD3 subunits could be potential biomarkers for cancers. *PLoS One* 2013;**8**:e78790
30. Chen B, Duan L, Yin G, Tan J, Jiang X. Simultaneously expressed miR-424 and miR-381 synergistically suppress the proliferation and survival of renal cancer cells – Cdc2 activity is up-regulated by targeting WEE1. *Clinics* 2013;**68**:825–33
31. Shalom-Feuerstein R, Serror L, De La Forest Divonne S, Petit I, Aberdam E, Camargo L, Damour O, Vigouroux C, Solomon A, Gaggioli C, Itskovitz-Eldor J, Ahmad S, Aberdam D. Pluripotent stem cell model reveals essential roles for miR-450b-5p and miR-184 in embryonic corneal lineage specification. *Stem cells* 2012;**30**:898–909
32. Li A, Qian J, He J, Zhang Q, Zhai A, Song W, Li Y, Ling H, Zhong Z, Zhang F. Modulation of miR122 expression affects the interferon response in human hepatoma cells. *Mol Med Rep* 2013;**7**:585–90
33. Tnani M, Bayard BA. Evidence for IRF-1-dependent gene expression deficiency in interferon unresponsive HepG2 cells. *Biochim Biophys Acta* 1999;**1451**:59–72
34. Dai X, Zhang W, Zhang H, Sun S, Yu H, Guo Y, Kou Z, Zhao G, Du L, Jiang S, Zhang J, Li J, Zhou Y. Modulation of HBV replication by microRNA-15b through targeting hepatocyte nuclear factor 1alpha. *Nucleic Acids Res* 2014;**42**:6578–90
35. Cheng M, Si Y, Niu Y, Liu X, Li X, Zhao J, Jin Q, Yang W. High-throughput profiling of alpha interferon- and interleukin-28B-regulated microRNAs and identification of let-7s with anti-hepatitis C virus activity by targeting IGF2BP1. *J Virol* 2013;**87**:9707–18
36. Wang KC, Garmire LX, Young A, Nguyen P, Trinh A, Subramaniam S, Wang N, Shyy JY, Li YS, Chien S. Role of microRNA-23b in flow-regulation of Rb phosphorylation and endothelial cell growth. *Proc Natl Acad Sci USA* 2010;**107**:3234–9
37. Salvi A, Sabelli C, Moncini S, Venturin M, Arici B, Riva P, Portolani N, Giulini SM, De Petro G, Barlati S. MicroRNA-23b mediates urokinase and c-met downmodulation and a decreased migration of human hepatocellular carcinoma cells. *FEBS J* 2009;**276**:2966–82
38. Goodwin D, Rosenzweig B, Zhang J, Xu L, Stewart S, Thompson K, Rouse R. Evaluation of miR-216a and miR-217 as potential biomarkers of acute pancreatic injury in rats and mice. *Biomarkers* 2014;**19**:517–29
39. Belver L, de Yebenes VG, Ramiro AR. MicroRNAs prevent the generation of autoreactive antibodies. *Immunity* 2010;**33**:713–22
40. Danger R, Braza F, Giral M, Soulillou JP, Brouard S. MicroRNAs, major players in B cells homeostasis and function. *Front Immunol* 2014;**5**:98
41. Choi MC, Jong HS, Kim TY, Song SH, Lee DS, Lee JW, Kim TY, Kim NK, Bang YJ. AKAP12/Gravin is inactivated by epigenetic mechanism in human gastric carcinoma and shows growth suppressor activity. *Oncogene* 2004;**23**:7095–103
42. Flotho C, Paulun A, Batz C, Niemeyer CM. AKAP12, a gene with tumour suppressor properties, is a target of promoter DNA methylation in childhood myeloid malignancies. *Br J Haematol* 2007;**138**:644–50
43. Noh JH, Chang YG, Kim MG, Jung KH, Kim JK, Bae HJ, Eun JW, Shen Q, Kim SJ, Kwon SH, Park WS, Lee JY, Nam SW. MiR-145 functions as a tumor suppressor by directly targeting histone deacetylase 2 in liver cancer. *Cancer letters* 2013;**335**:455–62
44. Cui SY, Wang R, Chen LB. MicroRNA-145: a potent tumour suppressor that regulates multiple cellular pathways. *J Cell Mol Med* 2014;**18**:1913–26
45. Xu N, Zhang J, Shen C, Luo Y, Xia L, Xue F, Xia Q. Cisplatin-induced downregulation of miR-199a-5p increases drug resistance by activating autophagy in HCC cell. *Biochem Biophys Res Commun* 2012;**423**:826–31
46. Shen Q, Cicinnati VR, Zhang X, Iacob S, Weber F, Sotiropoulos GC, Radtke A, Lu M, Paul A, Gerken G, Beckebaum S. Role of microRNA-199a-5p and discoidin domain receptor 1 in human hepatocellular carcinoma invasion. *Molecular cancer* 2010;**9**:227
47. Davis MM. A new trigger for T cells. *Cell* 2002;**110**:285–7

(Received January 20, 2016, Accepted April 6, 2016)

Original Research

Human microRNAs profiling in response to influenza A viruses (subtypes pH1N1, H3N2, and H5N1)

Jarika Makkoch[1], Witthaya Poomipak[2], Suthat Saengchoowong[3], Kritsada Khongnomnan[1], Kesmanee Praianantathavorn[1], Thananya Jinato[4], Yong Poovorawan[5] and Sunchai Payungporn[1,4]

[1]Department of Biochemistry, Faculty of Medicine, Chulalongkorn University, Bangkok 10330 Thailand; [2]Research affairs, Faculty of Medicine, Chulalongkorn University, Bangkok 10330 Thailand; [3]Joint Chulalongkorn University – University of Liverpool PhD Programme in Biomedical Sciences and Biotechnology, Bangkok 10330, Thailand; [4]Systems Biology Center, Research Affairs, Faculty of Medicine, Chulalongkorn University, Bangkok, 10330 Thailand; [5]Center of Excellence in Clinical Virology, Faculty of Medicine, Chulalongkorn University, Bangkok 10330, Thailand

Corresponding author: Sunchai Payungporn. Email: sp.medbiochemcu@gmail.com

Abstract

MicroRNAs (miRNAs) play an important role in regulation of gene silencing and are involved in many cellular processes including inhibition of infected viral replication. This study investigated cellular miRNA expression profiles operating in response to influenza virus in early stage of infection which might be useful for understanding and control of viral infection. A549 cells were infected with different subtypes of influenza virus (pH1N1, H3N2 and H5N1). After 24 h post-infection, miRNAs were extracted and then used for DNA library construction. All DNA libraries with different indexes were pooled together with equal concentration, followed by high-throughput sequencing based on MiSeq platform. The miRNAs were identified and counted from sequencing data by using MiSeq reporter software. The miRNAs expressions were classified into up and downregulated miRNAs compared to those found in non-infected cells. Mostly, each subtype of influenza A virus triggered the upregulated responses in miRNA expression profiles. Hsa-miR-101, hsa-miR-193b, hsa-miR-23b, and hsa-miR-30e* were upregulated when infected with all three subtypes of influenza A virus. Target prediction results showed that virus infection can trigger genes in cellular process, metabolic process, developmental process and biological regulation. This study provided some insights into the cellular miRNA profiling in response to various subtypes of influenza A viruses in circulation and which have caused outbreaks in human population. The regulated miRNAs might be involved in virus–host interaction or host defense mechanism, which should be investigated for effective antiviral therapeutic interventions.

Keywords: miRNAs, influenza A virus, expression profiles, next-generation sequencing

***Experimental Biology and Medicine* 2016; 241: 409–420. DOI: 10.1177/1535370215611764**

Introduction

The pandemic influenza virus usually infects a large population, not only human but also livestock, such as swine and poultry, resulting in problems in public health and loss of economic distress in terms of hospitalization.[1,2] More than 284,000 people worldwide died because of pH1N1 after a year of pandemic.[3] Some strains of influenza virus can be zoonotic, such as H5N1, leading to great losses in the poultry industry, and with high mortality rate in reported human cases (>60%).[4–8] Unlike being infected with seasonal influenza, H5N1 infection can cause multi-organ failure, hemorrhagic syndrome and cytokine storm, suggesting that host genes can respond in a different manner depending on the specific strain of influenza virus infection. Previous studies showed that influenza virus principally controls host genes to facilitate viral replication in multiple steps, and one of the potential mechanisms to control gene expression is microRNA (miRNA) regulation.[9–13]

MiRNAs are small (17–24 nt in length), endogenous, non-coding RNAs found in multicellular organisms.[14] They are acknowledged as vigorous tool regulator molecules that can trigger the targeted gene functions by the translational repression or mRNA degradation through the RNA interference pathway.[14–18] Previous studies showed that the genome of more than 150 species including viruses contain sequences of mature miRNAs, especially in the human genome, in which more than 1000 miRNAs have been characterized.[16,19–21] Studies have expressed that a broad range of cellular mechanisms are mediated by miRNAs, such as cell proliferation signaling, chromosome maintenance, cell differentiation and apoptosis.[9,14,22–24] Not only can viruses regulate host gene expression by using miRNAs to promote

the viral life cycle, but the host cell can also alter differential gene expression to respond against viral infection via the miRNA mechanism. The proportion of the miRNA level due to the encounter between host and virus will indicate the disease progression and outcome.[25,26] Multiple pieces of evidence have shown that both host and virus constructed miRNAs are essential for virus propagation. It has been reported that the influenza virus plays a critical role in the modulation of the miRNA mechanisms of infected cells and animal models.[9,27–29] In contrast, miRNAs can also react with the influenza virus replication process. Many previous studies have mentioned that influenza virus replication and propagation were inhibited due to cellular miR-323, miR-491, miR-654 and miR-146a expression which specifically bind to the PB1 gene of the virus.[30,31]

Many techniques have been used to validate the miRNA screening and target prediction of miRNA response to influenza virus infection, such as qPCR, luciferase assay and drug compound library screening.[9,12,28,31] Among these, microarray techniques have been used extensively to study the miRNA profiles in response to the pathogenesis of the influenza virus.[32–35] Although microarray technique can gain a large amount of data of miRNA expression, it cannot determine the significance of particular genes in the cellular mechanism which are not covered by the probe set, and may lead to some essential genes, which slightly change, being dismissed. The high-throughput next-generation sequencing (NGS) can cope with these problems, as the dataset generated from NGS will demonstrate the genome-wide miRNA expression profiles of infected host cells. This study aimed to investigate cellular miRNA expression profiles operating in response to three specific strains of influenza A virus responsible for causing outbreaks in the human population; Avian-origin highly pathogenic avian influenza (HPAI) H5N1, human pandemic (pH1N1) and seasonal H3N2 influenza A virus infection. The study also aimed to predict target genes which might be useful for understanding the host defense mechanism in terms of regulating viral infection.

Materials and methods

Cell culture

A549 (human lung carcinoma) cells used in this study were kindly provided by Prof. Jen-Ren Wang, Department of Medical Laboratory Science and Biotechnology, Center of Infectious Disease and Signaling Research, National Cheng Kung University. A549 cells were cultured in Dulbecco's modified eagle medium (DMEM) (Thermo Scientific) containing 10% heat inactivated fetal bovine serum (Thermo Scientific) and 1% (v/v) antibiotic/antimycotic (Gibco) under humidified atmosphere with 5% CO_2 at 37°C.

Virus infection

A549 cells were seeded (3×10^5 cells/well) in DMEM medium without antibiotic/antimycotic in 6-well plates. Then influenza A viruses subtype pH1N1 (A/Thailand/104/2009), H3N2 (A/Thailand/CU-H187/2010) and H5N1 (A/Thailand/NK165/2005) were prepared by diluting the virus stocks with DMEM medium to yield the desired concentration of 3×10^5 pfu/mL (MOI = 0.5). Each viral infection was performed in triplicate in a biosafety level 3 (BSL3) laboratory, Faculty of Medicine, Chulalongkorn University. When cells reached approximately 80% confluence, cell culture media were removed from each well and cells were washed with 3 mL of phosphate buffer saline (PBS). After that 500 µl of each virus suspension was added into each well and then incubated in a humidified atmosphere with 5% CO_2 at 37°C for 1 h with occasional shaking to allow the virus to adsorb into the cells. After incubation, the virus suspension was removed from each well and then washed by 3 ml of PBS. Finally, 3 ml of complete DMEM medium was added into each well and cells were incubated for 24 h. The protocol of this study was approved by the Institutional Review Board (IRB No. 121/55), Faculty of Medicine, Chulalongkorn University.

Library preparation

After 24 h post infection, triplicate wells were pooled together and microRNAs were extracted by using a microRNA purification kit (Norgen) following the manufacturer's protocol. The concentrations of microRNA were quantified by using Qubit fluorometer (Invitrogen) with a Quant-iT^{TM} RNA Assay kit (Invitrogen). Purified microRNA (0.2 µg) from each group (uninfected cells, pH1N1 infected cells, H3N2 infected cells and H5N1 infected cells) were used to construct four libraries with different indexes according to a TruSeq Small RNA sample preparation kit (Illumina). The length of DNA libraries were validated by using Agilent 2100 Bioanalyzer system (Agilent) with a high sensitivity DNA chip (Agilent). The concentrations of DNA libraries were quantified by using Qubit fluorometer (Invitrogen) with a Quant-iT^{TM} DNA Assay kit (Invitrogen). The four DNA libraries were pooled together with equal concentration and then high-throughput sequenced using a MiSeq platform (Illumina).

Analysis of microRNA expression profiles

MiSeq reporter software version 2.4 was used for analysis of sequencing data. Low-quality reads (Q-score < 30) were excluded whereas low-quality regions of sequences were trimmed. The passing filtered reads (Q-score ≥ 30) were aligned with human genomic DNA (hg19), mature & precursor human miRNA (from miRbase) and contaminant RNA (human tRNA, rRNA and mRNA) using the Bowtie algorithm (http://bowtiebio.sourceforge.net). The clusters which matched to the miRNA database but not contaminant RNA were considered as miRNA. The miRNAs were classified and counted based on the number of reads matched to the miRbase (www.mirbase.org/).

Differential expression analysis and data visualization

The data of validated miRNAs expressed in cell culture obtained from next-generation sequencing platform were demonstrated in form of fold change, compared to the amount of those miRNAs expressed in control experiment (mock infection). Differential expression analysis was calculated in terms of fold changes

$$\text{Fold changes} = \log_2\left(\frac{\text{Normalized expression in case}}{\text{Normalized expression in control}}\right)$$

$$\text{Normalized expression in control} = \frac{\text{miRNA of interest in control}}{\text{Total count of miRNAs in control}}$$

$$\text{Normalized expression in case} = \frac{\text{miRNA of interest in case}}{\text{Total count of miRNAs in case}}$$

The data visualization was performed by using the GraphPad Prism 5 software to demonstrate the up-regulated and deregulated miRNAs.

Analysis of microRNA-target genes and biological process classification

Identifications of target genes for selected miRNAs were analyzed by using the experimentally validated miRNA-target interactions data accumulated in miRTarBase version 4.5 (http://mirtarbase.mbc.nctu.edu.tw/). Briefly, the target genes of miRNAs were selected based on strong experimental evidence obtained from validation methods including reporter assay, qPCR or western blot. The PANTHER (Protein ANalysis THrough Evolutionary Relationships) classification system version 9.0 (http://www.pantherdb.org/)[36] was used to classify genes and proteins in order to facilitate high-throughput analysis. Each of the validated target genes of miRNA were classified based on biological processes including apoptotic process (GO:0006915), biological adhesion (GO:0022610), biogenesis (GO:0071840), biological regulation (GO:0065007), cellular process (GO:0009987), developmental process (GO:0032502), immune system process (GO:0002378), localization (GO:0051179), multicellular organismal process (GO:0032501), metabolic process (GO:0008152), reproduction (GO:0000003), and response to stimulus (GO:0050896).

Prediction of protein–protein interaction

The target genes of significant miRNAs from NGS experiment were performed for protein interaction. The interactions among the proteins in this study were analyzed from the STRING 9.1 database,[37,38] which merges and weighs information from various sources, covering conserved neighborhood, gene fusions, phylogenetic occurrence, co-expression, experiments, database imports, and text-mining.[39] The scores greater than 0.7 are considered as the high confidence.

Results

Analysis of human miRNAs by NGS based on MiSeq platform

After 24 h of infection, triplicate wells of each group were pooled together in order to generate 4 DNA libraries including uninfected control, pH1N1, H3N2 and H5N1 influenza A virus infected cells. Then the 4 libraries with different indexes were subjected to high-throughput sequencing using MiSeq platform. A total of 3,654,615 reads were obtained from a high-throughput sequencing process. After data filtering based on quality score ($Q \geq 30$), 2,225,781 high-quality filtered reads were obtained and used for further analysis. The overall reads with a perfect match compared to sequences of miRNA database (miRBase version 16.0) (www.mirbase.org/) were characterized and counted. According to miRBase data, the results showed that there were totally 19,732 reads belonging to human miRNAs, including 4604, 6482, 4509 and 4137 of identified reads which were obtained from non-infected, pH1N1-infected, H3N2-infected and H5N1-infected cells, respectively.

Differential expression of miRNA profiling

MiRNAs expression profiles of A549 cells infected with each subtype of influenza A virus were compared with uninfected cells. The list of differentially expressed miRNAs was identified and classified as upregulated (>1.5 fold increase) and downregulated (<1.5 fold decrease) compared to those miRNA levels in uninfected cells. The full list of miRNA profiling is shown in Figure 1. A549 infected with pH1N1 influenza A virus expressed 10 downregulated miRNAs and 29 upregulated miRNAs. Infection of H3N2 influenza A virus showed seven downregulated miRNAs and 20 upregulated miRNAs while A549 cells infected with HPAI H5N1 influenza virus revealed five downregulated and 23 upregulated miRNAs. The miRNA expression profiles of cells infected with each subtype of influenza A virus were compared both in upregulated (Figure 2a) and downregulated (Figure 2b) miRNAs in order to identify common miRNA responses to multiple subtypes of influenza A virus. The results showed that four miRNAs including hsa-miR-101, hsa-miR-193b, hsa-miR-23b and hsa-miR-30e* were found to have upregulated expression when infected with all three strains of influenza A virus. The hsa-miR-128, hsa-miR-130a, hsa-miR-181c, hsa-miR-301a, hsa-miR-127-3p and hsa-miR-769-5p were upregulated in cells infected with H3N2 and H5N1 while let-7e and hsa-miR-15b were upregulated by pH1N1 and H5N1 infection. For downregulated miRNAs, hsa-miR-125b was downregulated by H5N1 and pH1N1 infection while only hsa-miR-484 was downregulated by H5N1 and H3N2 influenza viruses.

Analysis of common miRNA profiles in response to influenza A virus infection

MiRNA expression profiles obtained from this study were compared to previous studies which were performed in various subtypes of influenza A virus and cellular

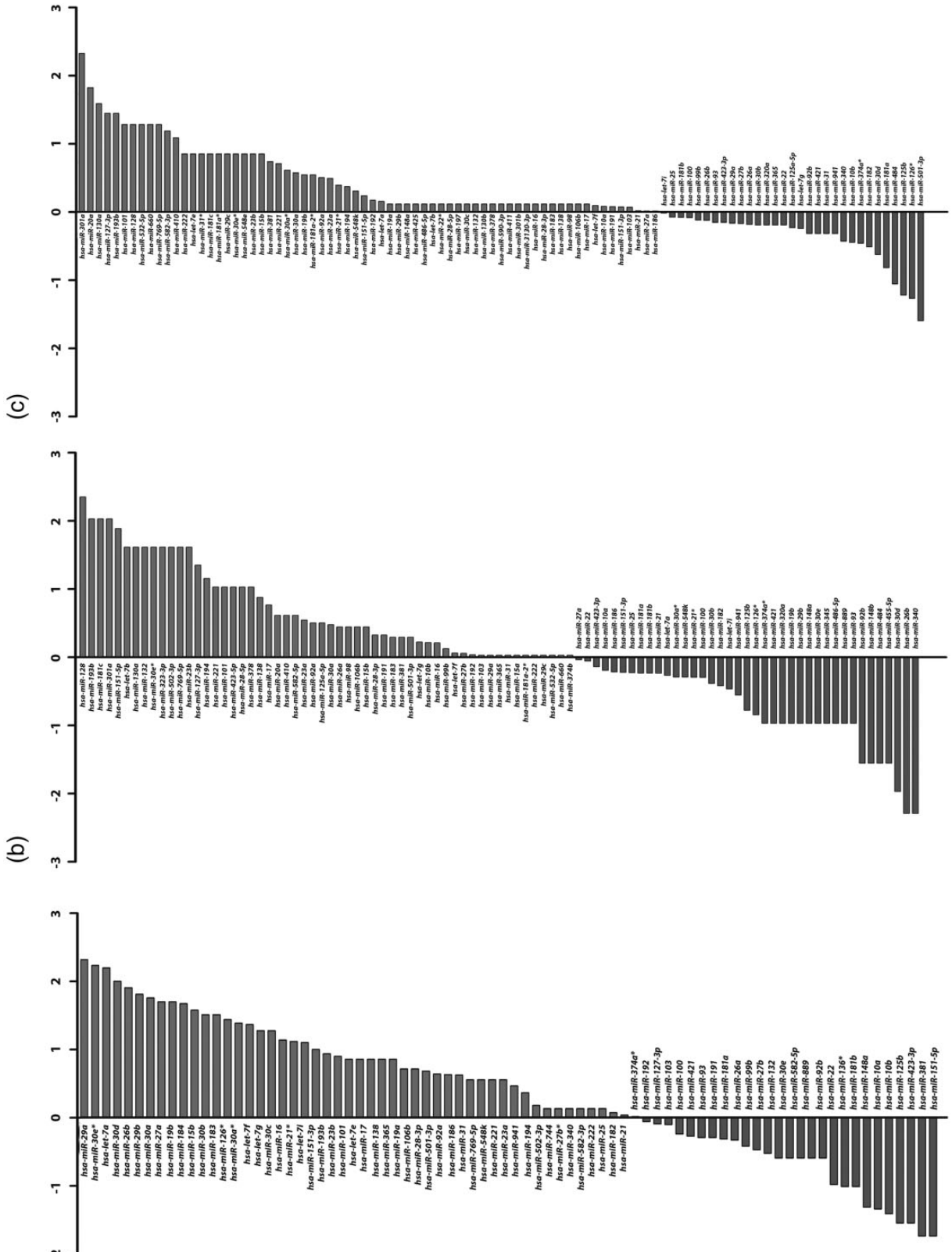

Figure 1 The miRNA expression profiles in each subtypes of influenza A virus infection. A549 cells were infected (MOI = 0.5) with three subtypes of influenza virus. (a) Seventy-eight miRNAs were expressed after infected with pH1N1 influenza virus, including 10 downregulated miRNAs, 29 upregulated miRNAs and 39 miRNAs that expressed in the similar level as control cells. (b) Infection of H3N2 influenza virus showed total of 95 miRNAs expression, including seven downregulated miRNAs, 20 upregulated miRNAs and 68 miRNAs that expressed in the similar level as control cells. (c) Ninety-nine miRNAs were responded in A549 cells infected with HPAI H5N1 influenza virus, five of which were downregulated, 23 miRNAs were upregulated and 71 miRNAs were expressed similar level compared to uninfected control

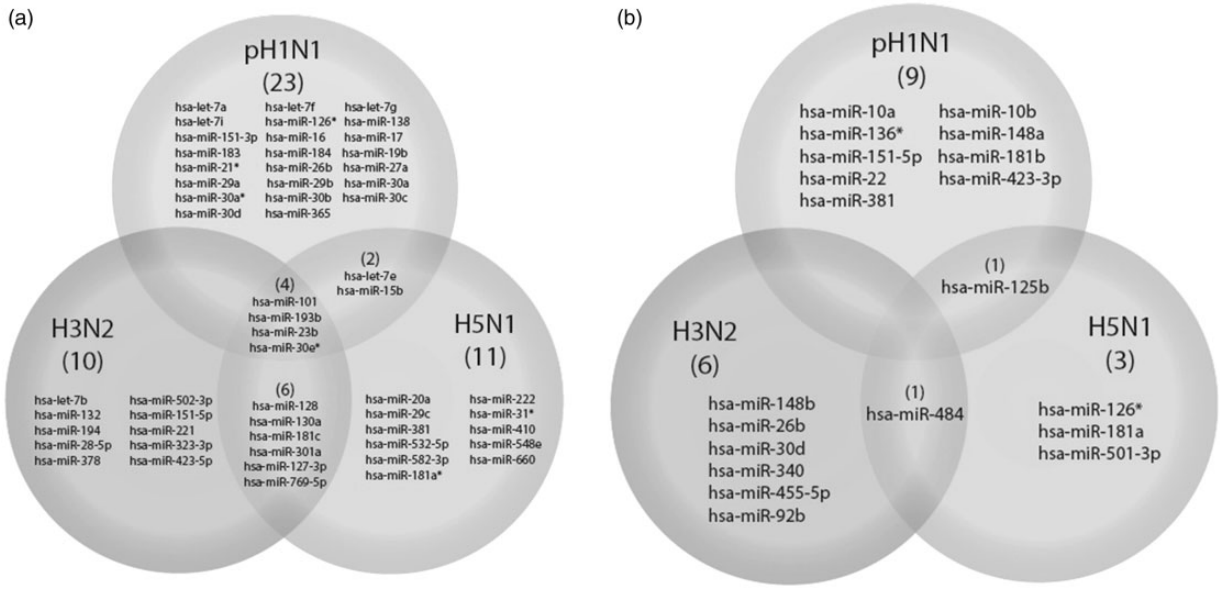

Figure 2 Venn-Euler diagram shows a summary of differentially expressed miRNAs in response to influenza A virus infection. (a) Upregulated miRNAs when infected with pH1N1, H5N1 and H3N2. (b) Downregulated miRNAs when the cells were infected by pH1N1, H3N2, and H5N1

models.[12,28,40–45] The comparative data suggested that there were 15 common miRNAs including let-7 family, miR-10, miR-15, miR-21, miR-29, miR-30, miR-34, miR-101, miR-132, miR-146, miR-148, miR-548, and miR-574 (Table 1).

Host target genes prediction of miRNA expression profile

After the analysis of common miRNA profiles in response to influenza A virus infection compared to several studies, 15 miRNAs were selected to be significant miRNAs that responded to influenza A virus infection. This study examined the target genes of miRNAs by miRNA-target interaction database called miRTarBase version 4.5 (http://mirtarbase.mbc.nctu.edu) and the PANTHER classification system. Using the information in the database for target prediction, the results showed that each miRNA could interact with hundreds of genes. We narrowed the targeted genes of miRNAs from the profile using strong experimental evidence of validation methods from previous studies. Using the PANTHER system, the number of target genes of the 15 selected miRNAs were summarized (Table 2). The number and percentages of miRNA target genes based on GO biological process classification of selected target genes were demonstrated. Each of the validated target genes for miRNAs was categorized based on types of biological processes, including apoptotic process (AP), biological adhesion (BA), biogenesis (BG), biological regulation (BR), cellular process (CP), developmental process (DP), immune system process (IP), localization (Lo), multicellular organismal process (MO), metabolic process (MP), reproduction (Re), and response to stimulus (Rs) (Table S1).

The protein–protein interactions provide information regarding most biological processes in an organism. In this study, the prediction of target proteins interaction via four deregulated miRNAs from our experiment, and therefore miR-101, miR-193b, miR-23b, and miR30a, were illustrated. The analysis of topology demonstrates important network illustrations created by interacting proteins. Therefore, the interactions between proteins from the STRING 9.1 database were used to form the target gene network of the differentially expressed microRNAs to determine several 'hub' nodes (Figure 3), which play an important role in apoptosis during the infection of influenza viruses. This finding may enlighten the understanding of the promising roles of the differentially expressed microRNAs.

Viral target genes prediction of miRNAs

Many previous studies showed that the cellular miRNAs can also target and modulate viral genes.[11,46] In this study, both the downregulated and upregulated miRNAs underwent the influenza virus target prediction compared to previous studies.[30,47,48] The result indicated that out of 11 miRNAs, nine of them were upregulated and targeted influenza virus genes. In this group, some of them can target only one viral gene, such as in the cases of miR-127, 128 and 29a, which target only PB1, PA, and HA gene, respectively, while some miRNAs, including miR-548, 222, and 16 can have multiple gene targets (Table 3). Most of the viral genes targeted by miRNAs in this study were related to polymerase activity (PB2, PB1 and PA).

Discussion

The present study provided miRNA profiling at an early stage of infection with three subtypes of influenza A virus (pH1N1, H3N2 and H5N1) by using next-generation sequencing. From the miRNA profiling results it was found that a number of host genes could be regulated by influenza A virus via the miRNA mechanism. The differential miRNA expressions can reveal the host-pathogen

Table 1 Common miRNAs expression profiles in response to influenza A virus infection obtained from several studies

Study description					Differentially expressed miRNAs (Δ = Up regulated; ∇ = Down regulated)													
Host	Cells/ tissues	Viral subtype	Infection time	Methods	let-7	miR-10	miR-15	miR-21	miR-29	miR-30	miR-34	miR-101	miR-132	miR-146	miR-148	miR-548	miR-574	References
Human	A549	pH1N1, H3N2, H5N1	24 h	NGS	Δ	∇	Δ	Δ	Δ	Δ		Δ	Δ		∇	Δ		This study
Human	A549	pH1N1	0, 4, 8, 24, 48, 72 h	qPCR	∇				∇	∇	Δ							9
Human	A549	H1N1, H3N2	24 h	qPCR										Δ				31
Human	A549	H1N1, H3N2	4, 24 h	Array		Δ	Δ		Δ			Δ			Δ			41
Human	A549	H1N1, H3N2	3 h	Array & qPCR												∇		42
Human	A549	H1N1, H3N2	8, 12, 24 h	Array & qPCR						Δ			Δ	Δ				40
Human	BEAS-2B	H1N1, H3N2	8, 12, 24 h	Array & qPCR	∇	Δ							Δ	Δ			Δ	40
Human	NCI-H292	H1N1, H5N1	3 h	Array & qPCR				Δ									Δ	12
Macaques	Lungs	H5N1, pH1N1 (1918)	1, 2, 4, 7 d	Array & qPCR	∇	∇		Δ	Δ	∇	∇	∇						28
Mice	Lungs	H5N1, pH1N1 (1918)	1, 3, 5 d	Array & qPCR	∇	∇		Δ	∇	∇	∇	∇						28
Mice	Lungs	H1N1	7 & 15 d	Array & qPCR	∇			Δ	∇	∇	∇							44
Dog	Lungs	H3N2	4 d	NGS & qPCR	Δ						Δ			∇				45
Pig	Lungs	H1N1, H3N2, H1N2	24 h, 72 h, 14 d	qPCR			Δ	Δ						∇				43

Table 2 Numbers of validated target genes of common miRNAs in response to influenza A virus

	Number and percentage of miRNA target genes based on GO biological process classification[a]												
miRNA family	**AP**	**BA**	**BG**	**BR**	**CP**	**DP**	**IP**	**Lo**	**MO**	**MP**	**Re**	**Rs**	**Total target genes**
let-7	13	9	5	35	51	25	8	13	13	51	8	9	240
	5.42%	3.75%	2.08%	14.58%	21.25%	10.42%	3.33%	5.42%	5.42%	21.25%	3.33%	3.75%	
miR-10	3	3	2	13	10	14	7	1	5	17	2	5	82
	3.66%	3.66%	2.44%	15.85%	12.20%	17.07%	8.54%	1.22%	6.10%	20.73%	2.44%	6.10%	
miR-15	5	1	0	15	18	8	2	3	2	16	4	5	79
	6.33%	1.27%	0.00%	18.99%	22.78%	10.13%	2.53%	3.80%	2.53%	20.25%	5.06%	6.33%	
miR-17	5	4	1	16	29	10	6	4	0	26	5	8	114
	4.39%	3.51%	0.88%	14.04%	25.44%	8.77%	5.26%	3.51%	0.00%	22.81%	4.39%	7.02%	
miR-20	2	1	1	15	22	7	5	2	1	23	4	6	89
	2.25%	1.12%	1.12%	16.85%	24.72%	7.87%	5.62%	2.25%	1.12%	25.84%	4.49%	6.74%	
miR-21	9	8	7	29	48	20	11	11	7	47	4	14	215
	4.19%	3.72%	3.26%	13.49%	22.33%	9.30%	5.12%	5.12%	3.26%	21.86%	1.86%	6.51%	
miR-29	2	11	7	12	20	14	7	8	9	11	2	10	113
	1.77%	9.73%	6.19%	10.62%	17.70%	12.39%	6.19%	7.08%	7.96%	9.73%	1.77%	8.85%	
miR-30	8	2	8	17	26	16	4	6	3	27	1	6	124
	6.45%	1.61%	6.45%	13.71%	20.97%	12.90%	3.23%	4.84%	2.42%	21.77%	0.81%	4.84%	
miR-34	2	2	0	10	10	6	3	0	3	11	2	1	50
	4.00%	4.00%	0.00%	20.00%	20.00%	12.00%	6.00%	0.00%	6.00%	22.00%	4.00%	2.00%	
miR-101	5	0	3	5	9	6	2	3	3	11	1	1	49
	10.20%	0.00%	6.12%	10.20%	18.37%	12.24%	4.08%	6.12%	6.12%	22.45%	2.04%	2.04%	
miR-132	0	0	2	8	9	1	0	0	0	8	2	1	31
	0.00%	0.00%	6.45%	25.81%	29.03%	3.23%	0.00%	0.00%	0.00%	25.81%	6.45%	3.23%	
miR-146	6	6	3	7	21	9	7	2	3	16	1	5	86
	6.98%	6.98%	3.49%	8.14%	24.42%	10.47%	8.14%	2.33%	3.49%	18.60%	1.16%	5.81%	
miR-148	1	3	1	3	10	5	3	2	2	8	1	3	42
	2.38%	7.14%	2.38%	7.14%	23.81%	11.90%	7.14%	4.76%	4.76%	19.05%	2.38%	7.14%	

Note: GO biological process of validated target genes was classified by PANTHER 9.0 classification system (http://www.pantherdb.org/) as the following: AP: apoptotic process (GO:0006915); BA: biological adhesion (GO:0022610); BG: biogenesis (GO:0071840); BR: biological regulation (GO:0065007); CP: cellular process (GO:0009987); DP: developmental process (GO:0032502); IP: immune system process (GO:0002378); Lo: localization (GO:0051179); MO: multicellular organismal process (GO:0032501); MP: metabolic process (GO:0008152); Re: reproduction (GO:0000003); Rs: response to stimulus (GO:0050896).

[a]Numbers of validated target genes were analyzed based on data (September 30, 2014) obtained from miRTarBase (http://mirtarbase.mbc.nctu.edu.tw/).

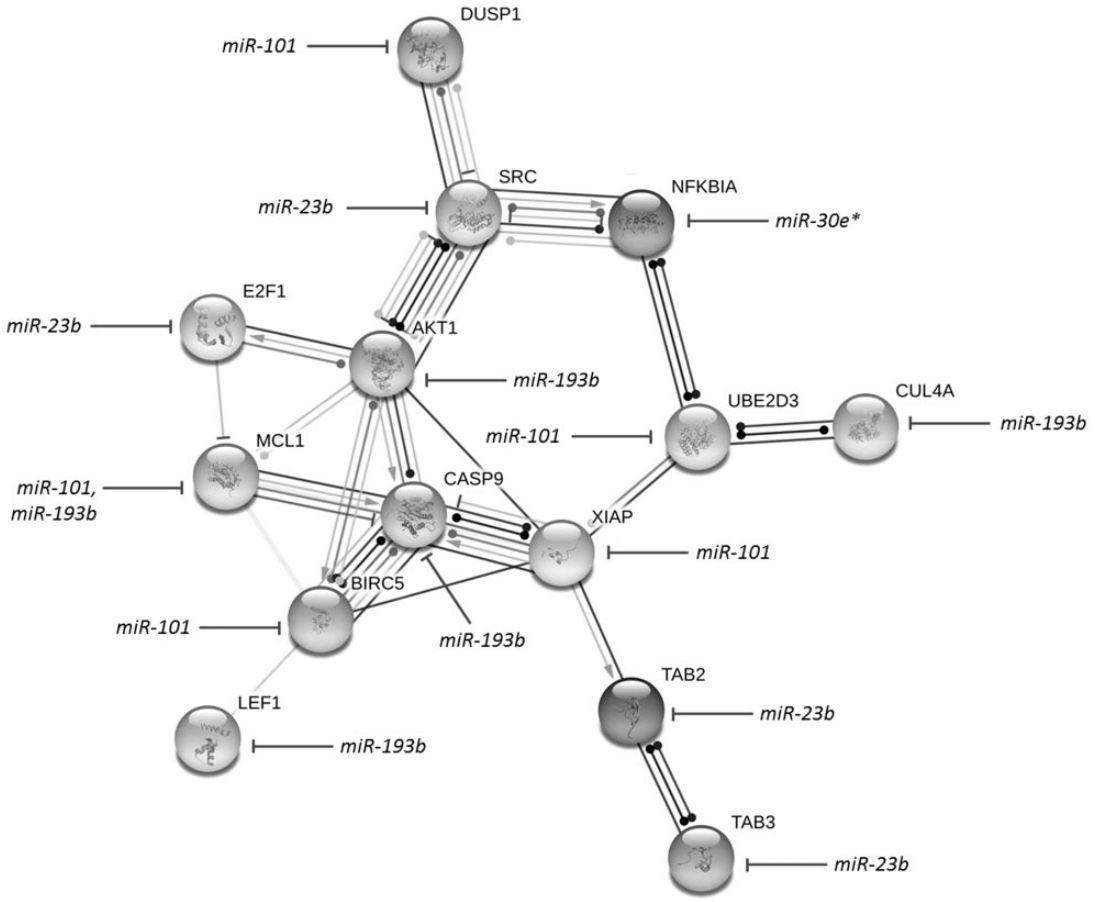

Figure 3 MicroRNA regulated network of target genes related to apoptosis in response to influenza virus infection. The STRING 9.1, together with data from Panther 9.0 constructed the interactions between proteins playing an important role in programmed cell death. As integrated with *in silico* analysis of microRNA target prediction, the pathway revealed the differentially expressed microRNAs controlling numerous target genes

Table 3 Viral targets of differentially expressed miRNAs in A549 infected with 3 subtypes of influenza virus

miRNAs	Ratios of infected/ non-infected (normalized)		Influenza virus segment
hsa-miR-127-3p	+1.35 (H3)		PB1
hsa-miR-128	+2.35 (H3)	+1.96 (H5)	PA
hsa-miR-29a	+9.25 (H1)	+1.74 (H5)	HA
hsa-miR-548	+1.15 (H5)		PB1, NS
hsa-miR-660	+1.74 (H5)		PA
hsa-miR-323	+1.62 (H3)		PB1
hsa-miR-let-7	+2.27 (H1)		M
hsa-miR-222	+2.22 (H5)	+2.22 (H5)	PB2, PB1,PA,NS1, NP, M
hsa-miR-16	+2.97 (H5)		PB2, PB1,PA,NS1, NP, M
hsa-miR-136	−0.38 (H1)		NP, HA
hsa-miR-92a	−1.55 (H3)		PB2

interaction in viral infection in two ways. First, the virus can hijack the host cellular mechanism by up- or downregulating the miRNAs involved in pathways that can promote viral replication. For example, the results showed that miR-181c was found to be upregulated in cells infected with H5N1 and H3N2 influenza A virus. The increase of this miRNA can target many genes associated with cellular immune defense, such as BCL2, IL-2, and Tnf,[49–51] and the deregulation of target genes can facilitate the influenza virus to avoid the suppressed host immune system. Second, the host cell can respond to viral infection via the miRNA mechanism by alteration of miRNAs which can have the effects on viral replication process to limit viral propagation. For example, the upregulation of miR-301 in H5N1 and H3N2 virus infection which can inhibit NKRF, the NFKB repressing factor, will promote the cytokine which indicates the innate and adaptive immunity response in mammalian cells.[52]

Many previous studies have suggested a correlation between influenza A virus infection and miRNA alteration. The infection of influenza virus can specifically activate the alteration of miRNAs including let-7 family, miR-30a-c, miR-132 and miR-30e* which might target in many genes function in lung repair.[44,53] However, the previous study found that miRNAs in let-7 family (let-7c, -7f, -7i), miR-30b and miR-26b were also upregulated by respiratory syncytial virus (RSV) infection,[53] implying that the alteration of these miRNAs are not only present against influenza virus infection but also other respiratory viruses.

The miRNA expression profiles were analyzed and compared to those from several studies which were obtained from different sample sources, viral strains, infection periods, and culture models, in order to discover the common miRNAs that overlapped between different systems. The results showed that some miRNAs were required to be considered. The miR-21, -29, -30, -34 and let-7 family were widely responsive to influenza virus infection in many systems. Interestingly, miR-15 and miR-21 were upregulated by influenza virus infection while miR-132, -30, and -101 were upregulated only in the human model system.

After the target prediction had been performed, most of the mechanisms due to virus infection were related to cellular processes, metabolic processes, developmental processes, and biological regulation (Table 2 and Table S1, Supplementary Information). Many miRNAs and their target genes should be considered and further discussed. MiR-101 can target MCL1, the anti-apoptosis gene and PRKDC, one of the large family of serine/threonine kinase,[54] which can play an important role in the receptor-mediated endocytosis process of the influenza life cycle, since the HA protein of the influenza virus can efficiently activate the PKC signaling pathway.[55,56] It has been reported that the influenza virus propagation process can be suppressed by a specific inhibitor of PKC.[57] Another miRNA that should be considered is the regulation of cell apoptosis via miR-29c (Figure 3) which was found to be upregulated in H5N1 infection. Much evidence suggests that this miRNA is involved in the virus-induced apoptosis pathway via the repression of anti-apoptotic agent, BCL2L2.[41] This is related to a previous study that found that the miR-29 family tends to be more upregulated due to influenza virus infection.[58] Moreover, some of the miRNA experimentally targeted genes play a critical role in immunoregulatory functions. For example, the upregulation of miR-15b suggests that infection of influenza virus can suppress the host immune response via miRNA mechanism. A previous study found that the IL-1B gene, the crucial regulator of inflammatory response, cellular activity including cell proliferation, differentiation and apoptosis, can decrease the expression of miR-let-7g and miR-26b.[53] Corresponding to this study, the high expression of let-7g and miR-26b indicated that the IL-1B has not been produced in the first 24 h after infection. In addition, our study showed that the upregulation of let-7 family (in all 3 subtypes infection), miR-29a, b (in pH1N1 infection) and mir-29c (in H5N1 infection) might have resulted from TNF-α and IL-4 still being inactive in the early phase of infection. However, the downregulation of miR-26b by H3N2 influenza virus infection should be considered, as it might be responsible for the different pathogenicity of H3N2 virus from pH1N1 virus and RSV.

A number of miRNAs have been found to be down regulated. Most of them can target genes associated with DNA methylation, protein degradation, and the signal transduction pathway. For example, the downregulation of miR-125b can trigger the MAPK signaling pathway, which regulates various cellular responses such as cell proliferation and apoptosis.[59,60] Previously, MAPK and CDK13 can be controlled by miR-548-3p and miR-138, which were, respectively,[61] identified as the mediators required for influenza virus replication. It is tempting to conclude that the upregulation of miR-548 (in H5N1 infection) and miR-138 (in pH1N1 infection) is the mechanism of the host response to limit influenza virus replication. Besides, a previous study suggested that the upregulation of MAPK protein can result from HA membrane accumulation due to the increase of polymerase activity. Interestingly, the upregulation of genes associated with DNA methylation via the decline of miRNA can cause the chromatin packaging, which can lead to the protein expression inhibition and may affect virus replication.

The difference of miRNA expression profile in cells infected with different subtypes might provide insight in the distinct pathogenicity of influenza virus. The result showed that there are four upregulated miRNAs including hsa-miR-101, hsa-miR-193b, hsa-miR-23b, and hsa-miR-30e*. Moreover, there were some strain-specific miRNAs which expressed in different levels in each subtype of influenza virus. The results showed that infection of H5N1 HPAI influenza virus can cause the highest amount of differential miRNA expression. Compared to a previous study, miR-31and miR-29c which are upregulated in H5N1 infection, and miR-29a and b, which are upregulated in pH1N1 infection, were confirmed to be potentially controlled during the early stage of influenza virus infection.[38] Interestingly, the results showed that miR-484 was found to be deregulated in cells infected with H5N1 and H3N2 influenza A virus. This miRNA can inhibit furin, the proteolytic enzyme that can cleave HA0 protein to facilitate influenza virus entry step. The downregulation of miR-484 will allow the host cell to produce more furin and promote the furin-dependent entry mechanism of the influenza viral life cycle.[62–64] One point of discussion should be considered, infection of the pH1N1 virus can recruit the miR-30 family, including miR-30a, miR-30a*, miR-30b, and miR-30c while only one member of miR-30 family was found to be deregulated in H3N2 infection, contrary to a previous study.[11] However, the previous study suggested that genetics of the subject might account for the regulation of miRNA expression,[65] so that genetic variation and a different cell culture system can affect the miRNA expression during influenza virus infection. While the previous study found that the change of miR-21*, miR-100*, miR-141, miR-574-3p, miR-1274a and b resulted from H5N1 infection in NCI-H292 cell line,[12] our results show the upregulation of miR-21* only. This suggested that the different cell culture might be responsible for various cellular responses via the miRNA mechanism. Moreover, compared to a previous study,[66] which investigated the miRNA profile of A/Udorn/72 (H3N2) infection, and suggested that the miRNA profile of the same subtype of influenza can be altered depending on the different genetic characteristics of the virus, the up-to-date virus infection can represent the virus that is presently circulating. In the study of Zhao et al.,[45] infection of canine influenza virus in lungs and trachea of dogs can cause the abundant expression of miR-143 and let-7. When compared to our study, the difference of miR-143 expression level may be due to the different characteristics of viral strains or host cells.

Infection with virus can alter many cellular mechanisms such as apoptosis which is one of the main machinery. Herein, we identified the genes and miRNAs observed in high-throughput sequencing that are involved in the apoptotic pathway by using STRING software (Figure 3). The pathway revealed the differentially expressed miRNAs controlling numerous target genes including NFKB, SOC, STAT, and IFN which can be regulated by many interesting miRNAs, including let-7 family, miR-101, miR-30, and miR-21, which might lead to development of miRNA therapeutics for influenza-like illness. However, many further experiments should be required such as western blot, *in vivo* study and pull down assays to make the refined observation and development.

Most of the upregulated miRNAs were predicted to target the influenza virus genome (Table 3). Most of them could bind to genes that have been reported in the early stage of influenza virus life cycle such as hemagglutinin and polymerase (PB2, PB1 and PA), which play the vital role in influenza virus entry mechanism and genome replication, respectively. In addition, a previous study suggested that miR-548an can mediate the influenza virus infection by regulation of non-structural-1A binding protein (NS1ABP),[42] corresponding to our study which found that the miR-548 was upregulated in H5N1 infection, implying that the host cell can produce more miR-548 against the exposure of influenza virus from an early stage of infection. Some miRNAs were found to be downregulated, suggesting that the virus can also trigger the miRNA pathway to fine-tune the miRNA mechanism to survive in host cells. The study in other time points after virus infection might reveal other differential miRNAs that can target other sites of the influenza virus genome, which may lead to the insight into the cellular mechanisms used to fight back against influenza virus infection. However, the built-on study by using widely used panel of robust tools, which are specific miRNAs inhibitors and miRNA mimics to knock down or increase the expression of miRNAs, is crucial to investigate the specific role of these candidate miRNAs.

Conclusion

In summary, this study provides the overall analysis of miRNA profiles in cell cultures infected with three different subtypes of influenza virus which have caused sporadic outbreaks in the human population, to gain insight into the overview of how the influenza virus can trigger the host cellular mechanism to facilitate itself to survive in host cells and also to find how cells can manipulate the cellular process to defend against influenza virus infection via the microRNA mechanism. This study provides information only in the early stage of infection, at 24 h post infection and can generate some potential candidate miRNAs and predicted target genes. This information can lead to the development of effective therapeutic agents, which have to interfere or control the influenza life cycle at an early stage of infection. Moreover, to explore the novel antiviral drugs, further analysis will be required such as miRNA profiling in late stages of infection or the study of knock-down and overexpression of candidate miRNAs.

Authors' contributions: JM analyzed the miRNA profiling and drafted the manuscript. WP carried out the NGS process, data processing and visualization. SS performed protein interaction network. KK assisted in cell culture and virus infection. KP assisted in NGS libraries preparation. TJ assisted in data analysis. YP provided stock of viruses and revised the manuscript. SP designed the study, data analysis, revised the manuscript and coordination. All authors read and approved the final manuscript.

ACKNOWLEDGEMENTS

The authors would like to gratefully acknowledge the Department of Biochemistry and Research affairs, Faculty of Medicine, Chulalongkorn University for their invaluable contribution to the success of this study. Funding for this study was supported by the Thailand Research Fund (TRF: RSA5680031); the Postdoctoral Scholarship, Ratchadapiseksompotch Fund (Faculty of Medicine, Chulalongkorn University); National Research University Project; Office of Higher Education Commission (WCU-007-HR-57); Centenary Academic Development Project (CU56-HR01); the Ratchadaphiseksomphot Endowment Fund of Chulalongkorn University (RES560530093); Research Chair Grant, National Science and Technology Development Agency (NSTDA) and Chulalongkorn Academic Advancement into its 2nd Century Project.

DECLARATION OF CONFLICTING INTERESTS

The authors hereby declare no personal or professional conflicts of interest with any aspect of this study.

REFERENCES

1. Baum M, Bielau S, Rittner N, Schmid K, Eggelbusch K, Dahms M, Schlauersbach A, Tahedl H, Beier M, Guimil R, Scheffler M, Hermann C, Funk JM, Wixmerten A, Rebscher H, Honig M, Andreae C, Buchner D, Moschel E, Glathe A, Jager E, Thom M, Greil A, Bestvater F, Obermeier F, Burgmaier J, Thome K, Weichert S, Hein S, Binnewies T, Foitzik V, Muller M, Stahler CF, Stahler PF. Validation of a novel, fully integrated and flexible microarray benchtop facility for gene expression profiling. *Nucleic Acids Res* 2003;**31**:e151
2. Smith GJ, Vijaykrishna D, Bahl J, Lycett SJ, Worobey M, Pybus OG, Ma SK, Cheung CL, Raghwani J, Bhatt S, Peiris JS, Guan Y, Rambaut A. Origins and evolutionary genomics of the 2009 swine-origin H1N1 influenza A epidemic. *Nature* 2009;**459**:1122–5
3. Dawood FS, Iuliano AD, Reed C, Meltzer MI, Shay DK, Cheng PY, Bandaranayake D, Breiman RF, Brooks WA, Buchy P, Feikin DR, Fowler KB, Gordon A, Hien NT, Horby P, Huang QS, Katz MA, Krishnan A, Lal R, Montgomery JM, Molbak K, Pebody R, Presanis AM, Razuri H, Steens A, Tinoco YO, Wallinga J, Yu H, Vong S, Bresee J, Widdowson MA. Estimated global mortality associated with the first 12 months of 2009 pandemic influenza A H1N1 virus circulation: a modelling study. *Lancet Infect Dis* 2012;**12**:687–95
4. Yuen KY, Chan PK, Peiris M, Tsang DN, Que TL, Shortridge KF, Cheung PT, To WK, Ho ET, Sung R, Cheng AF. Clinical features and rapid viral diagnosis of human disease associated with avian influenza A H5N1 virus. *Lancet* 1998;**351**:467–71
5. Tran TH, Nguyen TL, Nguyen TD, Luong TS, Pham PM, Nguyen v V, Pham TS, Vo CD, Le TQ, Ngo TT, Dao BK, Le PP, Nguyen TT, Hoang TL, Cao VT, Le TG, Nguyen DT, Le HN, Nguyen KT, Le HS, Le VT, Christiane D, Tran TT, Menno de J, Schultsz C, Cheng P, Lim W, Horby P, Farrar J, World Health Organization International Avian Influenza Investigative T. Avian influenza A (H5N1) in 10 patients in Vietnam. *New Engl J Med* 2004;**350**:1179–88

6. Chan PK. Outbreak of avian influenza A(H5N1) virus infection in Hong Kong in 1997. *Clin Infect Dis: an official publication of the Infectious Diseases Society of America* 2002;**34**:S58–64
7. Peiris JS, Yu WC, Leung CW, Cheung CY, Ng WF, Nicholls JM, Ng TK, Chan KH, Lai ST, Lim WL, Yuen KY, Guan Y. Re-emergence of fatal human influenza A subtype H5N1 disease. *Lancet* 2004;**363**:617–9
8. Komar N, Olsen B. Avian influenza virus (H5N1) mortality surveillance. *Emerg Infect Dis* 2008;**14**:1176–8
9. Loveday EK, Svinti V, Diederich S, Pasick J, Jean F. Temporal- and strain-specific host microRNA molecular signatures associated with swine-origin H1N1 and avian-origin H7N7 influenza A virus infection. *J Virol* 2012;**86**:6109–22
10. Meliopoulos VA, Andersen LE, Birrer KF, Simpson KJ, Lowenthal JW, Bean AG, Stambas J, Stewart CR, Tompkins SM, van Beusechem VW, Fraser I, Mhlanga M, Barichievy S, Smith Q, Leake D, Karpilow J, Buck A, Jona G, Tripp RA. Host gene targets for novel influenza therapies elucidated by high-throughput RNA interference screens. *FASEB J: official publication of the Federation of American Societies for Experimental Biology* 2012;**26**:1372–86
11. Wang Y, Brahmakshatriya V, Lupiani B, Reddy SM, Soibam B, Benham AL, Gunaratne P, Liu HC, Trakooljul N, Ing N, Okimoto R, Zhou H. Integrated analysis of microRNA expression and mRNA transcriptome in lungs of avian influenza virus infected broilers. *BMC Genomics* 2012;**13**:278
12. Lam WY, Yeung AC, Ngai KL, Li MS, To KF, Tsui SK, Chan PK. Effect of avian influenza A H5N1 infection on the expression of microRNA-141 in human respiratory epithelial cells. *BMC Microbiol* 2013;**13**:104
13. Wu Z, Hao R, Li P, Zhang X, Liu N, Qiu S, Wang L, Wang Y, Xue W, Liu K, Yang G, Cui J, Zhang C, Song H. MicroRNA expression profile of mouse lung infected with 2009 pandemic H1N1 influenza virus. *PloS ONE* 2013;**8**:e74190
14. Bartel DP. MicroRNAs: genomics, biogenesis, mechanism, and function. *Cell* 2004;**116**:281–97
15. Lagos-Quintana M, Rauhut R, Lendeckel W, Tuschl T. Identification of novel genes coding for small expressed RNAs. *Science* 2001;**294**:853–8
16. Lau NC, Lim LP, Weinstein EG, Bartel DP. An abundant class of tiny RNAs with probable regulatory roles in Caenorhabditis elegans. *Science* 2001;**294**:858–62
17. Lee RC, Ambros V. An extensive class of small RNAs in Caenorhabditis elegans. *Science* 2001;**294**:862–4
18. Ambros V. MicroRNAs and developmental timing. *Curr Opin Genet Develop* 2011;**21**:511–7
19. Lee RC, Feinbaum RL, Ambros V. The C. elegans heterochronic gene lin-4 encodes small RNAs with antisense complementarity to lin-14. *Cell* 1993;**75**:843–54
20. Griffiths-Jones S. The microRNA Registry. *Nucl Acids Res* 2004;**32**:D109–11
21. Griffiths-Jones S, Grocock RJ, van Dongen S, Bateman A, Enright AJ. miRBase: microRNA sequences, targets and gene nomenclature. *Nucleic Acids Res* 2006;**34**:D140–4
22. Calin GA, Sevignani C, Dumitru CD, Hyslop T, Noch E, Yendamuri S, Shimizu M, Rattan S, Bullrich F, Negrini M, Croce CM. Human microRNA genes are frequently located at fragile sites and genomic regions involved in cancers. *Proc Natl Acad Sci USA* 2004;**101**:2999–3004
23. John B, Enright AJ, Aravin A, Tuschl T, Sander C, Marks DS. Human microRNA targets. *PLoS Biol* 2004;**2**:e363
24. Wang B, Koh P, Winbanks C, Coughlan MT, McClelland A, Watson A, Jandeleit-Dahm K, Burns WC, Thomas MC, Cooper ME, Kantharidis P. miR-200a Prevents renal fibrogenesis through repression of TGF-beta2 expression. *Diabetes* 2011;**60**:280–7
25. Gottwein E, Cullen BR. Viral and cellular microRNAs as determinants of viral pathogenesis and immunity. *Cell Host Microbe* 2008;**3**:375–87
26. Skalsky RL, Cullen BR. Viruses, microRNAs, and host interactions. *Ann Rev Microbiol* 2010;**64**:123–41
27. Li Y, Chan EY, Li J, Ni C, Peng X, Rosenzweig E, Tumpey TM, Katze MG. MicroRNA expression and virulence in pandemic influenza virus-infected mice. *J Virol* 2010;**84**:3023–32
28. Li Y, Li J, Belisle S, Baskin CR, Tumpey TM, Katze MG. Differential microRNA expression and virulence of avian, 1918 reassortant, and reconstructed 1918 influenza A viruses. *Virology* 2011;**421**:105–13
29. Rogers JV, Price JA, Wendling MQ, Long JP, Bresler HS. Preliminary microRNA analysis in lung tissue to identify potential therapeutic targets against H5N1 infection. *Viral Immunol* 2012;**25**:3–11
30. Song L, Liu H, Gao S, Jiang W, Huang W. Cellular microRNAs inhibit replication of the H1N1 influenza A virus in infected cells. *J Virol* 2010;**84**:8849–60
31. Terrier O, Textoris J, Carron C, Marcel V, Bourdon JC, Rosa-Calatrava M. Host microRNA molecular signatures associated with human H1N1 and H3N2 influenza A viruses reveal an unanticipated antiviral activity for miR-146a. *J General Virol* 2013;**94**:985–95
32. Geiss GK, An MC, Bumgarner RE, Hammersmark E, Cunningham D, Katze MG. Global impact of influenza virus on cellular pathways is mediated by both replication-dependent and -independent events. *J Virol* 2001;**75**:4321–31
33. Severson WE, McDowell M, Ananthan S, Chung DH, Rasmussen L, Sosa MI, White EL, Noah J, Jonsson CB. High-throughput screening of a 100,000-compound library for inhibitors of influenza A virus (H3N2). *J Biomol Screen* 2008;**13**:879–87
34. Shih SR, Chu TY, Reddy GR, Tseng SN, Chen HL, Tang WF, Wu MS, Yeh JY, Chao YS, Hsu JT, Hsieh HP, Horng JT. Pyrazole compound BPR1P0034 with potent and selective anti-influenza virus activity. *J Biomed Sci* 2010;**17**:13
35. Borjabad A, Morgello S, Chao W, Kim SY, Brooks AI, Murray J, Potash MJ, Volsky DJ. Significant effects of antiretroviral therapy on global gene expression in brain tissues of patients with HIV-1-associated neurocognitive disorders. *PLoS Pathogen* 2011;**7**:e1002213
36. Mi H, Muruganujan A, Thomas PD. PANTHER in 2013: modeling the evolution of gene function, and other gene attributes, in the context of phylogenetic trees. *Nucl Acid Res* 2013;**41**:D377–86
37. Szklarczyk D, Franceschini A, Kuhn M, Simonovic M, Roth A, Minguez P, Doerks T, Stark M, Muller J, Bork P, Jensen LJ, von Mering C. The STRING database in 2011: functional interaction networks of proteins, globally integrated and scored. *Nucl Acid Res* 2011;**39**:D561–8
38. Song H, Wang Q, Guo Y, Liu S, Song R, Gao X, Dai L, Li B, Zhang D, Cheng J. Microarray analysis of microRNA expression in peripheral blood mononuclear cells of critically ill patients with influenza A (H1N1). *BMC Infect Dis* 2013;**13**:257
39. von Mering C, Jensen LJ, Snel B, Hooper SD, Krupp M, Foglierini M, Jouffre N, Huynen MA, Bork P. STRING: known and predicted protein-protein associations, integrated and transferred across organisms. *Nucl Acid Res* 2005;**33**:D433–7
40. Buggele WA, Johnson KE, Horvath CM. Influenza A virus infection of human respiratory cells induces primary microRNA expression. *J Biol Chem* 2012;**287**:31027–40
41. Guan Z, Shi N, Song Y, Zhang X, Zhang M, Duan M. Induction of the cellular microRNA-29c by influenza virus contributes to virus-mediated apoptosis through repression of antiapoptotic factors BCL2L2. *Biochem Biophys Res Commun* 2012;**425**:662–7
42. Othumpangat S, Noti JD, Blachere FM, Beezhold DH. Expression of non-structural-1A binding protein in lung epithelial cells is modulated by miRNA-548an on exposure to influenza A virus. *Virology* 2013;**447**:84–94
43. Skovgaard K, Cirera S, Vasby D, Podolska A, Breum SO, Durrwald R, Schlegel M, Heegaard PM. Expression of innate immune genes, proteins and microRNAs in lung tissue of pigs infected experimentally with influenza virus (H1N2). *Innate Immun* 2013;**19**:531–44
44. Tan KS, Choi H, Jiang X, Yin L, Seet JE, Patzel V, Engelward BP, Chow VT. Micro-RNAs in regenerating lungs: an integrative systems biology analysis of murine influenza pneumonia. *BMC Genom* 2014;**15**:587
45. Zhao FR, Su S, Zhou DH, Zhou P, Xu TC, Zhang LQ, Cao N, Qi WB, Zhang GH, Li SJ. Comparative analysis of microRNAs from the lungs and trachea of dogs (Canis familiaris) infected with canine influenza virus. *Infect Genet Evolut : journal of molecular epidemiology and evolutionary genetics in infectious diseases* 2014;**21**:367–74

46. Lecellier CH, Dunoyer P, Arar K, Lehmann-Che J, Eyquem S, Himber C, Saib A, Voinnet O. A cellular microRNA mediates antiviral defense in human cells. *Science* 2005;**308**:557–60
47. Scaria V, Hariharan M, Pillai B, Maiti S, Brahmachari SK. Host-virus genome interactions: Macro roles for microRNAs. *Cell Microbiol* 2007;**9**:2784–94
48. Khongnomnan K, Poomipak W, Poovorawan Y, Payungporn S. In silico Analysis of Human microRNAs Targeting Influenza a Viruses (subtype H1N1, H5N1 and H3N2). *World Acad Sci Eng Technol* 2012;**71**:433–9
49. Xue Q, Guo ZY, Li W, Wen WH, Meng YL, Jia LT, Wang J, Yao LB, Jin BQ, Wang T, Yang AG. Human activated CD4(+) T lymphocytes increase IL-2 expression by downregulating microRNA-181c. *Molecul Immunol* 2011;**48**:592–9
50. Ouyang YB, Lu Y, Yue S, Giffard RG. miR-181 targets multiple Bcl-2 family members and influences apoptosis and mitochondrial function in astrocytes. *Mitochondrion* 2012;**12**:213–9
51. Sun X, Icli B, Wara AK, Belkin N, He S, Kobzik L, Hunninghake GM, Vera MP, Registry M, Blackwell TS, Baron RM, Feinberg MW. MicroRNA-181b regulates NF-kappaB-mediated vascular inflammation. *J Clin Invest* 2012;**122**:1973–90
52. Chu WM, Ostertag D, Li ZW, Chang L, Chen Y, Hu Y, Williams B, Perrault J, Karin M. JNK2 and IKKbeta are required for activating the innate response to viral infection. *Immunity* 1999;**11**:721–31
53. Globinska A, Pawelczyk M, Kowalski ML. MicroRNAs and the immune response to respiratory virus infections. *Expert Rev Clin Immunol* 2014;**10**:963–71
54. Toker A. Signaling through protein kinase C. *Front Biosci: a journal and virtual library* 1998;**3**:D1134–47
55. Constantinescu SN, Cernescu CD, Popescu LM. Effects of protein kinase C inhibitors on viral entry and infectivity. *FEBS Lett* 1991;**292**:31–3
56. Kunzelmann K, Beesley AH, King NJ, Karupiah G, Young JA, Cook DI. Influenza virus inhibits amiloride-sensitive Na+ channels in respiratory epithelia. *Proc Natl Acad Sci USA* 2000;**97**:10282–7
57. Root CN, Wills EG, McNair LL, Whittaker GR. Entry of influenza viruses into cells is inhibited by a highly specific protein kinase C inhibitor. *J General Virol* 2000;**81**:2697–705
58. Zhang X, Dong C, Sun X, Li Z, Zhang M, Guan Z, Duan M. Induction of the cellular miR-29c by influenza virus inhibits the innate immune response through protection of A20 mRNA. *Biochem Biophys Res Commun* 2014;**450**:755–61
59. Pearson G, Robinson F, Beers Gibson T, Xu BE, Karandikar M, Berman K, Cobb MH. Mitogen-activated protein (MAP) kinase pathways: regulation and physiological functions. *Endocrine Rev* 2001;**22**:153–83
60. Dong C, Davis RJ, Flavell RA. MAP kinases in the immune response. *Ann Rev Immunol* 2002;**20**:55–72
61. Bakre A, Andersen LE, Meliopoulos V, Coleman K, Yan X, Brooks P, Crabtree J, Tompkins SM, Tripp RA. Identification of host kinase genes required for influenza virus replication and the regulatory role of microRNAs. *PloS ONE* 2013;**8**:e66796
62. Stieneke-Grober A, Vey M, Angliker H, Shaw E, Thomas G, Roberts C, Klenk HD, Garten W. Influenza virus hemagglutinin with multibasic cleavage site is activated by furin, a subtilisin-like endoprotease. *EMBO J* 1992;**11**:2407–14
63. Horimoto T, Nakayama K, Smeekens SP, Kawaoka Y. Proprotein-processing endoproteases PC6 and furin both activate hemagglutinin of virulent avian influenza viruses. *J Virol* 1994;**68**:6074–8
64. Luna C, Li G, Qiu J, Epstein DL, Gonzalez P. MicroRNA-24 regulates the processing of latent TGFbeta1 during cyclic mechanical stress in human trabecular meshwork cells through direct targeting of FURIN. *J Cell Physiol* 2011;**226**:1407–14
65. Bueno MJ, Perez de Castro I, Gomez de Cedron M, Santos J, Calin GA, Cigudosa JC, Croce CM, Fernandez-Piqueras J, Malumbres M. Genetic and epigenetic silencing of microRNA-203 enhances ABL1 and BCR-ABL1 oncogene expression. *Cancer cell* 2008;**13**:496–506
66. Buggele WA, Krause KE, Horvath CM. Small RNA profiling of influenza A virus-infected cells identifies miR-449b as a regulator of histone deacetylase 1 and interferon beta. *PloS ONE* 2013;**8**:e76560

(Received May 20, 2015, Accepted September 21, 2015)

Send Orders for Reprints to reprints@benthamscience.ae

MicroRNA, 2015, *4*, 123-130

Human miR-5193 Triggers Gene Silencing in Multiple Genotypes of Hepatitis B Virus

Apichaya Khlaiphuengsin[1,2], Nattanan Panjaworayan T-Thienprasert[3], Pisit Tangkijvanich[1,2], Nawarat Posuwan[4], Jarika Makkoch[1], Yong Poovorawan[4] and Sunchai Payungporn[1,2,5,*]

[1]*Department of Biochemistry, Faculty of Medicine, Chulalongkorn University, Bangkok, Thailand;* [2]*Research Unit of Hepatitis and Liver Cancer, Faculty of Medicine, Chulalongkorn University, Bangkok, Thailand;* [3]*Department of Biochemistry, Faculty of Science, Kasetsart University, Bangkok, Thailand;* [4]*Center of Excellence in Clinical Virology, Faculty of Medicine, Chulalongkorn University, Bangkok, Thailand;* [5]*Systems Biology Center, Research Affairs, Faculty of Medicine, Chulalongkorn University*

Sunchai Payungporn

Abstract: Hepatitis B virus (HBV) infection can lead to various disease states including asymptomatic, acute hepatitis, chronic hepatitis, liver cirrhosis and hepatocellular carcinoma (HCC), which remain a major health problem worldwide. Previous studies demonstrated that microRNA (miRNAs) plays an important role in viral replication. This study aimed to predict and evaluate human miRNAs targeting multiple genotypes of HBV. Candidate human miRNAs were analyzed by data obtained from miRBase and RNAhybrid. Then miRNAs were selected based on hybridization patterns and minimum free energy (MFE). The silencing effect of miRNA was evaluated by real-time PCR, the luciferase reporter assay and the ELISA assay. Five human miRNAs including miR-142-5p, miR-384, miR-500b, miR-4731-5p and miR-5193 were found to target several HBV genotypes. Interestingly, miR-5193 was found to be the most potent miRNA that could target against all HBV transcripts in almost all HBV genotypes with a highly stable hybridization pattern (5' canonical with MFE lower than -35 kcal/mol). Moreover, miR-5193 caused significant silencing in luciferase activity (53% reduction), luciferase transcript (60% reduction) and HBV surface antigen (HBsAg) production (20-40% reduction depending on genotypes). Therefore, miR-5193 might be useful and have a vital role for inhibition of HBV replication in the future.

Keywords: Gene expression, gene silencing, genotypes, hepatitis B virus, microRNAs, miR-5193.

INTRODUCTION

Hepatitis B virus (HBV) can be divided into 10 genotypes, genotypes A-J, depending on differences in genome sequence [1, 2]. The viral genome is a partially double-stranded DNA about 3.2 Kb and contains 4 overlapping open reading frames (ORFs) encoding for the viral core protein (HBc), the surface protein (HBs), the DNA polymerase (Pol) and the X regulatory protein [3, 4]. More than 350 million people worldwide are infected with chronic HBV, leading to various progressive disease states such as acute hepatitis, chronic hepatitis, liver cirrhosis and hepatocellular carcinoma (HCC) [5]. Progression of chronic HBV infection is related to several factors, including environmental factors (alcohol and alfatoxin consumption), viral factors (viral load and viral genotype) and host factors (age, sex, immunity and genetics). MicroRNAs (miRNAs) have been newly identified as a host factor regulating gene expression [6].

MiRNAs are non-coding RNAs that are transcribed from the host genome [7]. The process of miRNA biogenesis firstly begins within the nucleus to generate primary miRNA (pri-miRNA) consisting of hundreds to thousands of nucleotides with hairpin structures. The pri-miRNA is then trimmed by a nuclear RNase III protein, Drosha, to produce precursor miRNA (pre-miRNA) containing 60 to 100 nucleotides with a stem loop structure. After that the pre-miRNA is taken out of nucleus to cytoplasm by Exportin-5 [7]. The loop portion is then removed from the pre-miRNA by a ribonuclease III enzyme called Dicer to yield mature miRNA duplexes, approximately 22 nucleotides in length, with 2 nucleotide overhangs on the 5' and 3' ends [8]. The miRNA duplexes are then incorporated into the RNA-induced silencing complex (RISC) and one strand of miRNA is taken away by the helicase activity of the RISC. After strand separation, the single stranded miRNA strand guides RISC to bind to target mRNA. Consequently, miRNAs act as a key player in the regulation of gene expression in terms of gene silencing by mRNA degradation or translational repression. Therefore, miRNAs have been proposed as potential important biomolecules for clinical application [9].

Recently, many studies have shown that several miRNAs play a prominent role in regulation of viral infection and can be divided into 2 groups: viral miRNAs and cellular miRNAs. Previous reports have indicated that several viruses encode their own miRNAs including herpesviruses (HSVs) [10], Epstein–Barr-Virus (EBV) [11], Simian Virus 40

*Address correspondence to this author at the Department of Biochemistry, Faculty of Medicine, Chulalongkorn University, Rama 4 Rd. Pathumwan, Bangkok, Thailand 10330, Tel: +66-2256-4482; Fax: +66-2256-4482; E-mail: sp.medbiochemcu@gmail.com

2211-5374/15 $58.00+.00

(SV40) [12] and human immunodeficiency virus-1 (HIV-1) [13]. Viral miRNAs can target cellular mRNAs and interfere with cellular processes leading to pathogenesis. On the other hand, cellular miRNAs encoded by the host cell can target viral genes related to the replication of several infectious viruses such as primate foamy virus type 1 (PFV-1) [14], vesicular stomatitis virus (VSV) [15], hepatitis C virus (HCV) [16] and human papillomavirus (HPV) [17].

This study focused on the identification of human miRNAs targeting conserved regions among several HBV genotypes (A-J). Firstly, an *in silico* analysis was performed in order to predict the candidate human miRNAs targeting HBV genes. Then, the best candidate miRNA was evaluated based on silencing of a recombinant luciferase reporter gene and silencing of HBsAg production in cultured mammalian cells. This work identified hsa-miR-5193 as an effective silencer, implying that this miRNA might be useful and attractive for inhibition and treatment of HBV.

MATERIALS AND METHODS

Computational Analysis

The genome sequences of HBV were obtained from NCBI database (http://www.ncbi.nlm.nih.gov/). Ten HBV genotypes were used in this study, genotypes A (AM282986), B (DQ361535), C (AB246345), D (AB246347), E (AB091225), F (AB116654), G (AB056513), H (AY090457), I (AF241409) and J (AB486012). Each HBV genome sequence was separated into fragments, 50 bp in length. Each fragment had a 25 bp overlap with the fragment prior. Then, each 50 bp fragment was analyzed for sequence similarity against all human miRNAs in the miRBase database (http://www.mirbase.org/search.shtml). In miRBase, SSEARCH was used to find all human miRNAs that could align with HBV sequences. Mature human miRNAs with high sequence similarity to HBV sequences (> 40% match) were considered as candidate miRNAs. These candidate miRNAs further had their hybridization patterns and minimum free energy of base pairing predicted with HBV RNAs using RNAhybrid [18] (http://bibiserv.techfak.uni-bielefeld.de/rnahybrid/submission.html).

Criteria for Selection of MiRNAs

The potential hybridization patterns could be classified into 3 categories: 5'-seed, 5'-canonical and 3'-compensatory [19]. The 5'-seed pattern contains significant base pairing within the seed region (2-8 bp from the 5'-end of miRNA) whereas the 5'-canonical pattern has hybridization in the seed region and additional base pairing in 3'-end of the miRNA. The 3'-compensatory class is a hybridization pattern between miRNAs and their target RNAs by complimentary base pairing from the middle of the miRNAs to the 3′-end of miRNAs without base-pairing in the seed region. A minimum free energy (MFE) of less than -15 kcal/mol was used as another criterion for the selection of candidate miRNAs [20]. These criteria were successfully used for selection of miRNAs targeting HCV as described previously [21].

Constructions of a Reporter Vector and shRNA Expression Vectors

For a reporter vector construction, a partial HBV gene segment was ligated into the *Xho*I and *Nhe*I sites at the 3'-untranslated region (UTR) of a firefly luciferase gene, within a pGL3MS2/Basic vector, in order to generate a pGL3MS2/Basic-HBV reporter vector. The pGL3MS2/Basic vector was kindly provided by Dr. Brown, University of Otago, New Zealand [22]. This HBV partial segment was the predicted target of candidate human miR-5193. The pCMV-RLuc containing the *Renilla* luciferase reporter gene was used as a transfection control vector. For short hairpin RNA (shRNA) expression vectors, segments of miR-5193 or firefly luciferase genes were ligated into *BamH*I and *Hind*III restriction sites within a p*Silencer* 3.0-H1vector (Ambion®) to generate p*Silencer*-miR-5193 or p*Silencer*-Fluc, respectively (Table **1**).

Cloning Strategies

Top and bottom strand oligonucleotides (1 μg/μl) were mixed in 1X annealing buffer then denatured at 90°C for 3 min, followed by annealing at 37°C for 1 hour (Table **1**). After that the annealed fragment was ligated into a corre-

Table 1. Oligonucleotides used for vector constructions.

Oligos	Sequence (5'→3')	Vector name
HBV_TS	CTAGCCTTCAAAGACTGTGTGTTTACTGAGTGGGAGGC	pGL3MS2/Basic-HBV
HBV_BS	TCGAGCCTCCCACTCAGTAAACACACAGTCTTTGAAGG	
mir-5193_TS	GATCCGAACTGGGATGGGGGTTGGGGGGAGGTAAGAAGTCTCTGACTCCTCCTC-TACCTCATCCCAGTTTTTTTTGGAAA	p*Silencer*-miR-5193
mir-5193_BS	AGCTTTTCCAAAAAAAACTGGGATGAGGTAGAGGAGGAGTCAGAGACTTCT-TACCTCCCCCCAACCCCCATCCCAGTTCG	
siRNA-FLuc_TS	GATCCGCGCTGCTGGTGCCAACCCTTCAAGAGAGGGTTGGCACCAGCAGCGCTT-TTTTGGAAA	p*Silencer*-Fluc
siRNA-FLuc_BS	AGCTTTTCCAAAAAAGCGCTGCTGGTGCCAACCCTCTCTTGAAGGGTTGGCAC-CAGCAGCGCG	

sponding vector as previously described [23]. The recombinant plasmid was transformed into *E. coli* strain DH5α (RBS Bioscience) by a heat shock method and then a colony was selected with ampicillin resistance. The fidelity of each recombinant vector was confirmed via nucleotide sequencing.

Cell Cultures

Human hepatoblastoma HepG2 cells were cultured in Dulbecco's modified eagle medium (Thermo Scientific) containing 10% heat inactivated fetal bovine serum (Gibco) and 1% (v/v) antibiotic-antimycotic (Gibco) under humidified atmosphere with 5% CO_2 at 37°C.

Transfections of Reporter Vectors

Transfection was performed after seeding cells ($8x10^3$ cells/well) in medium without antibiotic-antimycotic in 96-well plates. When the cells reached approximately 80% confluence, the plasmids containing 100 ng of a reporter vector (pGL3MS2/Basic or pGL3MS2/Basic-HBV), 10 ng of a transfection control vector (pCMVRLuc containing *Renilla* luciferase reporter gene) and 50 ng of a shRNA expression vector (p*Silencer* scrambled negative silencing control or p*Silencer*-miR-5193 or p*Silencer*-Fluc positive silencing control) were diluted with Opti-MEM (Gibco) and then co-transfected into cells using 0.4 µl of Lipofectamine®2000 reagent (Invitrogen) following the manufacturer's instructions. The transfected cells were incubated in a humidified atmosphere with 5% CO_2 at 37°C for 72 hours and then harvested for the luciferase and real-time PCR assays.

Luciferase Assay

This assay was performed at 72 hours post-transfection by using the Dual-Luciferase Reporter assay system (Promega). According to the manufacturer's specification, the cells were washed with 100 µl phosphate buffer saline (PBS) and then lysed in 20 µl of the Passive Lysis Buffer. The suspensions were transferred into 96-well opaque bottom plate (Costar®). After that, 100 µl of Luciferase assay reagent II (LARII) was added into each well before measuring firefly luciferase activity at 560 nm, using a Multi-Mode Microplate reader (Synergy HT, BioTek). After that 100 µl of Stop and Glow reagent was added in order to stop the firefly luciferase and then *Renilla* luciferase activity was measured at 480 nm. The assay was performed in triplicates at least three independent experiments.

Real-time PCR Assay

RNA was extracted from the cell culture by RBC Real genomics total RNA extraction kit (RBC Bioscience) and treated with RQ1 RNase-Free DNase (Promega) to degrade single-stranded or double-stranded DNA. Then, cDNA was generated from the total RNA by using HelixCript™Thermo reverse transcriptase (Nanohelix) with random hexamers. GAPDH (Glyceraldehyde 3-phosphate dehydrogenase) and firefly luciferase genes were quantified by SYBR® Green-ER™ qPCR SuperMix universal (Invitrogen) using Step One Plus™ Real-time PCR Systems (Applied Biosystems). The GAPDH gene was used as an internal control to determine the relative expression levels of firefly luciferase. The qPCR primers used in this study were summarized in Table **2**. The thermal profile was 50°C for 2 min, 95°C for 3 min and 40 cycles of amplification (95°C for 15 sec, 58°C for 30 sec, 72°C for 1 min and 74°C for 30 sec with fluorescence detection at the end of each cycle). These data were analyzed by using Step One™ Software version 2.2 (Applied Biosystems). The relative quantification was calculated by using the comparative threshold (delta-delta Ct) method.

Transfection of HBV Plasmids and ELISA Assay

HepG2 cells were seeded ($5x10^4$ cells/well) in medium without antibiotic-antimycotic in 24-well plates. After 24 hours of incubation, 600 ng of the miRNA expression plasmid or pSlilencer-scramble was transiently co-transfected with 300 ng of each plasmid expressing the HBV genomes: A (AB246337), C (AB246345) and D (AB246347). All plasmids expressing HBV genomes were prepared as described previously [24]. These plasmids were generously provided by Prof. Yasuhito Tanaka, Nagoya City University Graduate School of Medical Sciences, Japan. After 72 hours of transfection, cell culture media and cell lysate were harvested for quantification of HBsAg levels by using the ARCHITECT i1000SR kit (Abbott) following the manufacturer's protocol based on the enzyme-linked immunosorbent assay (ELISA) [25].

Statistical Analysis

Difference between each group was analyzed by using the student's t test. A P value ≤ 0.05 was considered to be statistically significant.

RESULTS AND DISCUSSIONS

Prediction of Candidate Human MiRNAs Targeting HBV

During the viral replication cycle, HBV produces different RNA transcripts including pre-C/pre-genomic RNA (3.5 kb), pre-S1 (2.4 kb), pre-S2/S (2.1 kb) and X (0.9 kb). Therefore, those transcripts are proposed to be targeted by cellular miRNAs. Previously, Wu and colleagues [20] found 6 hu-

Table 2. Primers used for quantitative real-time PCR.

Primer name	Sequence (5'→3')	Gene	Size (bp)
FLuc_F FLuc_R	TCATAGAACTGCCTGCGTGAG ACATATCAAATATCCGAGTGTAGT	firefly luciferase	141
GAPDH_F GAPDH_R	GAGAAGGTCGGAGTCAACGGG TCAATGAAGGGGTCATTGATGG	GAPDH	106

man miRNAs, miR-7, miR-196b, miR-205, miR-345, miR-433 and miR-511, targeting conserved regions among HBV *adr*, *ayw* and *adw*2 subtypes. These miRNAs yielded the lowest minimum free energy (MFE) ranging from -21.12 to -25.71 kcal/mol. In addition, Potenza *et. al* (2001) identified 7 potential human miRNAs targeting conserved regions among HBV *ayw*, *adw* and *adr* subtypes. Those miRNAs consisted of miR-125a-5p, miR-125b, miR-151, miR-183, miR-326, miR-378 and miR-425 targeting the P/S ORF with a MFE ranging from -12.2 to -20.9 kcal/mol [23]. Moreover, miR-20a and miR-92a-1 were recently identified to target the HBV P/X ORF with a MFE of -22.1 and -23.1 kcal/mol respectively [26]. In previous studies different human miRNAs targeting HBV were identified using several variation factors such as accession number of HBV sequences, HBV genotypes, HBV subtypes, prediction softwares and criteria for miRNA selection.

In the present study, miRBase and RNAhybrid were used to predict candidate human miRNAs targeting HBV transcript among different genotypes (A-J). Candidate human miRNAs were analyzed based on their hybridization pattern and minimum free energy (MFE). This study predicted new miRNAs targeting HBV sequences that differed from those reported in the previous studies. According to the analysis across different genotypes of HBV, 5 human miRNAs, miR-142-5p, miR-384, miR-500b, miR-4731-5p and miR-5193, were found to target several HBV genotypes. The miR-142-5p targeted pre-C/pgRNA (3.5 kb) transcripts of HBV genotypes C, D, F and I with a 5' canonical hybridization pattern and MFE ranging from -17.0 to -17.2 kcal/mol. The miR-384 targeted to pre-C/pgRNA (3.5 kb) transcripts of HBV genotypes D, E, F and H with a 3' compensatory pattern and a MFE of approximately -23.8 kcal/mol. The miR-500b hybridized to pre-C/pgRNA (3.5 kb) transcripts of HBV genotypes E, G, I and J with a 3' compensatory pattern and MFE ranging from -21.0 to -23.1kcal/mol. The miR-4731-5p was predicted to target pre-C/ pgRNA (3.5 kb), pre S1 (2.4 kb) and pre S2/S (2.1 kb) transcripts of HBV genotypes C, D, E, G and J with a 5' canonical hybridization pattern and MFE of -26.6 to -29.5 kcal/mol. Interestingly, the miR-5193 performed complementary base pairing to all HBV transcripts in almost all genotypes of HBV (except genotype G) with a 5' canonical hybridization pattern and MFE ranging from -35.4 to -39.1 kcal/mol. Among the 5 predicted miRNAs targeting HBV, miR-5193 was found to be the most potent miRNA due to the ability to target all transcripts of HBV in almost all genotypes with the most stable hybridization. Based on the MFE, miR-5193 was more stable than other miRNAs targeting HBV described in previous reports. Therefore, miR-5193 was selected for *in vitro* analysis in order to evaluate the function of this miRNA. The hybridization pattern and MFE of each predicted miRNA were summarized in Table **3**.

Repression of Luciferase Activity Triggered by MiR-5193 Targeting HBV Segment

The evaluation of miRNA is based on the silencing of a reporter gene transfected in cultured mammalian cells. The candidate miRNA (miR-5193) was selected for constructing a miRNA expression vector. A partial HBV fragment containing a putative target site for human miR-5193 was cloned into the 3'-UTR of the firefly luciferase open reading frame in the pGL3MS2/Basic vector to generate a reporter-target vector: pGL3MS2/Basic-HBV. The pCMV-RLuc plasmid containing the *Renilla* luciferase reporter gene was used as a normalization reference gene. The recombinant plasmids were then co-transfected into HepG2 cells. Relative luciferase activity was measured 72 hours after transfection. The firefly luciferase signal was normalized against the *Renilla* luciferase signal, allowing accurate measurements of the expression level of the reporter gene. The basis for using this assay was that the binding of the miRNA (miR-5193) to the HBV viral target, transcribed together with the firefly luciferase gene, would repress firefly luciferase activity compared to the control.

For evaluation of luciferase activity repression, cells were divided into 6 groups (Fig. **1**). In each group, cells were transfected with equal amounts of the pCMV-RLuc control vector but with varying the reporter-target vector and the shRNA expression vector. Group A served as a negative silencing control as it was transfected with pGL3MS2/Basic (without HBV gene) and p*Silencer*-scramble (a scrambled sequence that is not complementary to any gene of the human genome). The mean of relative luciferase activity observed in group A was set as 100% for comparison with the other groups. Group B and E served as positive silencing controls as they were transfected with either pGL3MS2/ Basic (group B) or pGL3MS2/Basic-HBV (group E) and p*Silencer*-Fluc (specifically to hybridize and knockdown the firefly luciferase gene encoded by the reporter vector). The results showed that the relative luciferase activity observed in both group B (31.07% ± 7.36) and E (23.38% ± 15.02) was significantly lower than the control group (P = 0.008). The cells in group C were transfected with pGL3MS2/Basic and p*Silencer*-miR-5193 in order to test whether miR-5193 performed non-specific binding to the firefly luciferase gene. The results revealed no significant reduction (P = 0.304) of the relative luciferase activity in group C (84.01% ± 3.86), indicating that miR-5193 could not directly hybridize with the firefly luciferase gene. In group D, cells were transfected with pGL3MS2/Basic-HBV and p*Silencer*-scramble to test the silencing effect triggered by binding of endogenous cellular miR-5193 to the HBV gene within the 3'-UTR of the firefly luciferase gene. Result showed no significant difference (P = 0.788) of the relative luciferase activity between group D (103.87% ± 2.67) and the control, implying that endogenous cellular miR-5193 was expressed at insufficient levels to trigger silencing of the reporter gene. Finally, cells in group F were transfected with pGL3MS2/Basic-HBV and p*Silencer*-miR-5193 in order to investigate whether miR-5193 expressed from p*Silencer*-miR-5193 can bind to the HBV segment transcribed together with the firefly luciferase gene and trigger the repression of firefly luciferase activity. Interestingly, the relative luciferase activity in group F (47.62% ± 0.68) was significantly lower than those found in a control (P = 0.017), indicating that miR-5193 triggered a 53% reduction of the luciferase activity by targeting the HBV segment within the 3'-UTR of the firefly luciferase gene.

Table 3. Predicted miRNAs targeting multiple genotypes of HBV.

Human miRNAs (pattern)	Genotype	Hybridization of miRNA-target mRNA	MFE (kcal/mol)	HBV genome position	Target HBV transcript
miR-142-5p (5' canonical)	C	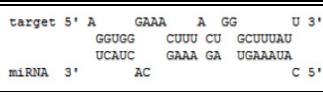	-17.2	2471-2495	pgRNA (3.5 kb)
	D	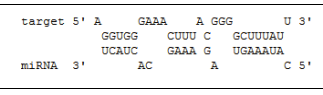	-17.1	2471-2495	
	F	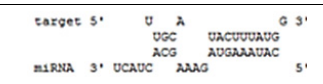	-17.1	2749-2761	
	I	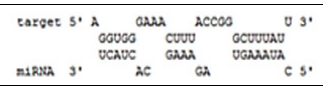	-17.0	2471-2495	
miR-384 (3' compensatory)	D	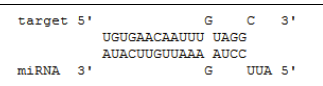	-23.5	2582-2598	pgRNA (3.5 kb)
	E	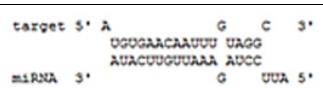	-23.8	2580-2596	
	F	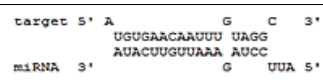	-23.8	2580-2596	
	H	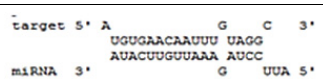	-23.8	2583-2599	
miR-500b (3' compensatory)	E	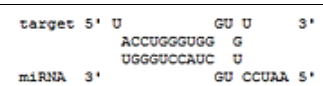	-21.0	2108-2120	pgRNA (3.5 kb)
	G	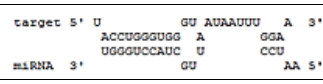	-22.5	2144-2166	
	I	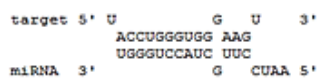	-23.1	2108-2121	
	J	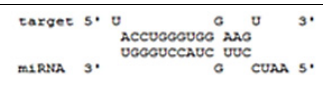	-23.1	2108-2121	
miR-4731-5p (5' canonical)	C	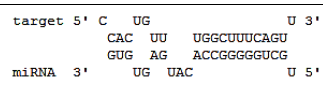	-26.6	718-735	pgRNA (3.5 kb), Pre S1 (2.4 kb), Pre S2/S (2.1 kb)
	D	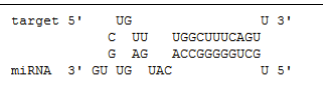	-22.6	720-735	
	E	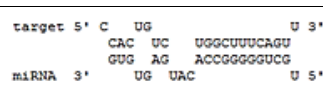	-27.7	718-735	
	G	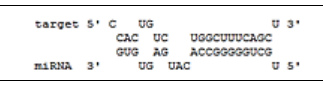	-29.5	718-735	
	J	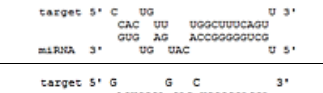	-26.6	718-735	
miR-5193 (5' canonical)	A	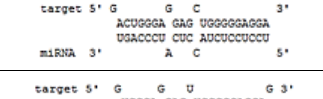	-38.3	1729-1750	pgRNA (3.5 kb), Pre S1 (2.4 kb), Pre S2/S (2.1 kb), X (0.9 kb)
	B	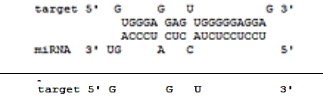	-35.4	1701-1720	
	C	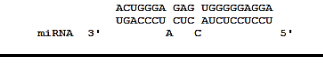	-38.3	1729-1750	

(Table 3) contd….

Human miRNAs (pattern)	Genotype	Hybridization of miRNA-target mRNA	MFE (kcal/mol)	HBV genome position	Target HBV transcript
miR-5193 (5' canonical)	D	target 5' G G U 3' ACUGGGA GAG UGGGGGAGGA UGACCCU CUC AUCUCCUCCU miRNA 3' A C 5'	-38.3	1729-1750	
	E	target 5' G G U 3' ACUGGGA GAG UGGGGGAGGA UGACCCU CUC AUCUCCUCCU miRNA 3' A C 5'	-38.3	1729-1750	
	F	target 5' G G C 3' ACUGGGA GAG UGGGGGAGGA UGACCCU CUC AUCUCCUCCU miRNA 3' A C 5'	-38.3	1729-1750	
	H	target 5' G G UC G 3' ACUGGGA GAG GGGGGAGGA UGACCCU CUC UCUCCUCCU miRNA 3' A CA 5'	-37.2	1732-1753	
	I	target 5' G G U G 3' ACUGGGA GAG UGGGGGAGGA UGACCCU CUC AUCUCCUCCU miRNA 3' A C 5'	-39.1	1729-1750	
	J	target 5' G G UC 3' ACUGGGA GAG AGGGGAGGA UGACCCU CUC UCUCCUCCU miRNA 3' A CA 5'	-36.4	1729-1750	

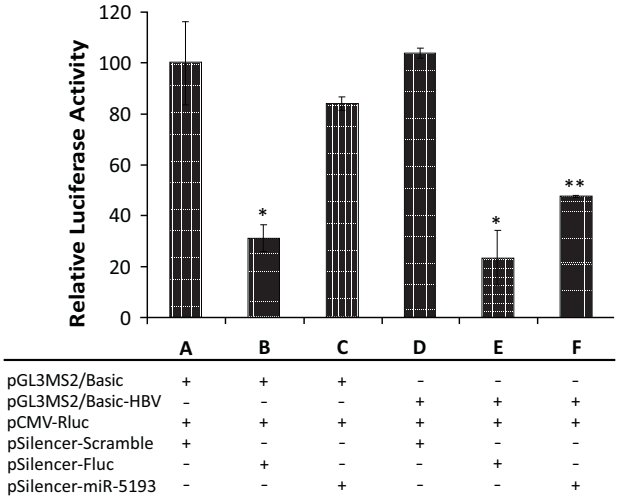

Fig. (1). Repression of luciferase activity. HepG2 cells were divided into 6 groups depending on different combination of transfected vectors including a control vector (pCMV-Rluc), a reporter vector (pGL3MS2/Basic or pGL3MS2/Basic-HBV) and a shRNA expression (p*Silencer*-Scramble or p*Silencer*-Fluc or p*Silencer*-miR-5193). After 72 hours post-transfection, relative luciferase acitivity was measured from firefly luciferase (Fluc) normalized with *Renilla* luciferase (Rluc) activities. Note that * indicates $P< 0.01$ whereas ** represents $P< 0.05$ when compared with a control group.

Degradation of Luciferase mRNA Triggered by MiR-5193 Targeting HBV Segment

Cells were co-transfected with a control vector, a reporter vector and a shRNA expression vector as described above. After 72 hours post-transfection, total RNAs were extracted from the cells in each group, followed by DNase treatment and cDNA synthesis. Then cDNA was used as a template for relative quantification by real-time PCR. The glyceraldehyde 3-phosphate dehydrogenase (GAPDH) gene served as an internal control for normalization of the firefly luciferase gene. In this experiment, cells were divided into 3 groups (Fig. **2**) depending on transfected vectors. The first group was a negative mRNA degradation control transfected with pGL3MS2/Basic and p*Silencer*-scramble. The mean of normalized luciferase mRNA level observed in the first group was set as 100% for comparison with other groups. The second group was a positive mRNA degradation control transfected with pGL3MS2/Basic and p*Silencer*-Fluc. The result showed that normalized firefly luciferase mRNA level in the second group (13.25% ± 8.13) was significantly lower than the control (P = 0.0002). The third group was transfected with pGL3MS2/Basic-HBV and p*Silencer*-miR-5193 in order to test the effect on mRNA degradation. The normalized firefly luciferase mRNA level in this group (40.63% ± 1.24) was significantly lower than that observed in the control group (P = 0.0002). This implied that the miR-5193 caused an approximate 60% reduction of the firefly luciferase mRNA level by targeting the HBV segment linked with the 3'-UTR of the firefly luciferase gene, triggering specific mRNA degradation.

Inhibition of Hepatitis B Surface Antigen (HBsAg) Production by MiR-5193

For evaluation of miR-5193's inhibition of HBsAg production, HepG2 cells were transiently co-transfected with 300 ng of plasmid expressing HBV genome genotypes A, C or D and 600 ng of p*Silencer* vector (scramble or miR-5193). After 72 hours post-transfection, the levels of HBsAg in cell lysates and supernatant were quantitated by the ELISA assay. As shown in the results (Fig. **3**), the levels of HBsAg in the control group (HBV genome plasmid and p*Silencer*-scramble co-transfected cells) were set as 100% in both the supernatant and cell lysate. In the supernatant, HBsAg secretion of HBV genotype A (84.35% ± 2.44; P = 0.0804), genotype C (65.66% ± 0.03; P = 0.0001) and genotype D (68.83% ± 4.29; P = 0.0049) were reduced by miR-5193 when compared to the control group (Fig. **3A**), implying that miR-5193 can inhibit the production and secretion of HBsAg in the supernatant. In addition, HBsAg expression in the cell

lysate transfected with the genome plasmid of HBV genotype A (88.59% ± 2.67; $P = 0.0150$), genotype C (84.82% ± 0.52; $P = 0.0019$) and genotype D (61.66% ± 0.45; $P = 0.0003$) were also significantly decreased by miR-5193 when compared to the control (Fig. **3B**), indicating that expression of HBsAg was suppressed by miR-5193.

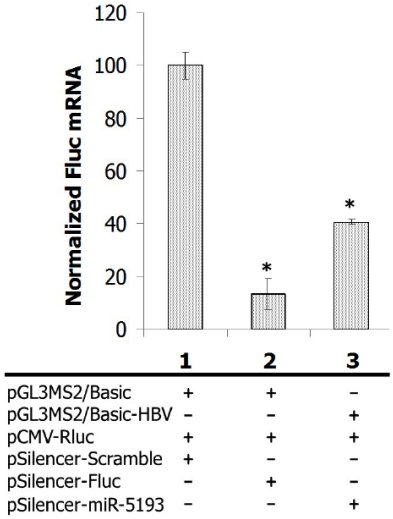

Fig. (2). Normalized mRNA level in cells transfected with different vectors. The amount of firefly luciferase (Fluc) was normalized with glyceraldehyde 3-phosphate dehydrogenase (GAPDH) internal control gene. Relative quantitation was performed by real-time PCR and calculated by delta-delta Ct method. Note that * indicates $P < 0.01$.

Other studies demonstrated that several miRNAs could regulate the silencing of HBV mRNAs or proteins. For example, miR-199a-3p and miR-210 have been proven to target HBV genes and able to suppress HBsAg expression [27]. In addition, miR-125a-5p was reported to interfere with HBsAg expression, reducing the amount of secreted HBsAg [23]. Recently, the miR-17-92 cluster including miR-20a and miR-92a-1 [26] were shown to target HBV mRNAs directly by the luciferase reporter assay and inhibit HBV replication.

In the present study, miR-5193 was shown to target HBV genomes by silencing of a luciferase reporter gene and revealed significant silencing in both mRNA and protein levels. Moreover, miR-5193 could suppress HBsAg translation in cell lysates and HBsAg production in the supernatant. However, the expression level of endogenous miR-5193 was quite low in HepG2 cell lines as implied by the results of the luciferase assay (Fig. **1**, group D). Moreover, the expression levels of miR-5193 were not significantly different between HepG2.2.15 and HepG2 cultured cells [28] implying that expression of miR-5193 was not altered by HBV infection. It is necessary to further investigate and identify a substance or components that could induce over-expression of endogenous miR-5193 in order to test whether enhancing of miR-5193 expression could inhibit HBV replication *in vivo* or not. In addition, recent studies have been developed cell culture models of HBV infection based on HepG2^{hNTCP} cells (human sodium taurocholate-cotransporting polypeptide transduction cells), which can turn the cell culture become more susceptible to HBV infection [29, 30], used to study cytolytic and non-cytolytic responses in HBV virus infection. These should be considered in order to expand the study of cellular response after HBV infection and to verify the genuine effects. Although the mechanisms of miRNA normally affect the endogenous cellular phenomenon, this cellular model would be used to imitate the natural processes in study of miRNAs which can affect the entry and propagation mechanism of HBV.

In summary, human miRNAs, miR-142-5p, miR-384, miR-500b, miR-4731-5p and miR-5193, were predicted to target several genotypes of hepatitis B virus. Among these predicted miRNAs, miR-5193 was selected for *in vitro* analysis as it could target all transcripts in almost all genotypes of HBV with a highly stable hybridization pattern during the *in silico* analysis. The miR-5193 revealed significant inhibition of luciferase mRNA and luciferase activity as well as HBsAg production. Therefore, miR-5193 might be useful and have a vital role for inhibition of HBV replication in the future.

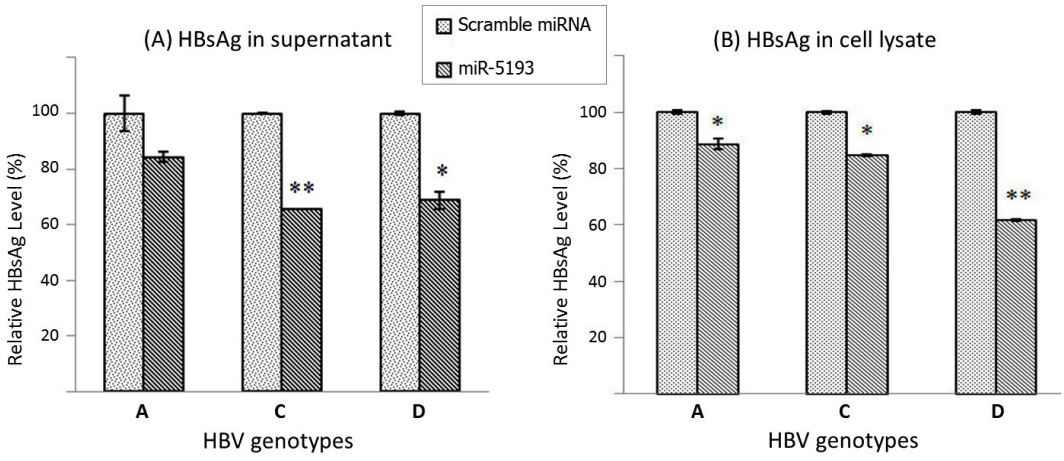

Fig. (3). Inhibition of HBsAg production by miR-5193. Hepatitis B surface antigen (HBsAg) was detected and quantitated by ELISA. (**A**) Levels of HBsAg secretion in supernatant. (**B**) Levels of HBsAg expression in cell lysates. Note that * indicates $P < 0.05$ and ** represents $P < 0.01$.

production. Therefore, miR-5193 might be useful and have a vital role for inhibition of HBV replication in the future.

CONFLICT OF INTEREST

The authors confirm that this article content has no conflict of interest.

ACKNOWLEDGEMENTS

We would like to thank Miss Emily Johnson, University of Liverpool, United Kingdom for grammatical corrections. This study was kindly supported by the Research Unit of Hepatitis and Liver Cancer and the Center of Excellence in Clinical Virology, Chulalongkorn University. Funding was supported by a Joint Research Program between Thailand and Japan (NRCT-JSPS); the Thailand Research Fund (RSA5680031); the Ratchadapiseksompotch Fund (Faculty of Medicine); the Research Chair Grant, the National Science and Technology Development Agency (NSTDA); CU GRADUATE SCHOOL THESIS GRANT; Ratchadapiseksompotch Endowment Fund of Chulalongkorn University (RES560530155) National Research University Project and Chulalongkorn Academic Advancement into Its 2nd Century Project.

AUTHOR'S CONTRIBUTIONS

AK carried out the computational analysis, *in vitro* experiment and drafted the manuscript. NPT carried out the plasmids' constructions and revised the manuscript. PT participated in data analysis. NP performed ELISA assay. JM and YP participated in revising the manuscript. SP conceived and designed the study, revised the manuscript and coordination. All authors read and approved the final manuscript.

REFERENCES

[1] Seeger C, Mason WS. Hepatitis B virus biology. Microbiol Mol Biol Rev 2000; 64: 51-68.

[2] Kurbanov F, Tanaka Y, Mizokami M. Geographical and genetic diversity of the human hepatitis B virus. Hepatol Res 2010; 40: 14-30.

[3] Liu WH, Yeh SH, Chen PJ. Role of microRNAs in hepatitis B virus replication and pathogenesis. Biochim Biophys Acta 2011; 1809: 678-85.

[4] Bar-Yishay I, Shaul Y, Shlomai A. Hepatocyte metabolic signalling pathways and regulation of hepatitis B virus expression. Liver Int 2011; 31: 282-90.

[5] Tian Y, Chen WL, Ou JH. Effects of interferon-α/β on HBV replication determined by viral load. PLoS Pathog 2011; 7: e1002159.

[6] Bartel DP. MicroRNAs: genomics, biogenesis, mechanism, and function. Cell 2004; 116: 281-97.

[7] Jin WB, Wu FL, Kong D, Guo AG. HBV-encoded microRNA candidate and its target. Comput Biol Chem 2007; 31: 124-6.

[8] Hsu PW, Lin LZ, Hsu SD, Hsu JB, Huang HD. ViTa: prediction of host microRNAs targets on viruses. Nucleic Acids Res 2007; 35(Database issue): D381-5.

[9] Zhang X, Hou J, Lu M. Regulation of hepatitis B virus replication by epigenetic mechanisms and microRNAs. Front Genet 2013, 4: 202.

[10] Pfeffer S, Sewer A, Lagos-Quintana M, *et al.* Identification of microRNAs of the herpesvirus family. Nat Methods 2005; 2: 269-76.

[11] Lo AK, To KF, Lo KW, *et al.* Modulation of LMP1 protein expression by EBV-encoded microRNAs. Proc Natl Acad Sci USA 2007; 104: 16164-9.

[12] Sullivan CS, Grundhoff AT, Tevethia S, Pipas JM, Ganem D. SV40-encoded microRNAs regulate viral gene expression and reduce susceptibility to cytotoxic T cells. Nature 2005; 435: 682-6.

[13] Omoto S, Ito M, Tsutsumi Y, *et al.* HIV-1 nef suppression by virally encoded microRNA. Retrovirology 2004; 1: 44.

[14] Lecellier CH, Dunoyer P, Arar K, *et al.* A cellular microRNA mediates antiviral defense in human cells. Science 2005; 308: 557-60.

[15] Otsuka M, Jing Q, Georgel P, *et al.* Hypersusceptibility to vesicular stomatitis virus infection in Dicer1-deficient mice is due to impaired miR24 and miR93 expression. Immunity 2007; 27: 123-34.

[16] Pedersen IM, Cheng G, Wieland S, *et al.* Interferon modulation of cellular microRNAs as an antiviral mechanism. Nature 2007; 449: 919-22.

[17] Nuovo GJ, Wu X, Volinia S, *et al.* Strong inverse correlation between microRNA-125b and human papillomavirus DNA in productive infection. Diagn Mol Pathol 2010; 19: 135-43.

[18] Krüger J, Rehmsmeier M. RNAhybrid: microRNA target prediction easy, fast and flexible. Nucleic Acids Res 2006; 34(Web Server issue): W451-4.

[19] Brennecke J, Stark A, Russell RB, Cohen SM. Principles of microRNA-target recognition. PLoS Biol 2005; 3: e85.

[20] Wu FL, Jin WB, Li JH, Guo AG. Targets for human encoded microRNAs in HBV genes. Virus Genes 2011; 42: 157-61.

[21] Plakunmonthon S, Panjaworayan T-Thienprasert N, Khongnomnan K, Poovorawan Y, Payungporn S. Computational prediction of hybridization patterns between hepatitis C viral genome and human microRNAs. J Comp Sci 2014; 5: 327-31.

[22] Rackham O, Brown CM. Visualization of RNA-protein interactions in living cells: FMRP and IMP1 interact on mRNAs. EMBO J 2004; 23: 3346-55.

[23] Potenza N, Papa U, Mosca N, Zerbini F, Nobile V, Russo A. Human microRNA hsa-miR-125a-5p interferes with expression of hepatitis B virus surface antigen. Nucleic Acids Res 2011; 39: 5157-63.

[24] Sugiyama M, Tanaka Y, Kato T, *et al.* Influence of hepatitis B virus genotypes on the intra- and extracellular expression of viral DNA and antigens. Hepatology 2006; 44: 915-24.

[25] Rukhsana J, Perrotta PL, Okorodudu AO, Petersen JR, Mohammad AA. Fit-for-purpose evaluation of architect i1000SR immunoassay analyzer. Clin Chim Acta 2010; 3: 798-801.

[26] Jung YJ, Kim JW, Park SJ, *et al.* c-Myc-mediated overexpression of miR-17-92 suppresses replication of hepatitis B virus in human hepatoma cells. J Med Virol 2013; 85: 969-78.

[27] Zhang GL, Li YX, Zheng SQ, Liu M, Li X, Tang H. Suppression of hepatitis B virus replication by microRNA-199a-3p and microRNA-210. Antiviral Res 2010; 88: 169-75.

[28] Liu Y, Zhao JJ, Wang CM, *et al.* Altered expression profiles of microRNAs in a stable hepatitis B virus-expressing cell line. Chin Med J (Engl) 2009; 122: 10-14.

[29] Hoh A, Heeg M, Ni Y, *et al.* Hepatitis B Virus-Infected HepG2hNTCP Cells Serve as a Novel Immunological Tool To Analyze the Antiviral Efficacy of CD8+ T Cells *In Vitro*. J Virol 2015; 89: 7433-8.

[30] Iwamoto M, Watashi K, Tsukuda S, *et al.* Evaluation and identification of hepatitis B virus entry inhibitors using HepG2 cells overexpressing a membrane transporter NTCP. Biochem Biophys Res Commun 2014; 44: 808-13.

Received: May 15, 2015 **Revised: July 16, 2015** **Accepted: August 18, 2015**

Original Research

Human miR-3145 inhibits influenza A viruses replication by targeting and silencing viral PB1 gene

Kritsada Khongnomnan[1], Jarika Makkoch[1], Witthaya Poomipak[2], Yong Poovorawan[3] and Sunchai Payungporn[1]

[1]Department of Biochemistry, Faculty of Medicine, Chulalongkorn University, Bangkok 10330, Thailand; [2]Research Affairs, Faculty of Medicine, Chulalongkorn University, Bangkok 10330, Thailand; [3]Center of excellent in clinical virology, Faculty of Medicine, Chulalongkorn University, Bangkok 10330, Thailand
Corresponding author: Sunchai Payungporn. Email: sp.medbiochemcu@gmail.com

Abstract

MicroRNAs (miRNAs) play an important role in the regulation of gene expression and are involved in many cellular processes including inhibition of viral replication in infected cells. In this study, three subtypes of influenza A viruses (pH1N1, H5N1 and H3N2) were analyzed to identify candidate human miRNAs targeting and silencing viral genes expression. Candidate human miRNAs were predicted by miRBase and RNAhybrid based on minimum free energy (MFE) and hybridization patterns between human miRNAs and viral target genes. *In silico* analysis presented 76 miRNAs targeting influenza A viruses, including 70 miRNAs that targeted specific subtypes (21 for pH1N1, 27 for H5N1 and 22 for H3N2) and 6 miRNAs (miR-216b, miR-3145, miR-3682, miR-4513, miR-4753 and miR-5693) that targeted multiple subtypes of influenza A viruses. Interestingly, miR-3145 is the only candidate miRNA targeting all three subtypes of influenza A viruses. The miR-3145 targets to PB1 encoding polymerase basic protein 1, which is the main component of the viral polymerase complex. The silencing effect of miR-3145 was validated by 3′-UTR reporter assay and inhibition of influenza viral replication in A549 cells. In 3′-UTR reporter assay, results revealed that miR-3145 triggered significant reduction of the luciferase activity. Moreover, expression of viral PB1 genes was also inhibited considerably (P value < 0.05) in viral infected cells expressing mimic miR-3145. In conclusion, this study demonstrated that human miR-3145 triggered silencing of viral PB1 genes and lead to inhibition of multiple subtypes of influenza viral replication. Therefore, hsa-miR-3145 might be useful for alternative treatment of influenza A viruses in the future.

Keywords: miRNA, miR-3145, silencing, inhibition, viral replication, influenza A virus

***Experimental Biology and Medicine* 2015; 240: 1630–1639. DOI: 10.1177/1535370215589051**

Introduction

Influenza A viruses are members of *Orthomyxoviridae* family. These enveloped viruses contain eight negative single strand RNA segments encoding for 11–12 viral proteins.[1] Infection of influenza A viruses can affect the upper respiratory system and cause asymptomatic to severe symptoms including fever, sneezing, coughing, runny nose, nasal congestion, and diarrhea.[1] Various subtypes of influenza A viruses can be classified by a combination of 17 different Hemagglutinin (HA) proteins and 10 various Neuraminidase (NA) proteins. The pH1N1, H5N1, and H3N2 subtypes cause serious worldwide public health concerns.[2,3] The therapeutic approaches are limited to targeting neuraminidase or M2 ion channels, as well as vaccines, which have been restricted due to seasonal antigenic drift. Recent studies suggest that cellular microRNAs (miRNAs) are involved in the regulation of viral replication; therefore, miRNAs might be useful for an alternative treatment against influenza A virus.

MiRNAs are small non-coding RNAs approximately 22 nucleotides in length.[4] MiRNAs are firstly transcribed as long hairpin RNAs called primary miRNAs (pri-miRNAs) which are continually cropped and trimmed to 60–100 nucleotides with a stem loop structure called precursor miRNAs (pre-miRNAs). The pre-miRNAs are then exported to cytoplasm by Exportin-5 protein. Cytoplasmic Dicer removes the loop structure of pre-miRNAs generating mature miRNA. Consequently, RNA-induced silencing complex (RISC) will assemble with miRNA duplexes and one strand of miRNA is removed by a helicase activity of the RISC while the remaining miRNA strand guides the RISC to a distinctive target mRNA via base pairing. MiRNAs regulate gene expression by mRNA degradation or translational repression, thus miRNAs play an important role in the

regulation of many cellular processes including cell proliferation, apoptosis, and homeostasis.[5] Moreover, cellular miRNAs also inhibit viral replications. For examples, hsa-miR-32 confines the accumulation of the primate foamy virus type 1 (PFV-1).[6] In 2010, Song et al. reported that miR-323 miR-491 and miR-654 target PB1 genes of H1N1 influenza A viruses (A/WSN/33), leading to viral gene silencing and blocking viral replication.[7] However, those miRNAs were proved to inhibit only one subtype (H1N1) of the influenza A virus in 1933, which may not represent the other subtypes or the recent strains of influenza A viruses infecting humans. Therefore, this study's purpose is to identify human miRNA targets in multiple subtypes of influenza A viruses such as pH1N1, H5N1 and H3N2, then to validate the candidate miRNA on viral gene silencing.

Materials and methods

Prediction of candidate miRNAs targeting influenza viral genes

Three subtypes of influenza A viruses including pH1N1 (A/Thailand/104/2009) [accession no. GQ169381-5, GQ205443, GQ229379 and GQ259597], H5N1 (A/Thailand/NK165/2005) [accession no. DQ372591-8] and H3N2 (A/Thailand/CU-H1817/2010) [accession no. CY074963-70] were used to predict human miRNAs that target them. Two web-based programs, miRBase[8–12] (www.mirbase.org) and RNAHybrid[13] (http://bibiserv.techfak.uni-bielefeld.de/rnahybrid/) were used to screen the human miRNAs that target viral genomes based on the principles of miRNA-target recognition[14] Hybridization patterns between the miRNAs and their target mRNAs can be classified into 5′ canonical, 5′ seed, and 3′ compensatory. Therefore, criteria for the selection of miRNAs targeting influenza viral genes is based on effective hybridization patterns (5′ canonical, 5′ seed, or 3′ compensatory) and minimum free energy (MFE) for base pairing less than −17.5 kcal/mol. Details of the computational prediction method was described in previous work.[15]

Construction of a reporter vector

Total viral RNA was extracted by the Guanidium-isothiocyanate method and then reverse transcribed by random hexamers with SuperScript® III reverse transcriptase (Invitrogen, Waltham, Massachusetts, USA) following the manufacturer's instruction. The targeting region fragment on viral PB1 genes was amplified by using *Nhe*I/PB1_ F and *Xho*I/PB1_R primers (Table 1). The thermal profile included an initial denaturation at 95°C for 3 min, 40 cycles of amplification (95°C for 15 s, 60°C for 15 s, and 72°C for 45 s) and final extension at 72°C for 7 min. These primers were designed with restriction sites of *Nhe*I and *Xho*I for ligation with a pGL3MS2/Basic reporter vector containing firefly luciferase (*FLuc*) as a reporter gene. The pGL3MS2/Basic vector and PB1 PCR product were digested by restriction enzymes *Nhe*I and *Xho*I (Thermo Scientific, Waltham, MA, USA). The digested products were analyzed by agarose gel electrophoresis and purified by HiYield™ Gel Extraction kit (RBC Bioscience, New Taipei City, Taiwan). Then, the partial PB1 DNA fragment was ligated into *Xho*I and *Nhe*I sites at 3′-UTR of a firefly luciferase gene within a pGL3MS2/Basic vector by T4 DNA ligase (Thermo Scientific). This constructed vector was called pGL3MS2/Basic_PB1.

Construction of silencing vectors

The pSilencer 3.0-H1 (Ambion®, Foster City, CA, USA) was used as a parent vector to construct the miRNA expression vector and positive silencing vector. For pSilencer_miR-3145 (encodes for hsa-miR-3145 short hairpin RNA), two oligonucleotides (1 μg/μL each) – miR-3145_TS (top strand) and miR-3145_BS (bottom strand) – were mixed in 1X annealing buffer then denatured at 90°C for 3 min, followed by annealing at 37°C for 1 h (Table 1). After that, the annealed fragment was ligated into *BamH*I and *Hind*III restriction sites within a pSilencer3.0-H1 according to the manufacturer's protocol. For pSilencer_FLuc (encodes for short hairpin RNA against firefly luciferase reporter gene), two oligonucleotides – shRNA-Luc_TS and shRNA-Luc_BS (Table 1) – were annealed and then inserted into pSilencer3.0-H1 with the same protocol as described above.

Plasmids propagation

Plasmids (pGL3MS2/Basic, pGL3MS2/Basic_PB1, pSilencer_scramble, pSilencer_FLuc and pSilencer_miR-3145) were transformed into competent cells (*E. coli* strain DH5α) (RBC Bioscience, New Taipei City, Taiwan) by a heat shock protocol and then a colony was selected based on ampicillin-resistant characteristics. Nucleotide sequencing was performed in order to confirm the fidelity of each recombinant vector. The concentration of each plasmid was measured by NanoDrop 1000 spectrophotometer (Thermo Scientific).

Cell culture

Human lung adenocarcinoma epithelial cells (A549) were cultured in DMEM (Thermo Scientific) containing 10% heat-inactivated fetal bovine serum (Thermo Scientific) and 1% (v/v) antibiotic-antimycotic (Gibco, Waltham, Massachusetts, USA) at 37°C under 5% CO_2 with 95% air atmosphere.

Plasmid transfection for 3′-UTR reporter assay

In 3′UTR reporter assay, A549 cells were seeded at 8×10^3 cells/well in medium without antibiotic-antimycotic in 96 well-plates and incubated for 24 hours. For transfection into each well, three plasmids including 100 ng of a reporter vector (pGL3MS2/Basic_PB1 or pGL3MS2/Basic), 50 ng of a silencing vector (pSilencer_scramble or pSilencer_miR-3145 or pSilencer_FLuc) and 10 ng of a control vector (pCMV_RLuc) were diluted with Opti-MEM (Gibco, Waltham, MA, USA) and then co-transfected into the A549 cells by using 0.4 μL of Lipofectamine®2000 (Invitrogen, Waltham, MA, USA) according to the manufacturer's protocol. The transfected cells were incubated in a humidified atmosphere with 5% CO_2 at 37°C for 72 hours and then harvested. The *Renilla* luciferase activity obtained

Table 1 Primers for quantitative PCR (qPCR) and oligonucleotides for plasmid construction used in this study

Primer/oligos	Sequence (5′ → 3′)	Strand	Application
PB1_ F	GACAGGGACATTTGAATTCAC	Sense	qPCR
PB1_R	GGTTTGATCCCACAGCTTCTT	Antisense	
GAPDH_F	GTGAAGGTCGGAGTCAACGG	Sense	qPCR
GAPDH_R	TCAATGAAGGGGTCATTGATGG	Antisense	
*Nhe*I/PB1_ F	TTGCTAGCGGATCCGACAGGGACATTTGAATTCAC	Sense	Reporter vector
*Xho*I/PB1_R	ACGGATCCTCGAGGTTTGATCCCACAGCTTCTT	Antisense	
miR-3145_TS	GATCCGTTCAACTCCAAACACTCAAAACTCATTGTTGAATGGAATGAG ATATTTTGAGTGTTTGGAATTGAATTTTTTGGAAA	Sense	Silencing vector
miR-3145_BS	AGCTTTTCCAAAAAATTCAATTCCAAACACTCAAAATATCTCATTCCA TTCAACAATGAGTTTTGAGTGTTTGGAGTTGAACG	Antisense	
shRNA-Luc_TS	GATCCGCGCTGCTGGTGCCAACCCTTCAAGAGAGGG TTGGCACCAGCAGCGCTTTTTTGGAAA	Sense	Silencing vector
shRNA-Luc_BS	AGCTTTTCCAAAAAAGCGCTGCTGGTGCCAACCCTCTCTT GAAGGGTTGGCACCAGCAGCGCG	Antisense	

Note: Underline indicates recognition sites of restriction enzymes.

from pCMV_RLuc was used for normalization of the relative luciferase assay.

Dual Luciferase Assay

The dual luciferase assay was performed by using Dual-Luciferase® Reporter Assay System (Promega, Madison, WI, USA) according to the manufacturer's instruction. Briefly, cells were washed with 100 µL of phosphate buffer saline and then lysed by adding 20 µL of the Passive Lysis Buffer. The suspensions were then transferred into a white opaque 96-well plate (Costar®). After that, 100 µL of Luciferase assay reagent II (LARII) was added into each well. The emissions of firefly luciferase activity at 560 nm were measured by Synergy HT Microplate reader (BioTek, Winooski, VT, USA). After that, 100 µL of Stop and Glow reagent was added in order to stop firefly luciferase and then measure *Renilla* luciferase activity at 480 nm. The assay was performed in triplicates in at least three independent experiments. The relative luciferase activity was calculated using signal intensities of firefly luciferase from a reporter vector divided by *Renilla* luciferase from a control vector.

Plasmid transfection for silencing of viral genes

In a 24-well plate, A549 cells were seeded at 5×10^4 cells/well in DMEM medium without antibiotic-antimycotic. After 24 h of incubation, 600 ng of a silencing vector (pSlilencer_ scramble or pSlilencer_miR-3145) was diluted with Opti-MEM (Gibco, Waltham, Massachusetts, USA) and then individually transfected into the A549 cells by using 1.25 µL of Lipofectamine®2000 (Invitrogen, Waltham, Massachusetts, USA). Then influenza A virus subtypes pH1N1 (A/Thailand/104/2009), H3N2 (A/Thailand/CU-H187/2010) and H5N1 (A/Thailand/NK165/2005) were prepared by diluting the virus stocks with DMEM medium to yield the desired viral titer. After 24 h post-transfection, cell culture media were removed from each well and cells were washed with 1 mL of phosphate buffer saline. After that, 500 µL of each virus suspension (MOI = 0.1) was added into each well and then incubated in a humidified atmosphere with 5% CO_2 at 37°C for 1 h with occasional shaking every 15 min to allow the virus to adsorb into the cells. After adsorption, the virus suspension was removed from each well and then washed with 1 mL of phosphate buffered saline. Finally, 1 mL of complete DMEM medium was added into each well and cells were incubated in a humidified atmosphere with 5% CO_2 at 37°C for 48 h. After that, supernatant and cell lysate were collected for further analysis. The experiments were performed in triplicates under a biosafety level 3 (BSL3) laboratory, Faculty of Medicine, Chulalongkorn University. The protocol of this study was approved by Institutional Review Board (IRB No. 121/55), Faculty of Medicine, Chulalongkorn University.

Real-time RT PCR

Total RNA was extracted from infected cell lysates by RBC Real genomics total RNA extraction kit (RBC Bioscience, New Taipei City, Taiwan) and then reverse transcribed with random hexamers by SuperScript® III reverse transcriptase (Invitrogen, Waltham, Massachusetts, USA). The viral PB1 gene and internal control GAPDH gene were quantified by Maxima SYBR Green/ROX qPCR Master Mix (Thermo Scientific). The primers used for amplifications of GAPDH and PB1 genes are summarized in Table 1. Real-time PCR amplification was carried out in Step One Plus™ Real-time PCR Systems (Applied Biosystems, Foster City, CA, USA). The thermal profile included one 3 min cycle at 95°C and 45 cycles of amplification (95°C for 15 s, 60°C for 15 s, 72°C for 45 s with fluorescence detection at the end of each cycle). After that, a melting curve analysis was performed by increasing the temperature from 60 to 95°C with a temperature transition rate of 0.5°C/s while continuously collecting the fluorescent signal. The results were analyzed using StepOne™ Software v.2.2 analysis. The relative quantitation was calculated by comparative C_T method to compare the viral gene

silencing between cells transfected with pSlilencer_miR-3145 and pSlilencer_scramble control.

Statistical analysis

Data obtained from relative luciferase activity and relative gene expression between each group was analyzed by Student's *t*-test. A $P \leq 0.05$ was considered statistically significant.

Results

Prediction of candidate human miRNA targeting multiple subtypes of influenza A viruses

Viral genomes obtained from three subtypes of influenza A viruses including pH1N1 (A/Thailand/104/2009), H5N1 (A/Thailand/NK165/2005) and H3N2 (A/Thailand/CU-H1817/2010) were used to predict human miRNA targets based on the miRNA-target recognition patterns (5′ canonical or 5′ seed or 3′ compensatory) and minimum free energy for base pairing (less than -17.5 kcal/mol) criteria. Computational prediction revealed that there were 76 human miRNAs targeting theninfluenza A viruses used in this study. Seventy miRNAs were found to specifically target each subtype of influenza A virus, 21 of which targeted H1N1 subtype, 27 targeted H5N1 subtype and 22 targeted H3N2 subtype (Figure 1). There were 6 miRNAs that targeted multiple subtypes of influenza A viruses including hsa-miR-216 b (target on NA gene of H5N1 and H3N2 subtypes), hsa-miR-3682 (target on NS gene of pH1N1 and H3N2 subtypes), hsa-miR-4513(target on PA gene of pH1N1 and H3N2 subtypes), hsa-miR-4753 (target on PA gene of pH1N1 subtype and PB1 gene of H5N1 subtype), hsa-miR-5693 (target on PA gene of H5N1 and H3N2 subtypes) and hsa-miR-3145 (target on PB1 gene of pH1N1, H5N1 and H3N2 subtypes). The hybridization pattern and MFE of each predicted candidate miRNA are summarized in Table 2.

Human miR-3145 targeting 3 subtypes of influenza A viruses

Interestingly, hsa-miR-3145 was the only candidate human miRNA targeting on PB1 gene of all three subtypes of

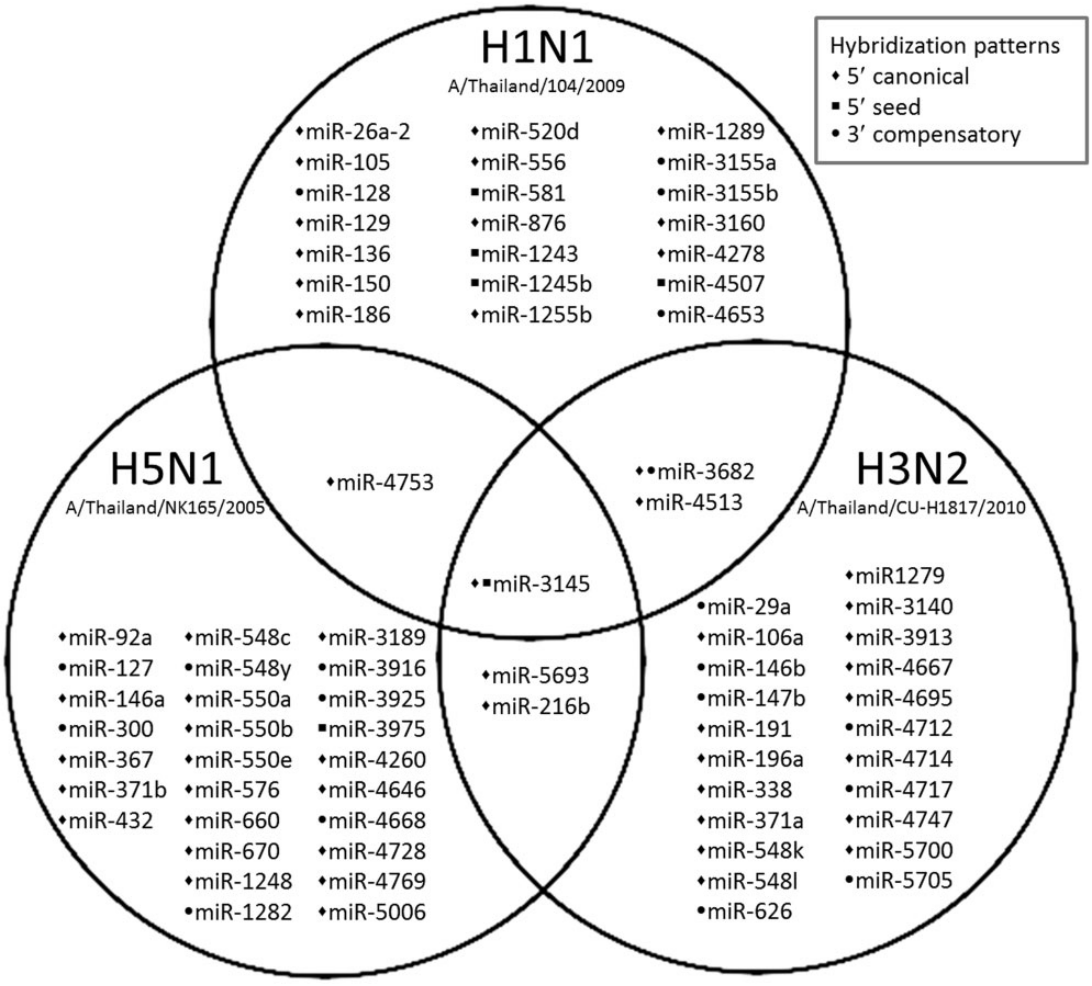

Figure 1 Venn-Euler diagram shows a summary of candidate human miRNAs targeting influenza A viruses subtype pH1N1, H5N1, and H3N2. Bullets refer to different types of hybridization patterns between miRNAs and target viral RNA. The prediction showed that 76 human miRNAs target influenza A viruses, including 70 miRNAs that targeted specific subtype (21 for pH1N1, 27 for H5N1 and 22 for H3N2) and 6 miRNAs (miR-216b, miR-3145, miR-3682, miR-4513, miR-4753 and miR-5693) that targeted multiple subtypes of influenza A virus

Table 2 Summary of candidate human miRNAs targeting multiple subtypes of influenza A viruses

Human miRNAs	Viral Subtype	Viral gene (position)	Hybridization pattern	MFE (kcal/mol)	Pairing pattern
miR-216 b	H5N1	NA (822–843)	target 5' A G G A 3' UCACAU UGU UGCAGGGAU AGUGUA ACG ACGUCUCUA miRNA 3' A G AA 5'	−31.3	5′canonical
	H3N2	NA (872–892)	target 5' G G G C 3' UCA AU UGUCUGCAGAGA AGU UA ACGGACGUCUCU miRNA 3' G A AAA 5'	−30.1	5′canonical
miR-3145	pH1N1	PB1 (1551–1570)	target 5' A C G 3' CC AGC UUUGGAGUGUCU GG UUG GAGUUUUAUAGA miRNA 3' GUUAA U U 5'	−18.2	5′seed
	H5N1	PB1 (1503–1541)	target 5' C UAUGGAGCUGCCC GU G 3' CAAUUUCAG A CUUGGAGUGUCU GUUAAGGUU U GAGUUUUAUAGA miRNA 3' GU 5'	−20.7	5′canonical
	H3N2	PB1 (1531–1549)	target 5' C U G 3' CCAG UUUGGAGUGUCU GGUU GAGUUUUAUAGA miRNA 3' GUUAA UGU 5'	−18.1	5′canonical
miR-3682	pH1N1	NS (1011–1028)	target 5' G UG GG U 3' U U UCCA GUAUCGUC A G AGGU CAUAGUAG miRNA 3' G UG GGA U 5'	−19.1	5′canonical
	H3N2	NS (580–600)	target 5' A UUC C 3' AUGAUAACACAG GAGU UACUAUUGUGUC UUCA miRNA 3' CAUC UC 5'	−22.6	3′compensatory
miR-4513	pH1N1	PA (587–609)	target 5' U A UU C 3' AUGGG UUCC UCGUCAGUC UACCC GAGG GGCAGUCAG miRNA 3' G UC A 5'	−32.3	5′canonical
	H3N2	PA (560–582)	target 5' U A UU C 3' AUGGG UUCC UCGUCAGUC UACCC GAGG GGCAGUCAG miRNA 3' G UC A 5'	−32.3	5′canonical
miR-4753	pH1N1	PA (1090–1115)	target 5' C AC ACAUG C 3' CAAGG AAAGA AAGAGAA GUUCC UUUCU UUCUCUU miRNA 3' UGU GA 5'	−20.9	5′canonical
	H5N1	PB1 (541–564)	target 5' A UUU C G 3' ACACA C AGAGAAAGAGAA UGUGU G UUUCUUUCUCUU miRNA 3' UCC A 5'	−20.9	5′canonical
miR-5693	H3N2	PA (1353–1370)	target 5' A UUU C G 3' ACACA C AGAGAAAGAGAA UGUGU G UUUCUUUCUCUU miRNA 3' UCC A 5'	−27.9	5′canonical
	H5N1	PA (1353–1370)	target 5' C G A 3' CAUU UAGAGCCACUG GUAA GUCUCGGUGAC miRNA 3' CUCAA A G 5'	−28.7	5′canonical

influenza A viruses. The hybridization patterns between hsa-miR-3145 and its viral PB1 target in different subtypes of influenza A viruses were slightly different (Table 2). For pH1N1, the hybridization was classified as ''5′seed'' with the pairing energy or minimum free energy (MFE) at −18.2 kcal/mol. With H5N1, hsa-miR-3145 was hybridized with a ''5′canonical'' pattern with MFE at −20.7 kcal/mol. The PB1 of H3N2 targeted a ''5′canonical'' pattern with

MFE at −18.1 kcal/mol. Moreover, alignment of PB1 genes obtained from various strains of human influenza A viruses revealed that PB1 target sites for the seed region of hsa-miR-3145 were conserved among various strains of the viruses (Figure 2). Implying that hsa-miR-3145 might be able to target PB1 of several strains of influenza A viruses. The silencing of PB1 expression by hsa-miR-3145 might have some effects on the replication of influenza A viruses. Therefore, hsa-miR-3145 was selected for further investigation.

Human miR-3145 targeted viral PB1 gene

To investigate the ability of hsa-miR-3145 to target viral PB1 gene, a 3′-UTR reporter assay was performed. According to the conserved target regions in PB1 genes among three viral subtypes, the pH1N1 virus was selected to be the representative for hsa-miR-3145 targeting validation. The pGL3MS2/Basic_PB1 reporter vector was constructed by adding a viral PB1 target region into 3′UTR of the firefly luciferase (*FLuc*) reporter gene in pGL3MS2/Basic vector. The pSilencer_scramble vector (a scrambled sequence that is not complemented by any gene of the human) and pSilencer_FLuc vector were constructed as negative silencing control vector and positive silencing control vector, respectively. The pSilencer_miR-3145 vector was constructed as a miR-3145 expression vector. The pCMV_RLuc vector was used for *Renilla* luciferase (*RLuc*) expression as a transfection control vector. The basis for using this assay is that the hybridization between miR-3145 and the viral PB1 target that linked with 3′-UTR of the firefly luciferase gene will trigger silencing of firefly luciferase activity compared to a control.

Basically, cells in each group were co-transfected with three plasmids including a reporter vector (pGL3MS2/Basic_PB1 or pGL3MS2/Basic), a silencing vector (pSilencer_scramble or pSilencer_FLuc or pSilencer_miR-3145) and a control vector (pCMV_RLuc). Each group was transfected with the same pCMV_RLuc control vector, but differed with respect to the types of reporter vector and silencing vector. Therefore, the transfected A549 cells were separated into six groups (Figure 3). In group 1, cells were transfected with pGL3MS2/Basic and pSilencer_scramble as the control group without target regions in the reporter vector and negative silencing control. In group 2, cells were transfected with pGL3MS2/Basic and pSilencer_FLuc was used as the positive silencing control due to the shRNA expression from pSilencer_FLuc specially targeting to *FLuc* reporter gene. As the results shown in Figure 3, the dual luciferase activity of group 2 was significantly lower ($P = 0.0132$) than those found in group 1, showing the effectiveness of the shRNA expression system. In group 3, pGL3MS2/Basic and pSilencer_miR-3145 were transfected into the cells in order to test whether miR-3145 triggered non-specific complementation with a firefly luciferase gene. Even the transfected cells could express hsa-miR-3145, but there was no target region in the reporter vector. As expected, the result revealed no significant difference ($P = 0.3162$) of the relative luciferase activity between group 3 and group 1, indicating that miR-3145 could not

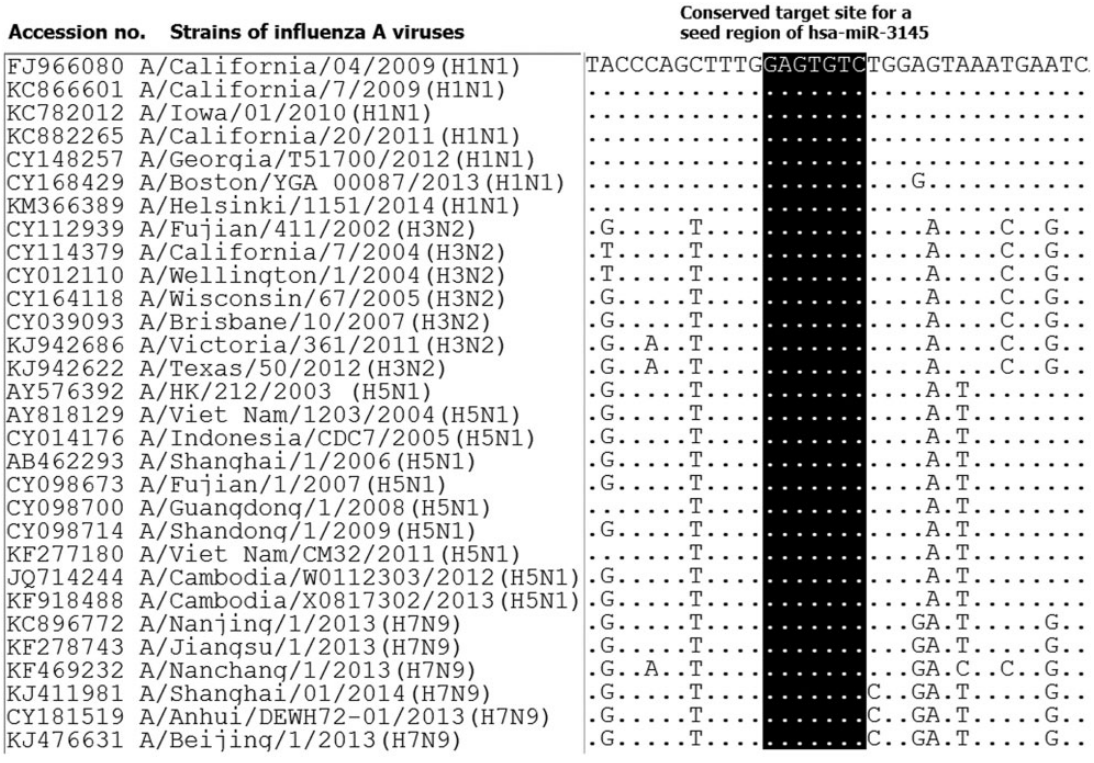

Figure 2 The alignment of viral PB1 gene revealed conserve target sites for seed region of hsa-miR-3145. Various strains in representative of four subtypes (pH1N1, H3N2, H5N1 and H7N9) of influenza A virus infecting humans were included in the alignment. The alignment was performed using Clastal W implemented in BioEdit software

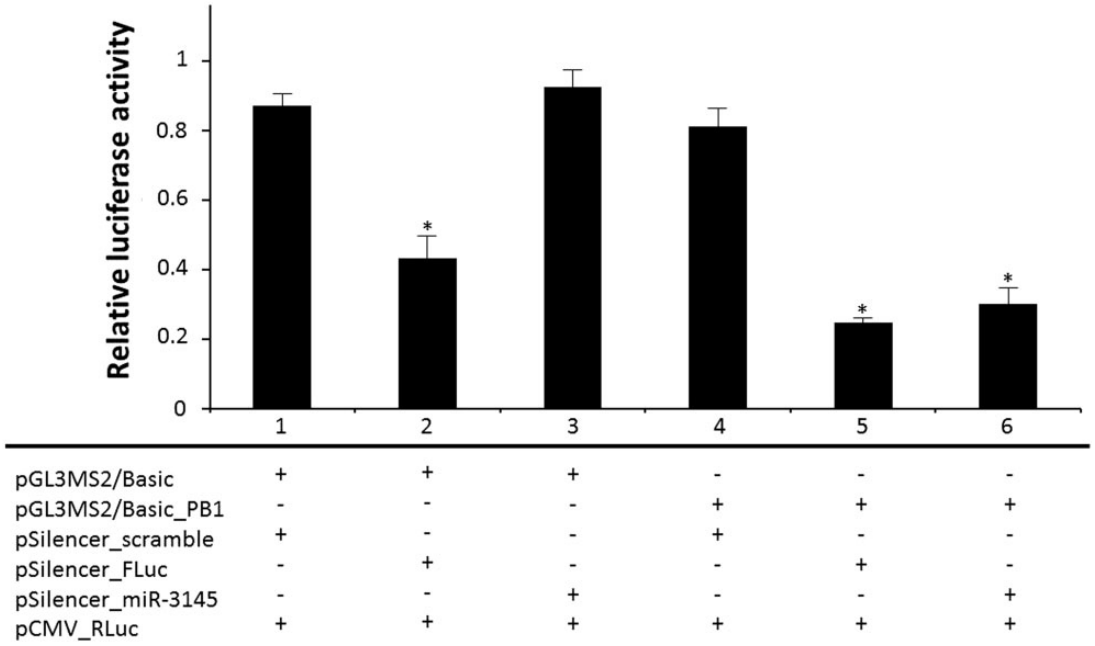

Figure 3 The bar graph shows the relative luciferase activity among groups of transfected cells. Group 1, cells were transfected with pGL3MS2/Basic and pSilencer_scramble as the control group; group 2, cells were transfected with pGL3MS2/Basic and pSilencer_FLuc was used as the positive silencing control; group 3, cells were transfected with pGL3MS2/Basic and pSilencer_miR-3145 in order to test whether miR-3145 triggered non-specific complementary with a firefly luciferase gene; group 4, cells were transfected with pGL3MS2/Basic_PB1 and pSilencer_scramble to test a silencing effect triggered by base complementation between an endogenous cellular miR-3145 and the PB1 gene within 3′-UTR of the firefly luciferase gene; group 5, cells were transfected with pGL3MS2/Basic_PB1 and pSilencer_FLuc as another positive silencing control; group 6, cells were transfected with pGL3MS2/Basic_PB1 and pSilencer_miR-3145 to test the silencing effect of miR-3145. The pCMV_RLuc control vector was transfected into cells in each group. '*' refers to significant differences from controls. Results revealed that the relative luciferase in groups 2, 5, and 6 were significantly lower ($P < 0.05$) than controls

directly bind to the firefly luciferase gene. For group 4, cells were transfected with pGL3MS2/Basic_PB1 and pSilencer_scramble to test a silencing effect triggered by base complementation between an endogenous cellular miR-3145 and PB1 gene within 3′-UTR of the firefly luciferase gene. Results from group 4 showed no significant reduction ($P = 0.3604$) of the relative luciferase activity between group 4 and group 1, implying that the endogenous cellular miR-3145 was not expressed or was expressed at a very low level that was not sufficient to silence the reporter gene. In another positive silencing control in group 5, cells were transfected with pGL3MS2/Basic_PB1 and pSilencer_FLuc. The significant reduction of luciferase activity in group 5 compared to those found in group 1 and group 4 ($P = 0.0026$ and 0.0063 respectively) showed the effectiveness of positive silencing control. There was no significant difference of the relative luciferase activity observed between groups 2 and 5, implying that no additional silencing effect occurred when adding the viral PB1 target region into the 3′-UTR of the reporter gene. In group 6, pGL3MS2/Basic_PB1 and pSilencer_miR-3145 were transfected into the A549 cells. In this group, the A549 cells could overexpress hsa-miR-3145 to hybridize with a viral PB1 target region presented at 3′-UTR of the reporter gene. Interestingly, the relative luciferase activity in group 6 was significantly lower than those found in group 1 and group 4 controls ($P = 0.0063$ and 0.0115, respectively), indicating that hsa-miR-3145 triggered approximately a 63% reduction of the luciferase activity by targeting the viral PB1 segment within the 3′-UTR of the firefly luciferase reporter gene.

Inhibition of influenza A virus replication triggered by hsa-miR-3145

After 24 h of post-transfection with a silencing vector (pSilencer_scramble or pSilencer_miR-3145), the A549 cells were infected with pH1N1 influenza virus (MOI = 0.1). To investigate the antiviral activity of hsa-miR-3145, cell lysate was collected at 48 h post-infection followed by RNA extraction and cDNA synthesis. Expression level of viral PB1 gene was normalized by the amount of host GAPDH internal control gene, which was quantitated by real-time PCR. The infected cells with an overexpression of hsa-miR-3145 showed a significant reduction of viral PB1 RNA expression ($P < 0.05$) compared to cells transfected with pSilencer_scramble negative silencing control in all three subtypes of viral infection (Figure 4). For the pH1N1 subtype, the PB1 expression was decreased by approximately 84.62% ($P = 0.0024$) while that in the H5N1 subtype was decreased for 98.95% ($P = 0.0004$) and PB1 expression of H3N2 subtype was repressed 60.00% ($P = 0.0001$). Thus, the overexpression of hsa-miR-3145 seemed to inhibit the viral PB1 expression. The PB1 is one of the viral polymerase complexes (PB2, PB1 and PA) required for viral transcription and replication. Therefore, silencing of the viral PB1 gene led to inhibition of viral replication.

Discussion

Although the computational tools of miRNA prediction are available, most of these tools can predict miRNAs target(s) only in some organisms, such as humans, mammals, fish,

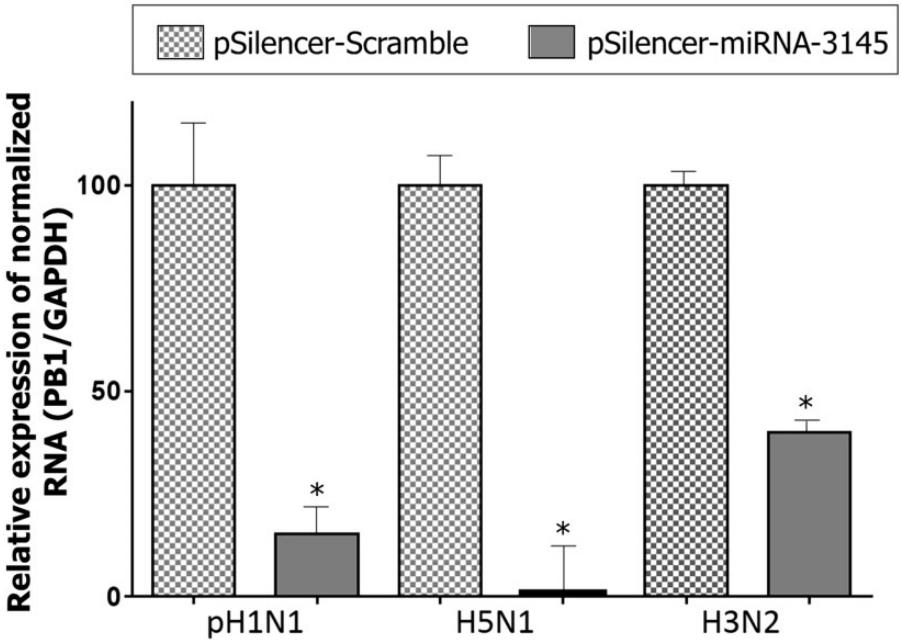

Figure 4 Percentage of relative expression of viral PB1 gene normalized with GAPDH gene quantitated by real-time PCR. The result demonstrated the significant reduction ($P < 0.05$) of viral PB1 gene in the presence of miRNA-3145 compared to mock infection in all three subtypes of influenza A virus including pH1N1, H5N1 and H3N2. '*' refers to significant differences from the control (mock infection)

flies or worms.[16,17] There are not many studies on predicting viral genes targeted by human miRNAs. The main category used in these tools is the complementary in the seed region of miRNA 5′ portion and their targets, leading to lots of false-positive and false-negative results.[18] In this study, we used the categories based on the principle of miRNA target recognition.[14] The hybridization patterns of miRNAs and their targets could be divided into three types; 5′ canonical, 5′ seed and 3′ compensatory. These patterns were used as the main criteria for the screening of candidate human miRNAs targeting various subtypes of influenza A virus. In addition, the pairing energy or minimum free energy (MFE) from the RNA Hybrid program was included in candidate miRNA selection. The criteria and prediction method used in this study was previously performed in order to identify miRNAs targeting HCV viral genes.[15]

In 2013, Zhang and colleagues reported that they identified miRNAs including hsa-miR-489, hsa-miR-325, hsa-miR-876-3p and hsa-miR-2117, which target H1N1 influenza A viral genes such as HA, PB2, MP and NS, respectively.[19] Similarly, the hsa-miR-876 was also found to be pH1N1-targeting miRNA in our study. Previous studies indicated that human miRNAs can inhibit influenza virus replication. The hsa-miR-146a was reported to inhibit the replication of H1N1 and H3N2 subtypes of influenza A viruses.[20] Ma et al. also verified that human miRNA let-7c can regulate the M1 expression of H1N1 influenza virus.[21] Hsa-miR-26a, which was predicted to target the H1N1 influenza virus in our study, was also reported to inhibit the replication of the H1N1 subtype in MDCK cells.[22] The hsa-miR-145 and hsa-miR-92a were suggested to target HA genes while hsa-miR-150 was reported to target PB2 genes of the H1N1 influenza A virus.[23]

However, most of the miRNAs targeting influenza viruses were differently identified in each study. This might be due to several factors including viral subtype, viral genome reference sequence, prediction software and miRNA selection criteria used in each individual study. According to the genetic variability of influenza A virus among different subtypes and strains, the aim of this study was to identify human miRNA targeting multiple subtypes of influenza A viruses infecting humans. Therefore, three subtypes of influenza A virus that infect humans, including pH1N1, H3N2 and H5N1, were analyzed. The result revealed that hsa-miR-3145 was the only human miRNA targeting influenza A viruses subtype pH1N1, H5N1, and H3N2. Interestingly, the target of this miRNA was the PB1 gene, which plays an important role in viral replication. Even the hybridizations between hsa-miR-3145 to three stains of influenza A viruses were slightly different, but the targets of miRNA seed region were conserved among various stains of the influenza A viruses as shown in the alignment of PB1 genes (Figure 2). H7N9 influenza A virus was recently reported to infect humans; therefore, the PB1 gene of H7N9 influenza A virus was also analyzed. Interestingly, H7N9 influenza A virus also contains conserved target sites for the seed region of hsa-miR-3145, implying that hsa-miR-3145 might be able to hybridize with PB1 gene of the H7N9 virus (Figure 2).

Similar to the study described by Song et al.,[7] the 3′-UTR reporter assay was performed to validate the targeting and silencing ability of candidate miRNAs. For hsa-miR-3145 evaluation, the target site on viral PB1 gene was ligated to the 3′-UTR of luciferase reporter gene. It revealed that hsa-miR-3145 can target the viral PB1 and lead to the silencing activity.

Real-time RT-PCR was used to determine viral PB1 expression in A549 infected cells. The PB1 gene expression was significantly decreased in viral infected cells that were transfected with hsa-miR-3145 expression vector, indicating that hsa-miR-3145 triggered silencing of the PB1 gene. Interestingly, H5N1 subtype infected cells show a dramatic decrease in PB1 expression when compared to the pH1N1 and H3N2 infected cells. This may be caused by strong hybridization between the H5N1 PB1 target gene and hsa-miR-3145. The silencing of the PB1 gene by hsa-miR-3145 was proved in both 3′-UTR reporter assay and *in vitro* viral replication (Figures 3 and 4). The PB1 gene plays an important role in viral replication by encoding polymerase basic protein 1, which is the component of viral polymerase complex. When the PB1 gene was repressed, the viral replication would be inhibited, leading to the decrease in viral production. Thus, hsa-miR-3145 might have an antiviral effect against multiple subtypes of influenza A viruses.

The hsa-miR-3145 miRNA was first reported in the Melanoma miRNAome study by deep sequencing.[24] Until now, its function or target has not been revealed. Unfortunately, the expression level of endogenous hsa-miR-3145 was very low in both uninfected and influenza viral-infected A549 cells (data not shown). This suggest that hsa-miR-3145 in the respiratory epithelial cell line is not constitutively expressed in normal conditions and not expressed in response to influenza viral infection. Therefore, further studies about induction mechanisms for endogenous hsa-miR-3145 expression might be useful for alternative antiviral approaches against influenza virus infection.

Conclusion

This study is the first report found that hsa-miR-3145 targeted multiple subtypes of influenza A viruses. The results revealed that hsa-miR-3145 targeted conserved regions in PB1 genes of influenza A viruses and triggered silencing of viral PB1. Thus, hsa-miR-3145 might be the best candidate for human miRNA inhibiting replication of influenza A viruses.

Authors' contributions: KK performed *in silico* and *in vitro* analysis as well as drafted the manuscript. JM carried out viral infection and edit the manuscript. WP assisted in BSL3 process, data processing and graphic visualization. YP provided stock of viruses and revised the manuscript. SP took part in designing the study, data analysis, revision of the manuscript and coordination. All authors read and approved the final manuscript.

ACKNOWLEDGEMENTS

We would like to appreciatively acknowledge the Department of Biochemistry and Research affairs, Faculty of Medicine, Chulalongkorn University, Thailand for their instrumental facilities. We would like to thank Prof. Jen-Ren Wang, Department of Medical Laboratory Science and Biotechnology, Center of Infectious Disease and Signaling Research, National Cheng Kung University, Taiwan for providing A549 cells. We also thank Assistant Prof. Nattanan Panjaworayan T-Thienprasert, Kasetsart University, Thailand for providing the original plasmids using in this study. Funding was supported by the Thailand Research Fund (TRF: RSA5680031); the Postdoctoral Fellowship, Ratchadapiseksompotch Fund (Faculty of Medicine, Chulalongkorn University); National Research University Project; Office of Higher Education Commission (WCU-007-HR-57); Centenary Academic Development Project (CU56-HR01); the Ratchadaphiseksomphot Endowment Fund of Chulalongkorn University (RES560530093), Research Chair Grant, National Science and Technology Development Agency (NSTDA) and Development and Promotion of Science and Technology Talents Project (DPST).

DECLARATION OF CONFLICTING INTERESTS

The authors hereby declare no personal or commercial conflict of interest with any aspect of this study.

REFERENCES

1. Fleming DM, Chakraverty P, Sadler C, Litton P. Combined clinical and virological surveillance of influenza in winters of 1992 and 1993-4. *BMJ* 1995;**311**:290–1
2. Centers for Disease C, Prevention. Update: Influenza A (H3N2)v transmission and guidelines – five states, 2011. *MMWR Morbid Mortal Weekly Rep* 2012;**60**:1741–4
3. Tran TH, Nguyen TL, Nguyen TD, Luong TS, Pham PM, Nguyen vV, Pham TS, Vo CD, Le TQ, Ngo TT, Dao BK, Le PP, Nguyen TT, Hoang TL, Cao VT, Le TG, Nguyen DT, Le HN, Nguyen KT, Le HS, Le VT, Christiane D, Tran TT, Menno de J, Schultsz C, Cheng P, Lim W, Horby P, Farrar J, World Health Organization International. Avian Influenza Investigative Team Avian influenza A (H5N1) in 10 patients in Vietnam. *New Engl J Med* 2004;**350**:1179–88
4. Ambros V. microRNAs: tiny regulators with great potential. *Cell* 2001;**107**:823–6
5. Hwang HW, Mendell JT. MicroRNAs in cell proliferation, cell death, and tumorigenesis. *Br J Cancer* 2007;**96 Suppl**:R40–4
6. Lecellier CH, Dunoyer P, Arar K, Lehmann-Che J, Eyquem S, Himber C, Saïb A, Voinnet O. A cellular microRNA mediates antiviral defense in human cells. *Science* 2005;**308**:557–60
7. Song L, Liu H, Gao S, Jiang W, Huang W. Cellular microRNAs inhibit replication of the H1N1 influenza A virus in infected cells. *J Virol* 2010;**84**:8849–60
8. Kozomara A, Griffiths-Jones S. miRBase: integrating microRNA annotation and deep-sequencing data. *Nucl Acid Res* 2011;**39**:D152–7
9. Kozomara A, Griffiths-Jones S. miRBase: annotating high confidence microRNAs using deep sequencing data. *Nucl Acid Res* 2014;**42**:D68–73
10. Griffiths-Jones S, Grocock RJ, van Dongen S, Bateman A, Enright AJ. miRBase: microRNA sequences, targets and gene nomenclature. *Nucl Acid Res* 2006;**34**:D140–4
11. Griffiths-Jones S. The microRNA Registry. *Nucl Acid Res* 2004;**32**:D109–11
12. Griffiths-Jones S, Saini HK, van Dongen S, Enright AJ. miRBase: tools for microRNA genomics. *Nucl Acid Res* 2008;**36**:D154–8
13. Rehmsmeier M, Steffen P, Hochsmann M, Giegerich R. Fast and effective prediction of microRNA/target duplexes. *RNA* 2004;**10**:1507–17
14. Brennecke J, Stark A, Russell RB, Cohen SM. Principles of microRNA-target recognition. *PLoS Biol* 2005;**3**:e85
15. Plakunmonthona S, T-Thienprasert NP, Khongnomnana K, Poovorawan Y, Payungporn S. Computational prediction of hybridization patterns between hepatitis C viral genome and human microRNAs. *J Computat Sci* 2014;**5**:327–31
16. Lewis BP, Shih IH, Jones-Rhoades MW, Bartel DP, Burge CB. Prediction of mammalian microRNA targets. *Cell* 2003;**115**:787–98

17. Krek A, Grün D, Poy MN, Wolf R, Rosenberg L, Epstein EJ, MacMenamin P, da Piedade I, Gunsalus KC, Stoffel M, Rajewsky N. Combinatorial microRNA target predictions. *Nat Genet* 2005;**37**:495–500
18. Hamzeiy H, Allmer J, Yousef M. Computational methods for microRNA target prediction. *Meth Mol Biol* 2014;**1107**:207–21
19. Zhang H, Li Z, Li Y, Liu Y, Liu J, Li X, Shen T, Duan Y, Hu M, Xu D. A computational method for predicting regulation of human microRNAs on the influenza virus genome. *BMC Syst Biol* 2013;**7**:S3
20. Terrier O, Textoris J, Carron C, Marcel V, Bourdon JC, Rosa-Calatrava M. Host microRNA molecular signatures associated with human H1N1 and H3N2 influenza A viruses reveal an unanticipated antiviral activity for miR-146a. *J General Virol* 2013;**94**:985–95
21. Ma YJ, Yang J, Fan XL, Zhao HB, Hu W, Li ZP, Yu GC, Ding XR, Wang JZ, Bo XC, Zheng XF, Zhou Z, Wang SQ. Cellular microRNA let-7c inhibits M1 protein expression of the H1N1 influenza A virus in infected human lung epithelial cells. *J Cell Molecul Med* 2012;**16**:2539–46
22. Liu H, Song L, Huang W. [MiR26a and miR939 regulate the replication of H1N1 influenza virus in MDCK cell]. *Wei sheng wu xue bao (Acta Microbiol Sinica)* 2010;**50**:1399–405
23. He T, Feng G, Chen H, Wang L, Wang Y. Identification of host encoded microRNAs interacting with novel swine-origin influenza A (H1N1) virus and swine influenza virus. *Bioinformation* 2009;**4**:112–8
24. Stark MS, Tyagi S, Nancarrow DJ, Boyle GM, Cook AL, Whiteman DC, Parsons PG, Schmidt C, Sturm RA, Hayward NK. Characterization of the Melanoma miRNAome by Deep Sequencing. *PloS ONE* 2010;**5**:e9685

(Received December 16, 2014, Accepted April 14, 2015)

Complete Genome Characterization and Phylogenetic Analysis of WU Polyomavirus in Thai Pediatric Patients with Respiratory Tract Infections in 2013

Prangwalai Chanchaem MSc*,
Yong Poovorawan MD**, Sunchai Payungporn PhD***

** Medical Science, Faculty of Medicine, Chulalongkorn University, Bangkok, Thailand*
*** Center of Excellence in Clinical Virology, Faculty of Medicine, Chulalongkorn University, Bangkok, Thailand*
**** Department of Biochemistry, Faculty of Medicine, Chulalongkorn University, Bangkok, Thailand*

Background: *The WU polyomavirus (WUPyV) is a small DNA virus (family Polyomaviridae) that contains a circular double-stranded DNA genome, approximately 5 kb in length. WUPyV was first discovered in the respiratory tract of children with acute respiratory symptoms.*
Objective: *This study focuses on the complete genome characterization and phylogenetic analysis of WUPyV obtained from Thai patients with respiratory diseases in 2013.*
Material and Method: *DNA was extracted from nasopharyngeal (NP) suction specimens (n = 614) from patients with respiratory tract infections. WUPyV was detected by using semi-nested PCR and then characterized by whole genome sequencing. The nucleotides and deduced amino acid sequences were analyzed by multiple sequences alignment and phylogenetic tree.*
Results: *Analysis revealed that 0.16% (1/614) of the sample was positive for WUPyV. Phylogenetic trees demonstrated that WUPyV (isolate CU_Chonburi 3) was closely related to previously described WUPyV. Moreover, whole genome sequences alignment of WUPyV showed several nucleotide variations within non-coding regions and amino acid changes in VP1 (position S347T); VP2 (positions L40V, G120R, Y121I, P123R, G127S, L137F, Q287R, and A327V); LTAg (positions Q357P, V369E, E377K, D378V, A381T, R382E, R383G, and D389G); and, STAg (positions R139S, K141E, R148K, and W153C).*
Conclusion: *Nucleotide variations within non-coding regions and critical amino acid substitutions in viral proteins may affect the rate of viral replication and viral adaptation; factors that may be linked to the susceptibility and severity of viral infection. Data obtained from this study may be useful in better understanding the genetic characterization and mutation patterns of WUPyV.*

Keywords: *WU polyomavirus, Characterization, Phylogenetic, Thailand*

J Med Assoc Thai 2015; 98 (Suppl. 1):
Full text. e-Journal: *http://www.jmatonline.com*

Respiratory tract infection is a major cause of hospitalization in infants and young children. The common respiratory viruses include influenza viruses, parainfluenza virus, rhinovirus, respiratory syncytial virus, coronaviruses, adenoviruses, and metapneumovirus[1]. Novel viruses that may cause respiratory illness have recently been identified. In 2007, WU (Washington University) polyomavirus (WUPyV) was first discovered in the respiratory tract of children with acute respiratory symptoms[2]. WUPyV is a small DNA virus belonging to the *Polyomaviridae* family. It contains a circular double-stranded DNA genome that is 5,229 bp in length[3]. The genome consists of three functional regions, including early, late, and non-coding regions. The early region encodes regulatory proteins, including large T antigen (LTAg) and small T antigen (STAg), which are responsible for viral DNA replication and gene expression. The late region encodes three capsid proteins: VP1, VP2, and VP3. The non-coding region encompasses the origin of replication and transcription control elements[3]. Accordingly, this virus contains 5 functional proteins: LTAg, STAg, VP1, VP2, and VP3. The large T-antigen is required for viral DNA replication, virion assembly, and transcription. The small T-antigen protein is also able to activate several cellular pathways that stimulate cell proliferation. The three capsid proteins include a major coat protein, VP1, and two minor coat proteins, VP2 and VP3.

Correspondence to:
Payungporn S, Department of Biochemistry, Faculty of Medicine, Chulalongkorn University, Rama IV Road, Patumwan, Bangkok 10330, Thailand.
Phone & Fax: 0-2256-4482
E-mail: sp.medbiochemcu@gmail.com

WU polyomavirus was observed in clinical specimens obtained from children with respiratory tract infection in several countries, including Australia (2.97%)[2], United Kingdom (1.02%)[4], France (2.42%)[5], China (2%)[6], Thailand (6.29%)[7], South Korea (6.99%)[8], and Canada (6.41%)[9]. The prevalence and molecular characterization of WUPyV in Thai patients were previously reported in 2008[7]. However, mutations in the viral genome may have occurred since that time. Therefore, this study focused on the complete genome characterization of WUPyV obtained from Thai pediatric patients with respiratory disease in 2013. Those findings were then compared with previously described characterizations of WUPyV. The comparative findings may provide insights into the viral mutation and genetic variability of WUPyV that may be responsible for the virulence and pathogenesis of this virus.

Material and Method

Clinical samples

Nasopharyngeal (NP) suction samples (n = 614) were collected from patients with influenza-like illness at King Chulalongkorn Memorial Hospital and Chonburi Hospital, Thailand. The protocol for this study was approved by the Institutional Review Board (IRB No. 457/56), Faculty of Medicine, Chulalongkorn University.

Detection of WUPyV by semi-nested PCR amplification

DNA was extracted from 100 µL of NP suction using a HiYield™ Viral Nucleic Acid Extraction kit (Real Genomics, USA), according to manufacturer protocol. Semi-nested PCR amplification within LTAg of WUPyV was performed using specific primers. The first round of PCR was amplified by WU_4337F: 5′-CATTATTAACWCCTTTACARAATAA-3′ and WU_4585R: 5′-TGTC WCAWGCTGTATTTAGTAA TA-3′; whereas, the second PCR was performed by WU_4390F: 5′-AAG TTATTAAYAGCACTAACTCTA TG-3′ and WU_ 4585R.

The expected semi-nested PCR product of WUPyV was approximately 215 bp. Moreover, amplification of the GAPDH gene (199 bp) using GAPDH_F404: 5′-CTTCACCACCATGGAGAAGG-3′ and GAPDH_R603: 5′-GTTGTCATGGATGACC TTGGC-3′ served as the internal control for detection.

Whole genome amplification of WUPyV

The complete genome of WUPyV was amplified directly from clinical samples, using 4 primer pairs in order to generate overlapping PCR products of the circular genome. All primers used for whole genome amplification were designed from nucleotide conserved regions from different strains of WUPyV, as previously described[7].

PCR conditions

The PCR reaction mixture comprised 1 µl of DNA, 2.5 µl of 10xPCR buffer minusMg, 0.5 µl of 10 mM dNTPs mixture, 0.75 µl of 50 mM $MgCl_2$, 0.5 µM of each primer, and 19.25 µl of distilled water for a final volume of 25 µl. Thermal profiles are described, as follows: initial denaturation at 94°C for 3 minutes; followed by, 40 amplification cycles consisting of 94°C for 30 seconds, 55°C for 30 seconds, and 72°C for 1.30 minutes; and, a final extension at 72°C for 7 minutes. Positive and negative controls were included in each run to ensure suitable detections.

Gel electrophoresis and nucleotide sequencing

PCR products were separated by 2% agarose gel electropholysis and then visualized by ethidium bromide staining under UV transillumination. The PCR amplified products were then purified using HiYield ™ Gel Extraction (RBC Bioscience, Taiwan). Nucleotide sequencing was then performed by First BASE Laboratories Sdn Bhd, Selangor, Malaysia.

Nucleotide sequences analysis

Nucleotide sequences were analyzed using the BLAST analysis tool (http://www.ncbi.nlm.gov/BLAST). Complete genome sequences were assembled using the contig assembly program (CAP) and aligned using ClustalW software, and implemented using the BioEdit Sequence Alignment Editor (version 7.0.4.1). The complete genome sequence of WU polyomavirus obtained from the present study was submitted to the GenBank database and assigned accession number: KJ725028. Other genome sequences of WUPyV analyzed in this study were obtained from the GenBank database, including: WUPyV reference strain (NC_009539); USA (EF444554 and FJ794068); Thailand (EU358768 and EU358769); China (EU296475, GQ926980, and FJ890981); Germany (EU711058); and, Australia (GU296363, GU296405, and GU296408). Nucleotide sequences were selected according to year and country of isolation. Redundant sequences were excluded from this analysis. The similarity of genome sequences between sample and WUPyV reference sequence were analyzed by Simplot version 3.5.1 (http://sray.med.som.jhmi.edu/SCRoftware/simplot).

Phylogenetic analysis

Phylogenetic trees were constructed by neighbor-joining (NJ) method with bootstrap (1000) and Tamura-Nei nucleotide substitution model implemented in Molecular Evolutionary Genetics Analysis (MEGA) program version 5.2 (http://www.mybiosoftware.com/phylogenetic-analysis/2334). All WUPyV genome sequences described above were included in the phylogenetic tree.

Results

Detection of WUPyV

The detection of WUPyV from Thai patients with respiratory diseases in 2013 revealed that 0.16% (1/614) of the sample was positive for WUPyV. BLAST analysis confirmed that this positive sample was closely related to WUPyV. This sample was assigned as WUPyV isolate CU_Chonburi 3 and the complete genome was further characterized. Other samples were negative for WUPyV, but were positive for GAPDH internal control; a result indicating appropriate sample collections and DNA extraction processes.

Complete genome analysis of WU polyomavirus

The genome of WUPyV (isolate CU_Chonburi 3) was closely related to the reference sequence of WUPyV (NC_009539), with 99% similarity. The genomes were then further compared by using the SimPlot software program (public domain). The result revealed that WUPyV (CU_Chonburi 3) was slightly different from WUPyV (NC_009539), as follows: non-coding region (positions 100-350); VP2 (positions 850-1,000); LTAg (positions 3,500-3,700); STAg (positions 4,650-4,800). The complete genome of WUPyV (CU_Chonburi 3) was then aligned with several WUPyV whole genome sequences from several countries, including Australia, USA, Germany, China, and Thailand during the timeframe of 2007-2011. Table 1 describes several nucleotide variations within non-coding regions, to include positions 37, 67, 73, 95, 130, 152, 173, 177, 180, 181, 206, 275, 293, 294, 350, 451, 499, 4522, and 5211. Table 2 illustrates amino acid changes in VP1 (position S347T); VP2 (positions L40V, G120R, Y121I, P123R, G127S, L137F, Q287R, and A327V); LTAg (positions Q357P, V369E, E377K, D378V, A381T, R382E, R383G, and D389G); and, STAg (positions R139S, K141E, R148K, and W153C).

Phylogenetic analysis

Phylogenetic trees were constructed based on analysis of nucleotide sequences within VP1, VP2, LTAg, and STAg (Fig. 2). The phylogenetic tree of the VP1 gene (Fig. 2A) demonstrated that WUPyV (isolate CU_Chonburi 3) was closely related to previously described WUPyV, such as WUPyV reference sequence (NC 009539), isolate MN 2726 from Australia in 2010 (GU296405), and isolate CLFF from China in 2008 (EU296475). Conversely, phylogenetic trees obtained from the analysis of VP2 (Fig. 2B), LTAg (Fig. 2C), and STAg (Fig. 2D), revealed that WUPyV (isolate CU_Chonburi 3) was quite unrelated to other strains of WUPyV.

Discussion

According to the previous study, the prevalence of WUPyV in Thailand in 2008 was 6.29% (19/302)[7]. However, the present study observed a prevalence of only 0.16% (1/614) in Thai patients with respiratory disease during 2013. When comparing the current and previous studies, there was no difference in specimen type (NP suction) or detection technique (semi-nested PCR). Moreover, the sample size used in this study was double the sample size used in the previous report. Accordingly, type of specimen, detection method, and sample size were not responsible for the low prevalence of WUPyV observed in the present study. A possible explanation may be a difference in antibody response against WUPyV. WUPyV contains VP1 as a major coated protein to target cell receptors; as such, VP1 protein becomes the main target of host neutralizing antibodies. According to the analysis in the present study, the VP1 gene of WUPyV (isolate CU_Chonburi 3) was relatively conserved (only one amino acid change: S347T), consistent with the previous descriptions of WUPyV (Fig. 1 and 2A). This finding implies that WUPyV in 2013 should be neutralized by antibodies against the VP1 protein. Consequently, the prevalence of WUPyV in 2013 should be very low, as compared to prevalence rates reported in the previous studies[2,4-15].

Phylogenetic analysis based on the VP1 gene revealed that WUPyV isolated from several countries, including Australia, USA, Germany, China, and Thailand, from 2007 to 2013 were closely related. The phylogenetic trees of WUPyV (isolate CU_Chonburi 3) based on VP2, LTAg, and STAg were located a considerable distance from other strains of WUPyV. However, additional WUPyV genome sequences from several countries should be chronologically investigated in order to understand better the evolution of this virus.

Mutations within viral proteins (LTAg, STAg,

Table 1. Nucleotide variations within non-coding regions

Isolate name	Country	Year	Nucleotide variations within non-coding regions*																		Accession No.
			37	67	73	95	130	152	173	177	180	181	206	275	293	294	350	451	499	4522	5211	
WU Ref strain	Australia	2007	g	g	g	g	c	g	c	c	g	g	a	a	t	a	c	c	c	a	g	NC_009539
S5	USA	2007	g	g	g	g	c	g	c	c	g	g	a	a	t	a	c	c	c	g	a	EF444554
CU-295	Thailand	2008	g	g	g	g	c	g	c	c	g	g	a	a	t	a	c	c	c	g	a	EU358768
CU-302	Thailand	2008	g	g	g	g	c	g	c	c	g	g	a	a	t	a	c	c	c	g	g	EU358769
CLFF	China	2008	g	g	g	g	c	g	c	c	g	g	a	a	t	a	c	c	c	a	g	EU296475
GD-WU709	China	2009	g	g	g	g	c	g	c	c	g	g	a	a	t	a	c	c	c	g	a	GQ926980
Rochester-7029	USA	2009	g	g	g	g	c	g	c	c	g	g	a	a	t	a	c	c	c	g	a	FJ794068
Wuerzburg	Germany	2009	g	g	g	g	c	g	c	c	g	g	a	a	t	a	c	c	c	g	a	EU711058
O91	Australia	2010	g	g	g	g	c	g	c	c	g	g	a	a	t	a	c	c	c	g	a	GU296363
MN2726	Australia	2010	g	g	g	g	c	g	c	c	a	g	a	a	t	a	c	c	c	g	a	GU296405
O3	Australia	2010	g	g	g	g	c	g	c	c	g	g	a	a	t	a	c	c	c	g	a	GU296408
FZ18	China	2011	g	g	g	g	c	g	c	c	g	g	a	a	t	a	c	c	c	g	a	FJ890981
CU_Chonburi 3	Thailand	2013	c	c	a	c	a	t	a	a	t	a	c	g	g	g	a	t	t	g	t	KJ725828

* Position refers to NC_009539 (WU Ref strain)

Table 2. Amino acid changes in VP1, VP2, LTAg, and STAg

Isolate name	Country	Year	Amino acid changes*																					Accession No.
			VP1	VP2								LTAg								STAg				
			347	40	120	121	123	127	137	287	327	357	369	377	378	381	382	383	389	139	141	148	153	
WU Ref strain	Australia	2007	S	L	G	Y	P	G	L	Q	A	Q	V	E	D	A	R	R	D	R	K	R	W	NC_009539
S5	USA	2007	S	L	G	Y	P	G	L	Q	A	Q	V	E	G	A	R	R	D	R	K	R	W	EF444554
CU-295	Thailand	2008	S	L	G	Y	P	G	L	Q	A	Q	V	E	D	A	R	R	D	R	K	R	W	EU358768
CU-302	Thailand	2008	S	L	G	Y	P	G	L	Q	A	Q	V	E	D	A	R	R	D	R	K	R	W	EU358769
CLFF	China	2008	S	L	G	Y	P	G	L	Q	A	Q	V	E	D	A	R	R	D	R	K	R	W	EU296475
GD-WU709	China	2009	S	L	G	Y	P	G	L	Q	A	Q	V	E	D	A	R	R	D	R	K	R	W	GQ926980
Rochester-7029	USA	2009	S	L	G	Y	P	G	L	Q	A	Q	V	E	D	A	R	R	D	R	K	R	W	FJ794068
Wuerzburg	Germany	2009	T	L	G	Y	P	G	L	E	A	Q	V	E	D	A	R	R	D	R	K	K	W	EU711058
O91	Australia	2010	T	L	G	Y	P	G	L	Q	A	Q	V	E	D	A	R	R	D	R	K	K	W	GU296363
MN2726	Australia	2010	S	L	G	Y	P	G	L	Q	A	Q	V	E	D	A	R	R	D	R	K	R	W	GU296405
O3	Australia	2010	T	L	G	Y	P	G	L	Q	A	Q	V	E	D	A	R	R	D	R	K	R	W	GU296408
FZ18	China	2011	T	L	G	Y	P	G	L	Q	A	Q	V	E	D	A	R	R	D	R	K	R	W	FJ890981
CU_Chonburi 3	Thailand	2013	T	V	R	I	R	S	F	R	V	P	E	K	V	T	E	G	G	S	E	K	C	KJ725828

* Position refers to NC_009539 (WU Ref strain)

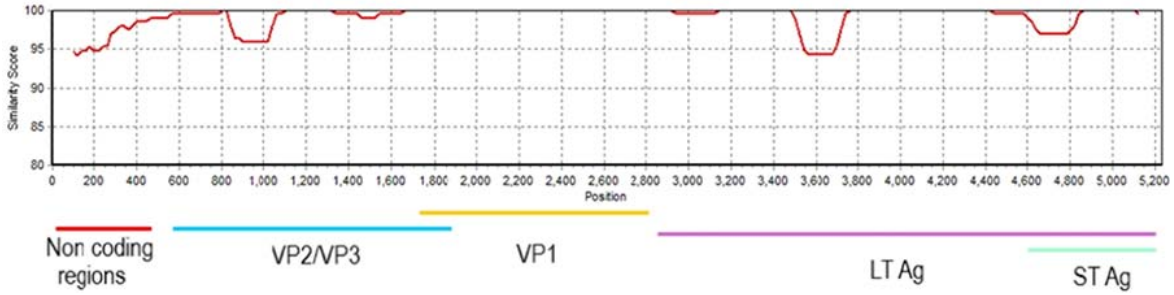

Fig. 1 Similarity plot of complete genome sequences between WUPyV (CU_Chonburi 3) and WUPyV reference sequence (NC_009539).

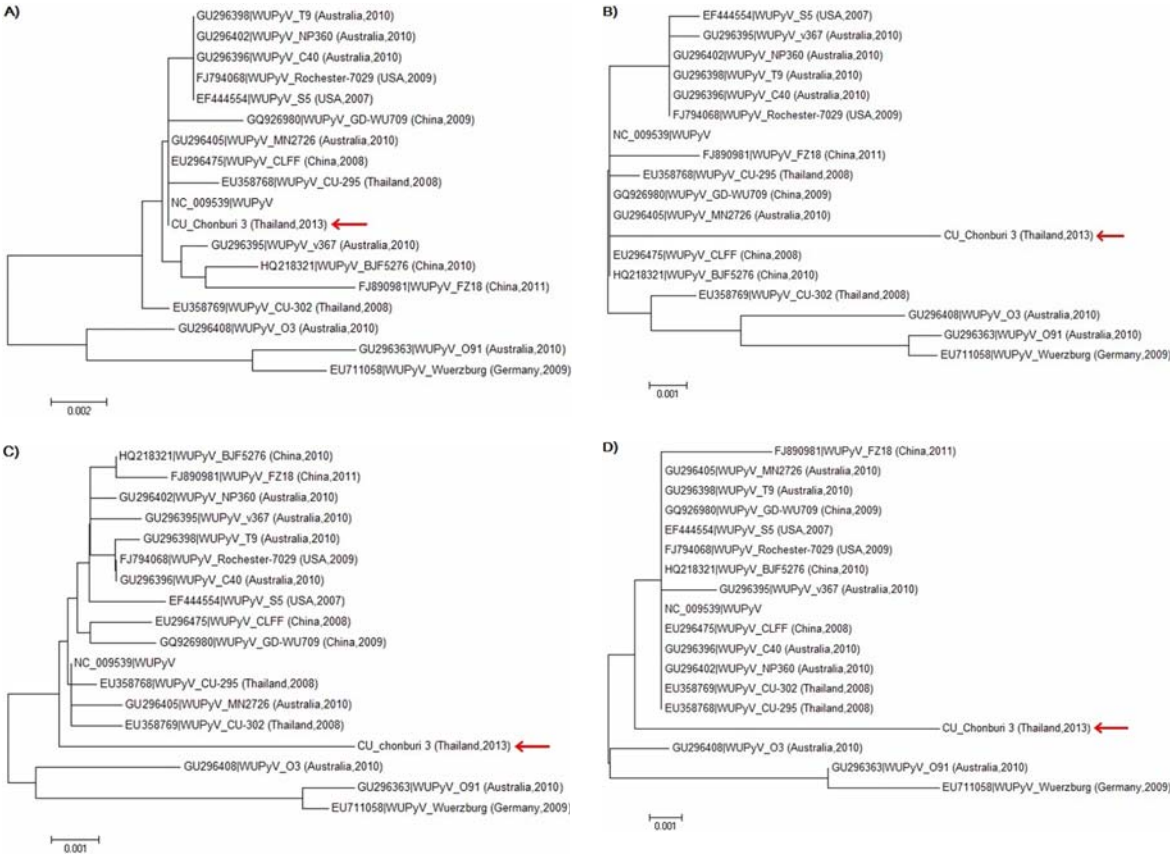

Fig. 2 Phylogenetic analysis of WUPyV based on (A) VP1, (B) VP2, (C) LTAg, and (D) STAg genes.

VP1, and VP2) were determined by whole genome comparison. Amino acid changes can be divided into 2 groups, including non-critical and critical amino acid changes. Changes in non-critical amino acids may not affect the function of the proteins, because the properties of amino acids are similar (including: VP1 (position S347T); VP2 (positions L40V, Q287R, and A327V); and, STAg (position R148K)). On the other hand, changes in critical amino acids may influence the function of the proteins by triggering properties specific to individual amino acids, to include: charge, ring structure, glycosylation site, and disulfide linkage. The critical amino acid changes observed in this study include: VP2 (positions G120R, Y121I, P123R, G127S, and L137F); LTAg (positions Q357P, V369E, E377K, D378V, A381T, R382E, R383G, and D389G); and, STAg (positions R139S, K141E, and W153C).

Conclusion

Nucleotide variations within non-coding

regions and critical amino acid substitutions in viral proteins may affect the rate of viral replication and viral adaptation, which may be linked to susceptibility and severity of viral infection. However, further experimental investigation is required in order to confirm the impact of each non-synonymous mutation on the characteristics of WUPyV and the specific immune response to this particular virus.

Acknowledgement

The authors of the present study wish to acknowledge with gratitude the Department of Biochemistry, Faculty of Medicine, Chulalongkorn University and the Center of Excellence in Clinical Virology, Faculty of Medicine, Chulalongkorn University for their invaluable contribution to the success of the present study.

Funding disclosure

Funding for this study was provided by the Thailand Research Fund (TRF: RSA5680031) and the Ratchadapiseksompotch Fund, Faculty of Medicine, Chulalongkorn University.

Potential conflicts of interest

None.

References

1. Kleines M, Hausler M, Kruttgen A, Scheithauer S. WU Polyomavirus (WUPyV): A Recently Detected Virus Causing Respiratory Disease? Viruses 2009; 1: 678-88.
2. Gaynor AM, Nissen MD, Whiley DM, Mackay IM, Lambert SB, Wu G, et al. Identification of a novel polyomavirus from patients with acute respiratory tract infections. PLoS Pathog 2007; 3: e64.
3. Allander T, Andreasson K, Gupta S, Bjerkner A, Bogdanovic G, Persson MA, et al. Identification of a third human polyomavirus. J Virol 2007; 81: 4130-6.
4. Norja P, Ubillos I, Templeton K, Simmonds P. No evidence for an association between infections with WU and KI polyomaviruses and respiratory disease. J Clin Virol 2007; 40: 307-11.
5. Foulongne V, Brieu N, Jeziorski E, Chatain A, Rodiere M, Segondy M. KI and WU polyomaviruses in children, France. Emerg Infect Dis 2008; 14: 523-5.
6. Ren L, Gonzalez R, Xu X, Li J, Zhang J, Vernet G, et al. WU polyomavirus in fecal specimens of children with acute gastroenteritis, China. Emerg Infect Dis 2009; 15: 134-5.
7. Payungporn S, Chieochansin T, Thongmee C, Samransamruajkit R, Theamboolers A, Poovorawan Y. Prevalence and molecular characterization of WU/KI polyomaviruses isolated from pediatric patients with respiratory disease in Thailand. Virus Res 2008; 135: 230-6.
8. Han TH, Chung JY, Koo JW, Kim SW, Hwang ES. WU polyomavirus in children with acute lower respiratory tract infections, South Korea. Emerg Infect Dis 2007; 13: 1766-8.
9. Abed Y, Wang D, Boivin G. WU polyomavirus in children, Canada. Emerg Infect Dis 2007; 13: 1939-41.
10. Goh S, Lindau C, Tiveljung-Lindell A, Allander T. Merkel cell polyomavirus in respiratory tract secretions. Emerg Infect Dis 2009; 15: 489-91.
11. Csoma E, Sapy T, Meszaros B, Gergely L. Novel human polyomaviruses in pregnancy: higher prevalence of BKPyV, but no WUPyV, KIPyV and HPyV9. J Clin Virol 2012; 55: 262-5.
12. Abedi KB, Vallely PJ, Corless CE, Al Hammadi M, Klapper PE. Age-related pattern of KI and WU polyomavirus infection. J Clin Virol 2008; 43: 123-5.
13. Bialasiewicz S, Whiley DM, Lambert SB, Wang D, Nissen MD, Sloots TP. A newly reported human polyomavirus, KI virus, is present in the respiratory tract of Australian children. J Clin Virol 2007; 40: 15-8.
14. Bialasiewicz S, Whiley DM, Lambert SB, Nissen MD, Sloots TP. Detection of BK, JC, WU, or KI polyomaviruses in faecal, urine, blood, cerebrospinal fluid and respiratory samples. J Clin Virol 2009; 45: 249-54.
15. Babakir-Mina M, Ciccozzi M, Campitelli L, Aquaro S, Lo CA, Perno CF, et al. Identification of the novel KI Polyomavirus in paranasal and lung tissues. J Med Virol 2009; 81: 558-61.

การศึกษาจีโนมและการจำแนกสายพันธุ์ของ WU polyomavirus ในผู้ป่วยติดเชื้อระบบทางเดินหายใจในประเทศไทยปี พ.ศ. 2556

ปรางวลัย จันทร์แจ่ม, ยง ภู่วรวรรณ, สัญชัย พยุงภร

ภูมิหลัง: เชื้อ WU polyomavirus (WUPyV) เป็นดีเอ็นเอไวรัสที่มีขนาดเล็กจัดอยู่ใน family Polyomaviridae ซึ่งมีสารพันธุกรรมเป็นดีเอ็นเอสายคู่ ขนาดประมาณ 5 kb ถูกค้นพบครั้งแรกจากเด็กที่มีการติดเชื้อในระบบทางเดินหายใจ

วัสดุและวิธีการ: งานวิจัยนี้ศึกษาลักษณะทางพันธุกรรมของเชื้อ WU polyomavirus ในประเทศไทยปี พ.ศ. 2556 โดยตรวจสอบเชื้อ WU polyomavirus ด้วยวิธี semi-nested PCR และหาลำดับสารพันธุกรรมทั้งจีโนมจากนั้นทำการวิเคราะห์ multiple sequences alignment และ Phylogenetic tree

ผลการศึกษา: จากการศึกษาระบาดวิทยานั้นพบว่ามีการระบาดของ WU polyomavirus (WUPyV) คิดเป็น 0.16% (1/614) เท่านั้น จากการศึกษา Phylogenetic tree พบว่า WUPyV (isolate CU_Chonburi 3) มีความสัมพันธ์ใกล้เคียงกับ WUPyV ที่มีรายงานก่อนหน้านี้ (ความเหมือน 99%) นอกจากนี้สารพันธุกรรมทั้งจีโนมของ WUPyV (isolate CU_Chonburi 3) นั้นมีการเปลี่ยนของลำดับนิวคลีโอไทด์บริเวณ non-coding regions หลายตำแหน่งและมีการเปลี่ยนของกรดอะมิโนของโปรตีน VP1 (ตำแหน่ง S347T), VP2 (ตำแหน่ง L40V, G120R, Y121I, P123R, G127S, L137F, Q287R และ A327V), LTAg (ตำแหน่ง Q357P, V369E, E377K, D378V, A381T, R382E, R383G และ D389G) และ STAg (ตำแหน่ง R139S, K141E, R148K และ W153C)

สรุป: ข้อมูลที่ได้จากการศึกษานี้สามารถใช้เป็นข้อมูลพื้นฐานทางด้านระบาดวิทยาและการจำแนกสายพันธุ์ระดับโมเลกุลของเชื้อฮิวแมนโพลีโอมาไวรัส ซึ่งอาจมีประโยชน์ต่อไปในอนาคต